Neuronal circuits underlying visual attention during naturalistic behaviour in zebrafish larvae

Pedro Miguel Dias Henriques

A dissertation submitted in partial fulfillment

of the requirements for the degree of

Doctor of Philosophy

of

University College London.

Department of Neuroscience, Physiology and Pharmacology

University College London

March 12, 2019

I, Pedro Miguel Dias Henriques, confirm that the work presented in this thesis is my own. Where information has been derived from other sources, I confirm that this has been indicated in the work.

Abstract

To survive, animals need to sustain behavioural responses towards specific environmental stimuli to achieve an overall goal. One example is the hunting behaviour of zebrafish larvae, which is characterised by a set of discrete visuomotor events that begin with prey detection, followed by target-directed swims and end with prey capture. Several studies have begun elucidating the neuronal circuits that govern prey detection and initiation of hunting routines, which are largely dependent on the midbrain optic tectum (OT). However, it is not known how the brain is able to sustain a behavioural routine directed towards a specific target, especially in complex environments containing distractors.

In this study, I have discovered that the nucleus isthmus (NI), a midbrain nucleus implicated in visual attention in other vertebrates, is required for sustained tracking of prey during hunting routines in zebrafish larvae. NI neurons co-express cholinergic and glutamatergic markers and possess two types of axonal projection morphology. The first type targets the ipsilateral OT and AF7, a retinorecipient pretectal region involved in hunting. The second type projects bilaterally to the deep OT layers. Laser ablation of the NI followed by tracking of naturalistic hunting behaviour, revealed that while hunting initiation rates and motor kinematics were unaltered, ablated animals showed an elevated probability of aborting hunting routines midway. Moreover, 2-photon calcium imaging of tethered larvae during a closed-loop virtual reality hunting assay, showed that NI neurons are specifically active during hunting.

These results suggest that the NI supports the maintenance of action

sequences towards specific prey targets during hunting, most likely by modulating pretectal and tectal activity. This in turn supports its presence at the centre of an evolutionarily conserved circuit to control selective attention to ethologically relevant stimuli in the presence of competing distractors.

Impact Statement

This thesis was able to bridge several methodologies in the field of neuroethology to understand how neuronal circuits mediate behaviours. The work reported here used state-of-the-art tools to interrogate the role of a specific neuronal circuit in the behaviour of a vertebrate system. This is likely to project onto the general goal of systems neuroscience to understand the computational, algorithmic and implementation levels employed by the nervous system, linking sensory perception to behaviour. In this context, future studies might use similar frameworks to provide clear insights on how nervous systems generate behaviour, and how evolution has shaped brain circuits to meet different ecological demands. On a more applied level, this study might provide in the future the possibility to design paradigms to test the impact of specific drugs on selective attention in a high throughput manner. This might enable drug discovery for the treatment of ailments in humans related to impairments of selective attention, such as ADHD.

Acknowledgements

I would first like to thank my supervisor, Isaac Bianco. Isaac couldn't have done anything better. He was always friendly and lively despite the odd incompetence of his PhD student. He was always there to help, to stimulate my thought process, to give helpful suggestions, to go through the experiments again, to support me when I failed and to cheer when I succeeded. His door was always open. Mine will always be to you.

Joanna was there too. And there she kept, waiting to show me another dog video. I hope you don't get tired of showing me yet another. You were a good PhD sis. I also have to my two current desk neighbours, since they had to endure my endless staring at the MATLAB console, not paying attention to them. Thank you Anya, for being a clever silly person and thank you Shannon for making me think about the meaning of my life and for asking all the deep, complex and unexpected questions that put me on my toes. Thank you Leo, who was the happiest man alive and the best of friends. Thank you Julie for going to all those parties with me, you'll always be my friend. A special thanks to Ana. I would be nothing without you and will forever regret leaving you. You taught me a lot. Thanks to my Geek buddies Marcus and Eirinn. Boy did we have a good time!!

A special thanks to all the members of the Bianco lab, both permanent and temporary. I hope I was good enough to greet you

in.

There's not enough space to thank all the people that deserve, and that collectively have made my passing through the First Floor Fish lab the most amazing experience. I'll thank you in person with with a pint in hand.

Thanks to my Me & You bros. No matter how many seas we're apart, we're bonded forever.

Last but not least, I thank my parents, my sister, my grandma and my aunt. You are the most loving family and I'm incredibly grateful to all of you and your support. I love you all.

Contents

List of Figures

Chapter 1

Introduction

Animals are required to face the challenges of an ever-changing environment if they are to survive. The dangers of an incoming predator, or on the other hand, the rewards of an evading prey, provide an immediate need for the nervous system to quickly and accurately process information that maximizes the success of the animal's current goals. Physical and physiological constraints make such a task invariantly to require some form of selection to decide which stimuli are more relevant to the animal's current needs. This mechanism, formally known as attention, is present across many vertebrate species, from humans to mice, birds, amphibians, fish and even in insects, arguing for its origins to be deeply rooted in evolutionary history. Moreover, such stimulus selectivity needs to be maintained for the amount of time required for the animal's current goal to be achieved. A task made more challenging in the context of complex and dynamic interactions between the animal and its target.

This thesis is concerned with the question as to how the nervous system is able to implement sustained behaviour towards ethologically relevant stimuli in a goal-oriented fashion. More specifically, it investigates the role of an evolutionarily ancient structure of the vertebrate brain, the Nucleus Isthmi (NI), in mediating such behaviours in the young larva of zebrafish (*Danio rerio*). In this chapter, I will start by giving a summarized description of goal-oriented behaviours and how they might use selective attention to allow sustained responses towards target stimuli, providing insights on brain circuits that are

likely to mediate these responses. Then, I will give an overview of selective attention, focusing on behaviours and the evolutionarily conserved brain circuits that mediates them across several non-mammalian vertebrate species. Finally, I will concentrate on discussing why the prey-catching behaviour of zebrafish larvae provides a good model to investigate the brain mechanisms involved in goal-oriented behaviour and specifically, in how the brain is able to allow the maintenance of sequences of actions targeted on relevant environmental stimuli.

1.1 Goal-oriented behaviours

Animals interact with their environment by producing behaviour. When a motivation, brought by internal and external factors, produces an instrumental action of the subject onto the world, this behaviour might be called goal-oriented. This process requires a dynamic interaction between the agent and its environment, generating a sequence of discrete actions that ultimately lead to the completion (or not) of the original goal.

At the core of goal-oriented behaviours is the interplay between motivational state, sensory input and action selection. Motivation, such as hunger, can up or down-regulate the threshold required to initiate or terminate some goal-oriented action. In turn, action selection can rely on both on innate or learned programmes that are triggered on integrated sensory evidence, which can then be updated based on "error" signals that compare reward expectation with action outcome.

Progress has been made identifying neural circuits involved in inducing specific behaviours, modulating features of behaviour and controlling the timing and serial execution of motor sequences (Long et al., 2010; Seeds et al., 2014). However, little is known about neural mechanisms that explicitly maintain a behavioural state so as to facilitate the progression of action sequences to support task completion.

In classic neuroethology, "*stimulus-response chains*" have been proposed in

which a stereotyped sequence of sensorimotor transformations occurs because the outputs from one action act as the "*releasing stimulus*" for the next (Evans, 1966; Ewert, 1974). However, for complex behaviours such as those involving interactions between animals, the sequence of sensory inputs might be less reliable. Added to this, competing sensory information during goal-oriented behaviour adds uncertainty to sustaining a targeted action sequence, a problem that as we will see bellow, might be solved by mechanisms of selective attention.

Many behaviours require complex and dynamic interactions between sensory input and motor output, but arguably one of the most striking is the case of predator-prey interactions that happen in hunting/prey-capture sequences.

1.1.1 Prey-capture

Many animals predate on some other organism and are themselves a target of predation. Prey-capture offers a significant advantage in understanding goal-oriented behaviours because the goal the organism that is behaving is known a priori, which is to capture its prey. In the case of prey-capture pursuit strategies, as opposed to a sit-and-wait strategy employed by some animals (Ewert et al., 2001), the active pursuit of a prey using discrete targeted actions can help identify specific sensory-motor transformations that are used at every step of a sequence of targeted actions, which can lead to insights on the algorithms used to implement them.

Despite the recent advancements in understanding how certain neurons might contribute to generate complex goal-oriented behaviours, one would like to be able to monitor and causally disrupt the function of several neurons during the production these behaviours in a setting that is ethologically relevant to the animal. Such approach might arguably provide insights on how different neuronal populations causally interact to implement specific sensory-motor patterns during complex goal-oriented behaviours (Krakauer et al., 2017). One of the most well studied examples following this experimental framework is the case of the prey-catching behaviour of the dragonfly (*Plathemis lydia*).

Dragonflies hunt for small insects flying overhead by deploying a series of

manoeuvres that follow both predictive and reactive strategies. On the first step, a small moving shadow of a specific range of angular size and speed directly above the dragonfly's head initiates a flight to intercept the prey (Lin and Leonardo, 2017). A set of specialized feature detector neurons in the dragonfly's lobula plate termed "small target motion detectors" (STMD) seem to be important at for this detection stage (Olberg, 2012; Combes et al., 2013). During pursuit, the dragonfly moves to intercept its prey by predicting its future location, considering that it moves a constant direction and velocity (Olberg et al., 2000). This is in contrast to a reactive strategy, where the animals act to maintain a constant bearing to its target by correcting for orientation errors. Crucially, the prey is kept constantly fixated in a small fovea of the eye with high resolution by rotations of the head with an almost zero lag with respect to the retinal slip generated by both self and prey motion (Olberg et al., 2007; Mischiati et al., 2015). Such small lag is difficult to account by a sensory reactive strategy, but instead is likely to rely on internal models of self and prey motion to allow it to predict with high accuracy the future position of the target (Mischiati et al., 2015).

The problem of maintaining a behaviour sequence directed towards a single target is further challenged by the fact that at any one time during behaviour, multiple competing stimuli might present a "*distraction*" from the current objective. In the dragonfly, a specific class of neuron located in the lobula plate, named CSTMD1 (Geurten et al., 2007; Bolzon et al., 2009), seem to play a role in this selection. These neurons, which are sensitive to prey-like visual features, selectively respond to a single stimulus among competing targets (Wiederman and OCarroll, 2013) and their response to a target moving stimulus (probe) is facilitated by the short presentation of a cue stimulus (primer) outside its receptive field. This happens especially for primers moving in a trajectory that predicts location of the probe (Wiederman et al., 2017), thus allowing for a "hot-spot" of selective attention at the future location of the target prey.

In the next section, we will see how selective attention has evolved in many animals to allow selection of relevant environmental stimuli from the multitude of sensory information that at any one time arrives at the senses.

1.2 Selective attention

As we have discussed, a critical aspect of goal-oriented behaviour is the requirement for a continuous interaction between the relevant sensory input and the motor output that produces movements to allow animals to achieve their goal. In a dynamic environment, uncertainty, noise and irrelevant/distracting stimuli are likely to disrupt this delicate link. To cope with this, the central nervous system evolved a set of mechanisms to selectively enhance the representation of stimuli which are more salient or relevant for the animals' current goal, while blocking competing eligible signals (Krauzlis et al., 2018; Knudsen, 2018; Ewert et al., 2001). These mechanisms are generally called selective attention (James, 1890; Nobre and van Ede, 2018; Treisman, 1969; Driver, 2001).

In human and non-human primate studies, a distinction is usually made between selection based on the exogenous cues (bottom-up), which depend on the physical features of stimulus (eg., size, color, movement) or endogenous influences (top-down), which reflect the "voluntary" processing of certain features or locations depending on the animal's current behavioural goal. This distinction can be classically described by the influential cueing task first introduced by Michael Posner in human subjects (Posner and Keele, 1968; Posner, 1980). In these experiments, subjects are required to fixate at a central point. In a top-down attention task, the subjects is presented with a cue at fixation point (endogenous cue), like an arrow pointing to the direction where the target is going to appear next. Then, after a brief period of time (100-1000 ms), a target is presented to either the left or right side of the fixation point, to which the subject is required to respond. The benefits of attention are readily observed by a decrease in the response time when the cue is valid (ie., signals

the correct location of the target) than when it's invalid. Similarly, in experiments designed to uncover the effects of bottom-up attention, a salient cue, such as a bright spot, is presented to the left or right sides before the target appears with the subjects instructed to have their eyes fixated at the centre. Presenting a valid or invalid target afterwards reveals the same effects as for top-down cues, even when the cue has no predictive value on the location of the target, indicating that salient stimuli are effective at shifting our attention (Posner, 1980).

The behavioural flexibility, ease of training and similarities with the human brain have made non-humane primates the primary animal model to study the neuronal mechanism of selective attention, of which visual attention has been investigated the most. This has led to the discovery of a fronto-parietal network that direct attention to spatial locations, different sensory modalities, specific stimulus features or objects (Buschman and Kastner, 2015). These act on the neuronal level increasing neuronal sensitivity, gain, decorrelating activity between neighbouring neurons, synchronizing activity between brain regions and sharpening receptive field tuning (Nandy et al., 2017; Zirnsak et al., 2014; Bartsch et al., 2017).

Despite the overwhelming unbalance in studies investigating the cortical control of selective attention, several lines of evidence indicate that subcortical, and specifically midbrain circuits are crucially involved in some more basic forms of attention, which in some cases can even override cortical control (Goddard et al., 2012). Crucially, many of these insights have come from studies of behavioural and neuronal signs of selective attention using non-mammalian species which lack a neocortex, providing a new perspective on the evolutionary roots of these mechanism.

1.2.1 The Superior colliculus/Optic tectum

While several sub-cortical structures have been found to participate in selective attention, such as the thalamus (Saalmann and Kastner, 2011) and the striatum (Grillner and Robertson, 2016), the Superior colliculus (SC), or Op-

tic tectum (OT) in non-mammalian species, has recently received increased investigation due to its seemingly conserved role in spatial selective attention (Krauzlis et al., 2013). Indeed, while forebrain networks seem to work to select information based on task demands and salience of stimuli (Buschman and Kastner, 2015), the SC seems to be primarily concerned with the relative priority of stimuli based on their spatial location in the environment (Krauzlis et al., 2018; Knudsen, 2018; Fecteau and Munoz, 2006; Crapse et al., 2018). This specificity can probably be understood considering its structure and connectivity.

Located on the roof of the vertebrate midbrain, the SC/OT is organized by several laminae, which can be separated into superficial, intermediate and deep layers. The superficial layers mainly receive sensory input, which is topographically organized to the map of the visual space. In general, SC neurons respond to visual cues on the contralateral visual field, although exceptions exist depending on the species. In mammals, SC neurons receive direct input from the retina, and while in primates only $\approx$ 10% of RGCs project to the SC (Perry and Cowey, 1984), 85% – 90% of RGCs project to the SC in mice (Ellis et al., 2016). In non-mammalian species, the retina provides the majority, if not all the visual input (Huerta, 1984). In the intermediate and deep layers, neurons also respond to other sensory modalities such as auditory or somatosensory stimuli, while another group of neurons generate activity related to pre-motor commands for orientation towards or away from a stimulus, by way of movements of different effectors such as eyes (saccades), head, whiskers or pinnae (Gandhi 2011). This goal-orienting function of the SC/OT has long been recognized to be related to the allocation of overt spatial attention (Krauzlis et al., 2013), but it's its function in mediating covert attention (ie., without targeted saccades) that's most interesting. This covert allocation of attention by the SC is well characterized by an experiment in monkeys performing a visual detection task (Figure 1.1, Lovejoy and Krauzlis (2010)). In this experiment, monkeys were trained to discriminate the motion direction of a random-dot

patch stimulus that appeared at a previously cued location. Importantly, a competing patch is presented in another uncued location, which the animal must ignore. Inactivation of the SC in an area representing the cued location severely impairs monkeys' performance in a way that the reported motion is biased towards that of the competing patch. When a stimulus is presented alone in the cued location, performance is only slightly impaired, indicating that this effect is not due to a defect in visuo-motor processing.

This evidence seems to suggest that the SC acts to control how sensory evidence is interpreted by the brain, providing a "priority" signal when conflicting information is present. Indeed, its spatial topographical organization and multisensory integration properties make it a likely candidate for establishing a priority map of the surrounding environment (Fecteau and Munoz, 2006; Mysore and Knudsen, 2014; Boehnke and Munoz, 2008; Itti and Koch, 2001). Some theories argue that this signal is then transmitted into higher cognitive areas, like the visual cortex, biasing representations there for action selection. However, evidence suggests that this might not be so simple. For example, in a similar task as described above in monkeys where the SC was inactivated, activity in the visual cortex continues to show typical neuronal signatures of attention (increased discharge rates, decreased inter-neuronal correlations and ratio of variance to the mean, also known as Fano factor), despite obvious impairments in behaviour (Zénon and Krauzlis, 2012), contradicting the view that the SC acts to regulate how sensory signals are perceived in the cortex.

One prominent hypothesis to explain this discrepancy is that different aspects of sensory perception might be differentially regulated by different brain regions. For example, in the context of signal detection theory, the attentional benefit in a stimulus discrimination task can be divided by changes in the criterion (c), of sensitivity (d') (Macmillan and Creelman, 2005). Criterion is likened to the subject's strategy in reporting a stimulus. A more liberal approach leads to more targets being correctly reported (hits), but also increases the reported number of non-targets (false-alarm rate). On the other

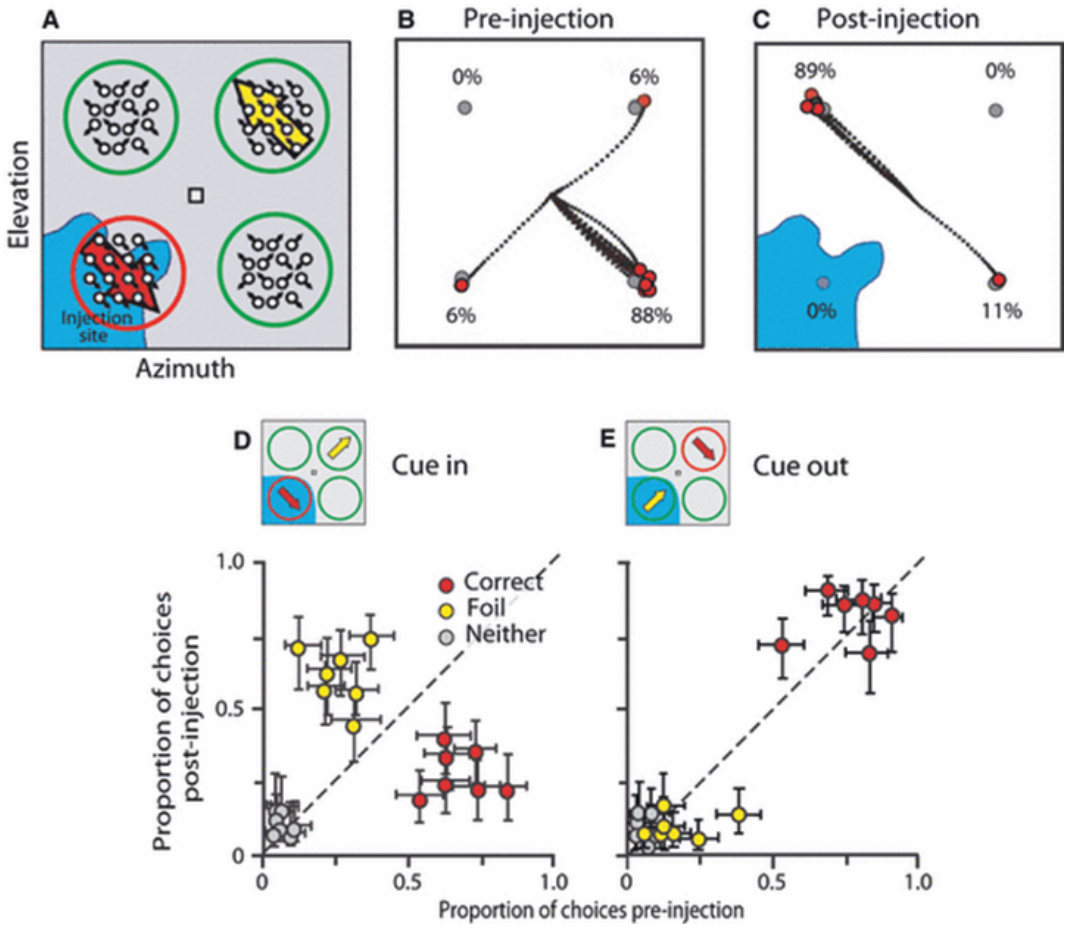

Figure 1.1: Inactivation of the Superior Colliculus in monkeys causes a deficit in spatial-attention. (A) Monkeys are cued by a red circle to attend to the direction of a pulse of coherently moving dots and to report the direction of motion (red arrow) with an eye movement in the corresponding direction. Coherent motion in the opposite quadrant (foil stimulus, yellow arrow) and random-motion in the other two quadrants were instructed (by training) to be ignored. The SC was then inactivated in the region corresponding to the cued location (Blue patch). (B) Before inactivation, eye saccades are manly directed towards the direction of the cued motion. (C) In contrast, after SC inactivation saccades are directed in the direction of the motion of the foil stimulus. (D) Difference in saccade directions before and after SC inactivation when the cued stimulus was located in the inactivation portion of the visual field. (E) Same comparison when the inactivation corresponds to the location of the foil stimulus. Adapted from (Knudsen, 2011). Original from (Lovejoy and Krauzlis, 2010).

hand, a subject's sensitivity relates to its ability to discriminate a target from a non-target, increasing the number of hits but also decreasing the amount of false-alarms. The SC has been found to be related to changes in criterion (McPeek and Keller, 2004; Sridharan et al., 2017), but not sensitivity (Crapse et al., 2018), while neuronal modulations in the cortex seems instead to arise from behavioural changes in sensitivity (Luo and Maunsell, 2015).

Although some discrepancies exist between different studies (Lovejoy and Krauzlis, 2017), these results indicate that the OT seems to be more concerned with biasing responses towards particular locations of the visual field, irrespective of their features. Thus, while in mammals the neocortex has evolved to deal with more complex properties of selective attention, such as feature tuning, a spatial selection bias might be a more ancient feature with which species that lack a neocortex might predominantly require (Knudsen, 2018; Krauzlis et al., 2018). Indeed, recent work on non-mammalian species have started to shed light on the evolutionary conservation of selective attention.

Perhaps one of the best examples of selective attention in a non-mammalian species comes from the work of Eric Knudsen on birds. In one noteworthy experiment, chickens were trained to report the vertical location of a target stimulus, which was also displaced to one of the sides and was accompanied by a distractor stimulus on the other side (Sridharan et al., 2014). When the contrast of the distractor is higher than the target's, the detection performance of chickens suffers, indicating that the presence of the distractor imposes a competition based on its relative salience to that of the target. However, when a preceding cue is presented to the left or right side, predicting the horizontal, but not vertical location of the target, responses are more accurate and faster than in no cue trials, indicating a clear attentional benefit. This shows that chickens can also use top-down cues to allocate attention to specific locations of the visual space, similarly to what has been described in primates. What brain areas might modulate these behavioural effects? Several lines of work point to a network involving the OT and its satellite nuclei, the Nucleus

isthmi (NI) (Knudsen, 2018).

1.2.2 The midbrain attention network - conservation across vertebrates

The Nucleus isthmi, whose mammalian homologue structure is the Parabigeminal nucleus (PBN, Gruberg et al. (2006)), is an incredibly conserved population of cholinergic neurons situated in the midbrain tegmentum across a vast number of vertebrate species (Constantine-Paton and Ferrari-Eastman, 1981; Dunn-Meynell and Sharma, 1984; Glasser and Ingle, 1978; Graybiel, 1978; Grobstein et al., 1978; Gruberg and Lettvin, 1980; Sakamoto et al., 1981; Méndez-Otero et al., 1980; Tay and Straznicky, 1980; Udin and Fisher, 1985; Caine and Gruberg, 1985; Gaybriel and Ragsdale, 1978; Gruberg et al., 2006).

1.2.2.1 Birds

Early seminal works in pigeons established that both the OT and the NI are required for visual discrimination of objects (Hodos and Bonbright, 1974; Jarvis, 1974). More recent studies have however directly implicated both structures in modulating spatial attention. While in most species the NI has been described as a single cholinergic population of neurons, in birds and reptiles, these achieve a greater complexity as three sub-nuclei can be anatomically and molecularly distinguished (Sereno and Ulinski, 1987; Wang et al., 2006, 2004). These are the cholinergic nucleus isthmi pars parvocellularis (Ipc) and pars semilunaris (SLu), and the GABAergic isthmi pars magnocellularis (Imc).

In birds, a circuit composed of the OT and the Ipc/SLu and Imc subpopulations has been shown to mediate selective attention to specific locations of space by acting through a focal facilitation and global inhibition of responses in the OT space map (Figure 1.2, Knudsen (2011, 2018)). The distinctive feature of this network is the interconnectivity between its components. The first circuit establishes a space-specific amplification of the highest priority stimulus. In the deep layer 10 of the bird's tectum, "shepherd's crook" neurons send topographical focal projections to all Ipc, SLu and Imc nuclei (Wang et al.,

2006). These neurons have radial, bipolar dendrites which innervate several superficial and intermediate layers of the OT, receiving direct retinal and multimodal sensory input, as well as endogenous cues from the forebrain (Mysore and Knudsen, 2014). In turn, the cholinergic Ipc and SLu neurons send feedback projections to the same portion of the OT space map (Wang et al., 2006). Ipc terminals have a columnar organization which extensively innervate superficial OT layers. These are thought to facilitate glutamate release in retinotectal afferents mediated by the binding of ACh into presynaptic nAChRs, thereby amplifying retinal input (Edwards and Cline, 1999; Binns and Salt, 2000; Dudkin and Gruberg, 2003). Indeed, inactivation of Ipc neurons reduces the gain and spatial tuning of corresponding OT unit responses to visual stimuli (Asadollahi and Knudsen, 2016), and Ipc lesions impairs the discrimination of visual stimuli, even when no competitors are present (Knudsen et al., 2017). At the same time, ACh release from Ipc neurons also synchronizes gamma-band oscillations (25-60 Hz) across the network, which is transmitted to the thalamus and basal ganglia by OT and SLu projections (Hellmann et al., 2001; Goddard et al., 2012; Bryant et al., 2015; Marín et al., 2005). This synchronization is thought to enhance the transmission of visual responses in the OT at specified locations of the space map that correspond to the highest priority stimulus (Sridharan and Knudsen, 2015).

A parallel circuit implements a global-competition to inhibit responses to competing, less salient stimuli. For example, when barn owls are presented with two competing looming visual stimuli, neuronal responses in the deep OT represent the stimulus with the highest salience (eg., higher looming speed). This selection is represented by a sharp decrease of neuronal responses to a target stimulus when the salience of a competitor, anywhere else in the visual field, surpasses that of the target (Mysore et al., 2010, 2011). This global inhibitory mechanism is mediated by the Imc GABAergic population, which after receiving topographical input from the OT, sends feedback anti-topographical global projections to the OT, Ipc and SLu (Wang et al., 2004; Lai

et al., 2010; Mysore et al., 2010; Mysore and Knudsen, 2013). In response to this, neuronal responses in the Ipc representing a target stimulus also sharply decline when the competitor becomes more salient (Asadollahi et al., 2010). At the same time, long range projections within the Imc provide lateral inhibition (Goddard et al., 2014), which is responsible for implementing a circuit motif of "mutual inhibition of lateral inhibition", which has been shown to allow rapid categorization of the strongest stimulus when multiple stimuli are in competition (Mysore and Knudsen, 2012).

1.2.2.2 Anurans

The behavioural responses of predation and avoidance in anuran species rely crucially on the OT. In these species, the OT is innervated by most RGCs, where some visual features related to behaviourally relevant stimuli, like the small convex shaped "bug detectors" of Letvin are already computed (Lettvin et al., 1959). In the tectum, certain classes of tectal ganglion cells respond to optimal prey and threat stimuli (Ewert et al., 2001) and activation of prey-like tectal neurons triggers prey-catching responses that are targeted to the mapped location of visual space where the activation occurred (Ewert, 1974). Maybe unsurprisingly, OT ablation abolishes behavioural responses to both prey and threat stimuli in the side contralateral to the ablation (Ingle, 1973; Ingle and Cook, 1977; Kostyk and Grobstein, 1982, 1987).

The NI is also crucial for the deployment of these behaviours. Like many other species, the anuran NI is composed of cholinergic cells located in the midbrain tegmentum (Gruberg and Udin, 1978; Desan et al., 1987; Wallace et al., 1990). In frogs, a cell body layer forms the "cortex" of the nucleus, which wrap around the neuropil (medulla) except for a small gap where the fibres pass through, forming a "taco" like shape where the fibres extend laterally in the brain (Gruberg and Udin, 1978). The rostral-most NI cells also make reciprocal topographical connections with the ipsilateral OT, while the caudal cells only project contralaterally. There does not seem to be evidence so far for bilateral projections from single NI neurons (Dudkin et al., 2007). When the NI

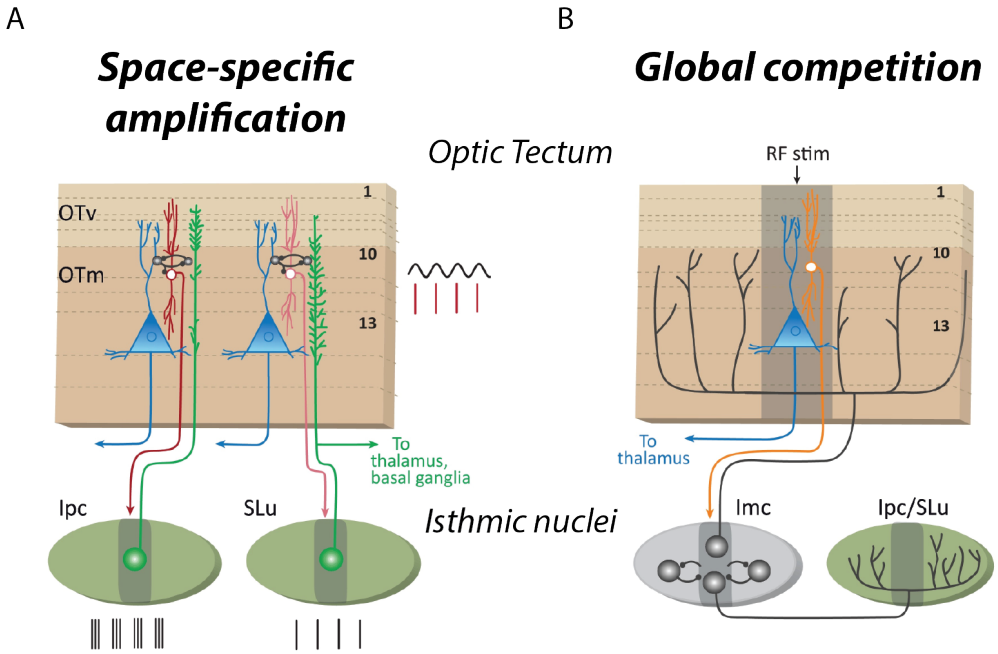

Figure 1.2: Circuit mechanisms of the midbrain attention network in birds. (A) Space-specific amplification by the midbrain network. GABAergic neurons (black) in the OT layer 10 periodically depolarize neurons of the same layer that project to the cholinergic Ipc or SLu (black circles). Periodic spikes from these neurons (red lines) evoke periodic spike bursts in Ipc neurons (black lines) and periodic single spikes in SLu neurons (single black lines). Ipc and SLu neurons project back topographically across the visual (OTv) and multimodal (OTm) layers of the Optic tectum. SLu neurons also send projections to the thalamus and basal ganglia. The resulting synchronization of activity across OT layers can enhance the transmission of visual responses within the OT, specifically for this location in the space map. (B) Global competitive selection by the midbrain network. Neurons in OT layer 10 project to the nucleus Imc (Orange neuron). GABAergic inhibitory neurons in the Imc project back to the OT in an anti-topographical fashion across the rest space map, innervating multiple layers in the OTm (Black neurons). Other neurons in the Imc also project to the Ipc and SLu in a similar fashion, while another class of local interneurons are responsible for lateral inhibition in the Imc. Both these mechanism act to facilitate space specific responses in the OT and to synchronize activity across the network and with high-order thalamic nuclei (nucleus rotundus), which might be required for biasing top-down selective attention. OT, optic tectum; OTm, multimodal OT; OTv, visual OT; RF, receptive field; RF stim, centre of the region activated by a small, salient stimulus; SLu, nucleus isthmi pars semilunaris. Modified from (Knudsen, 2018).

is ablated unilaterally, frogs do not respond to either prey or visual threats in the contralateral visual field at locations mapped to the corresponding ablation (Gruberg et al., 1991; Caine and Gruberg, 1985). Intriguingly, however, one study reported that bilateral NI ablations in toads do not seem to impair prey-catching responses (Collett et al., 1987). No argument has been however proposed for theses discrepancies.

Is there evidence that the anuran midbrain is involved in selective attention? In a classical experiment in frogs, a prey-like stimulus was moved in one portion of the visual field such that elicited low prey-catching rate (Ingle, 1975). After a brief pause, if the stimulus is moved again, the prey-catching rate increases dramatically. This "priming" effect seems to be local since it happens only if the second stimulus is located close to the location of the first. The same study also reported the presence of tectal responses resembling "attention units", which were selective for prey-like stimuli and had a delayed response to the presentation of the priming stimulus, suggesting that such units might be responsible for lowering the response threshold of tectal output, facilitating responses at that location for the following stimulus presentation.

Although the role of the NI in the context of selective attention has not been explicitly investigated in anurans, isthmo-tectal projections seem to have a faciliatory effect on retino-tectal transmission, as co-stimulation of the NI and optic tract enhances the calcium influx of retinal afferents by double the amount of nerve stimulation alone (Dudkin and Gruberg, 2003). As retino-tectal fibre terminals have been shown to contain nicotinic ACh receptors (Sargent et al., 1989), it was suggested that this effect might be mediated by ACh release from isthmo-tectal projections. Frogs also have a bias to respond to prey in the rostral visual field if challenged with two competing prey (Stull and Gruberg, 1998), even if they were located further away (Dudkin et al., 2011), indicating that the rostral visual field is somehow biased for prey-catching responses. Whether this bias is mediated by the NI is still undetermined.

1.2.2.3 Teleost fish

As is the case of other vertebrates, the OT of teleost (bony) fish plays a crucial role in visually-guided behaviours (Roeser and Baier, 2003). I will describe in more detail the structure of the OT of zebrafish and its impact on the behaviour of zebrafish larvae on Chapter 4, which bears resemblance with that of many other teleosts. Here, I will focus on the known interaction between the OT and the NI in adult teleosts.

The NI of teleost is composed of a cholinergic population of neurons (Mueller et al., 2004; Pérez et al., 2000) and is described as a "shell" of cell bodies enveloping on the rostral part of the nucleus a "core" of neuropil (Figure 1.3, Sakamoto et al. (1981); Ito et al. (1982)). The OT type XIV neurons in the tectal deep layers (SPV) project topographically to the core of the ipsilateral NI. These neurons have dendritic arborizations in the tectal superficial layers (SO and SFGS), receiving largely retinal input, but also in deeper layers (SGC) where multimodal input converges. In turn, NI neurons send feedback topographical projections to both OT (Johnson et al., 2013; Dunn-Meynell and Sharma, 1984) and pretectal nuclei (Striedter and Northcutt, 1989; Yáñez et al., 2018; Folgueira et al., 2008). It is not known, however, if single NI neurons send bilateral projections to the OT, or whether isthmotectal projections are different from those innervating the pretectum.

The NI of goldfish and sunfish vehemently responds to looming stimuli approaching in the contralateral visual field and its responses increase gradually with decreasing distance between the fish and the stimulus independently of stimulus size or speed and using only monocular cues (Gruberg et al., 2006), indicating that it might encode some form of proximity to a visual stimulus. Other visual stimuli also seem to elicit, albeit comparatively smaller responses, including stimuli moving parallel to the fish's body axis (Gruberg et al., 2006), light spots (Northmore, 1991; Northmore and Gallagher, 2003). Despite its topographical inputs, however, recordings from opposite ends of the NI seem to respond with near zero lag to stimulation anywhere in the contralateral visual

field, as if the whole nucleus responds as a unit (Northmore and Gallagher, 2003), possibly mediated by electrical coupling (Williams et al., 1983). This strange response has led to the idea that the NI in teleosts mediates an arousal or attention function, specifically considering its preferential responses to novel stimuli, which habituates relatively fast (Gallagher and Northmore, 2006), and are inhibited by two simultaneously presented stimuli (Northmore, 1991). No studies have however reported causal manipulations of NI neurons while observing behaviour in teleosts. Despite this, these observations suggest that the NI is likely to modulate visual responses in the OT. But has the OT in teleost fish been associated with any form of visual selective attention?

1.2.2.4 Attention in teleosts – the archerfish

A phenomenal example of goal-oriented behaviour in fish is the ballistic prey-catching behaviour of the archerfish. As the name suggests, archerfish catch their prey (usually stationary insects like flies, or spiders perched on overhanging vegetation) by shooting a highly directed squirt of water from their mouth to tumble their prey onto the water bellow (Timmermans, 2001). Remarkably, they do this while overcoming the refraction of light due to the air-water interface between the fish and its prey, which changes the perceived location of a stimulus than if it was observed entirely underwater. Moreover, they are able to accurately predict the location where its prey will fall and rapidly move to retrieve it (Rossel et al., 2002) and can learn to improve their accuracy by observing other fish (Schlegel et al., 2006).

Of particular importance here, archerfish also exhibit properties of visual selective attention. For example, when presented with multiple potential targets to shoot on a screen, but one of the stimuli has differing visual features than its competitors (singleton), such as different speed or direction of motion, archerfish will shoot at the different stimulus more often than expected by chance, as if it "popped out" (Ben-Tov et al., 2015). Importantly, the reaction times to shoot the target in these conditions are independent of the number of distractor stimuli, indicating that archer fish are able to use a

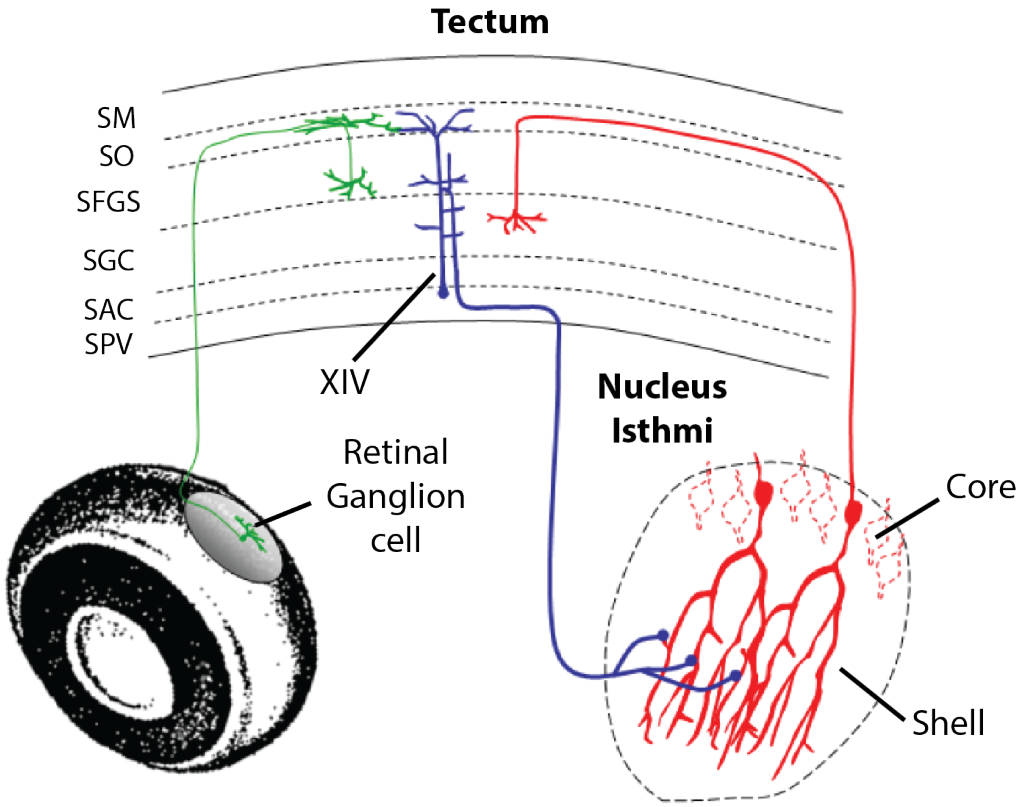

Figure 1.3: The NI-OT circuit of teleosts. Retinal ganglion cells in the retina project to the most superficial layers if the OT. Here, type XIV neurons receive visual input relayed from the retina and transmits it to the NI in the midbrain tegmentum by synapsing in its "core" of neuropil. NI cells, whose cell bodies are arranged around the core in the "shell" project topographically to the same region of the OT space map, innervating deeper tectal layers in the SGC. SM, Stratum marginale; SO, Stratum opticum; SFGS, Stratum fibrosum et griseum superficiale; SGC, Stratum griseum centrale; SAC, Stratum album centrale; SPV, Stratum periventriculare. NI, Nucleus isthmi. Modified from (Northmore, 2011).

parallel visual search mechanism for finding visual objects of interest, a task that was thought to exclusively belong to mammalian species (Treisman and Gelade, 1980; Itti and Koch, 2001). Some evidence also suggests that the OT is involved in computing this target selection, as some speed-selective OT neurons show increased activity if the speed of the stimulus in their receptive field was higher than the competing stimuli outside of it (Ben-Tov et al., 2015). Archerfish also possess a NI (Karoubi et al., 2016), however it has not been tested if it plays any role in these selective attention paradigms.

Like selective attention paradigms in humans (Posner, 1980), archerfish also show smaller reaction times to shoot a target on a screen when a cue precedes its appearance (Gabay et al., 2013). Moreover, this effect is dependent on the time lag between the cue and the appearance of the target, showing a characteristic U shape, where longer reaction times are seen with very short or long delays, known as inhibition of return (IOR) (Posner and Cohen, 1984). This is suggested to result in an optimal foraging strategy that promotes the exploration of new unseen locations, avoiding already attended ones (Klein, 2000). Investigating similar paradigms in other species of fish or other vertebrates will be able to tell if this is a specialization of archerfish, however, the remarkable comparison of visual attention task in humans and archerfish argues that this might be a more general characteristic of the vertebrate nervous system, inviting the design of similar experimental test in other species.

These accounts provide an overview of how selective attention is likely to be an evolutionarily ancient strategy for animals to cope with the vast amount of available information that is available to the senses at any time. However, despite the advancements in understanding the neural mechanisms of selective attention across several species, a good model on how the nervous system implements these strategies during ethologically relevant behaviour is still lacking. What behaviour models are likely to be more useful to address this issue?

1.3 The zebrafish larvae as a model organism for systems neuroscience

The brain of zebrafish develops rapidly. By 72 hours-post-fertilization (dpf) retinal ganglion cells (RGCs) have already started establishing connectivity with the contralateral OT neuropil (Stuermer, 1988). By 4-5 dpf, a retinotopic map is fully established, where the dorsal-ventral and medial-lateral visual field is represented in the dorsal-ventral and rostral-caudal tectum (Niell and Smith, 2005).

RGCs leaving the retina innervate 10 different arborization fields (AFs) after crossing to the contralateral side through the optic chiasm (Burrill and Easter Jr, 1994). In the tectum, which is innervated by AF10 arbours, RGCs are distributed into 10 distinct laminae composed of combinations of different RGC types (Robles et al., 2013), which also differentially respond to different visual features (Gabriel et al., 2012; Nikolaou and Meyer, 2012), indicating that parallel streams of visual information are already segregated in the tectum.

The number of neurons on both eyes of the zebrafish larva represent about half the total amount of neurons in the brain (Zimmermann et al., 2018). As such, zebrafish extensively rely on visually-guided behaviours (Portugues and Engert, 2009). As young as 5 days-post-fertilization, larvae are able to freely swim and produce a set of innate behaviours that help them survive in the river streams of the south-eastern Himalayan region from where they originate (Spence et al., 2008; Portugues and Engert, 2009). By this age, optokinetic (OKR) and Optomotor (OMR) responses can be elicited, which allow the eyes and body to maintain a stabilized sense of the world in response to whole-field visual motion cues (Neuhauss et al., 1999; Easter Jr and Nicola, 1996). These behaviours do not require the OT, as tectal ablations do not seem impair their deployment (Roeser and Baier, 2003). Instead, they are likely be mediated through pretectal and thalamic neurons which receive inputs from other arborization fields (Naumann et al., 2016). To escape predation, zebrafish larvae also rely on fast manoeuvres that direct them away from a perceived threat.

These can be readily elicited by looming dark spots (Dunn et al., 2016; Temizer et al., 2015), a stimulus that shows similar aversive responses in many other vertebrate and invertebrate species (Muijres et al., 2014); (Evans et al., 2018; Fotowat and Gabbiani, 2011). This behaviour is likely mediated by the OT and in fish involves the deployment of a specialized circuit of neurons in the hindbrain along with the large Mauthner cell (Dunn et al., 2016).

From a systems neuroscience perspective, the small brains of zebrafish larvae ($\approx$ 100.000 neurons, Naumann et al. (2010)), transparency and genetic amenability (Wyatt et al., 2015), has allowed the simultaneous monitoring of neuronal activity in the entire brain, during tethered (Ahrens et al., 2013; Naumann et al., 2016; Dunn et al., 2016; Haesemeyer et al., 2018) or free-swimming behaviour (Cong et al., 2017; Kim et al., 2017). Combined with tools to causally disrupt neuronal circuits, such as optogenetics (Förster et al., 2017; Wyart et al., 2009), laser (Bianco et al., 2012; Roeser and Baier, 2003; Barker and Baier, 2015; Semmelhack et al., 2014) or chemical (Barker and Baier, 2015) ablations, and used in combination with monitoring of behaviour (Bianco and Engert, 2015; Dunn et al., 2016; Haesemeyer et al., 2018; Oteiza et al., 2017) and circuit tracing (Robles et al., 2014), have allowed the investigation and discovery of detailed brain circuits that mediate behaviour (Naumann et al., 2016; Dunn et al., 2016; Koyama et al., 2016).

1.3.1 Prey-catching behaviour of zebrafish larvae

Perhaps the most striking example of visually guided behaviour in the larval zebrafish is prey-catching/hunting, which is first apparent at around 5 dpf. As in many goal-oriented behaviours, the hunting routines of zebrafish larval can be characterized by a series of discrete sensory-motor transformations (Patterson et al., 2013; Bianco et al., 2011; Trivedi and Bollmann, 2013; McElligott and OMalley, 2005). Hunting begins after the detection of prey by discriminating prey specific visual features like small ($\approx 5°$) and moving (30 - 90°/s) dark spots (Bianco et al., 2011; Bianco and Engert, 2015; Semmelhack et al., 2014). Several motor kinematics distinguish hunting from other behaviours.

The most stereotypical event is a convergence of both eyes (Bianco et al., 2011). This is thought to enable larvae to perceive the depth of prey during hunting routines, since this allows a significant portion of their anterior visual field to receive binocular visual cues (Bianco et al., 2011). Moreover, convergences are not symmetric, as the eye contralateral to the location of the visual prey tends to converge more than the ipsilateral eye (Bianco and Engert, 2015). At almost the same time as the eyes converge, a low-frequency lateralized tail swim, so-called J-turn (McElligott and OMalley, 2005) is deployed, which orients the fish such that its target is placed close to front of the fish's visual field (Bianco et al., 2011; Marques et al., 2018). Larvae usually begin hunting routines with prey at distances of around 1.5 mm (Bianco et al., 2011) and located in azimuth within 100° (Trivedi and Bollmann, 2013). Then, a series of discrete target-oriented swim bouts are deployed, which correct for azimuth displacements of the prey with respect to the centre of the larva's visual field, and gradually reduce it distance (Patterson et al., 2013; McElligott and OMalley, 2005; Trivedi and Bollmann, 2013). When target is at a striking distance (< 1 mm), larvae produce a capture swim, which can either be a fast strike "ram-like" manoeuvre or a suction of the prey, if it's very close to the mouth (Patterson et al., 2013).

Several recent studies have begun elucidating the brain circuits involved in the detection of prey and initiation of hunting routines (Figure 1.4). Visual features such as object size and movement direction are computed in the retina (Antinucci et al., 2016; Preuss et al., 2014) and transmitted to the contralateral OT. Here, neurons specifically tuned to conjunctions of prey-like features, termed non-linear mixed selectivity (NLMS) neurons can be observed and are thought to be responsible for target detection (Bianco and Engert, 2015). It is possible that NLMS neurons achieve their specific tuning properties by combining inputs from retinal, extra- and intra-tectal neuronal populations (Barker and Baier, 2015). Several neurons in the tectum PVN cell body layer are observed to fire in unison in assemblies, which correlate with the laterality of the

convergence saccades (Bianco and Engert, 2015; Romano et al., 2015). These observations suggest that OT cell assemblies might correspond to pre-motor activity that sends information to downstream oculomotor neurons to drive convergence saccades, and to specific reticulospinal neurons in the hindbrain that in turn are responsible to generate targeted orienting movements of the tail (Gahtan and O'Malley, 2003; Thiele et al., 2014). Specific retinal input from the rostral visual field to the AF7 (Robles et al., 2014) might also be required to produce hunting behaviour, as prey-like visual features and live paramecia induce responses in AF7 retinal afferents and selective ablation of the AF7 neuropil reduces hunting responses to live paramecia in tethered fish (Semmelhack et al., 2014).

Although these observations begin to explain how zebrafish larvae detect and initiate hunting behaviours, much less is known about how larvae are able to sustain a hunting routine targeted on a single prey. For example, do zebrafish larvae have some internal predictive representation of the future target location after an orientation bout? To answer such questions, recording of behaviour at high enough temporal and spatial resolution combined with clever manipulations of visual stimuli are imperative. For example, using a closed-loop paradigm where tethered zebrafish larvae were presented with prey-like virtual targets on a screen while mounted on an agarose dish, but where the eyes and tail were able to move, Trivedi et al. found that the inter-bout-interval between the first hunting bout and the second was shorted if the target was manipulated to appear closer to the centre of the fish's visual field, than if positioned at more eccentric locations (Trivedi and Bollmann, 2013). This suggests the existence of a focal facilitation of responses at the centre of the visual field, where most hunting bouts in free swimming larvae attempt to position the prey. Whether this is true for all bouts in a hunting routine, or if this facilitation takes into consideration the self and the target's motion is still undermined.

It is also unknown of zebrafish larvae display some sort of selective atten-

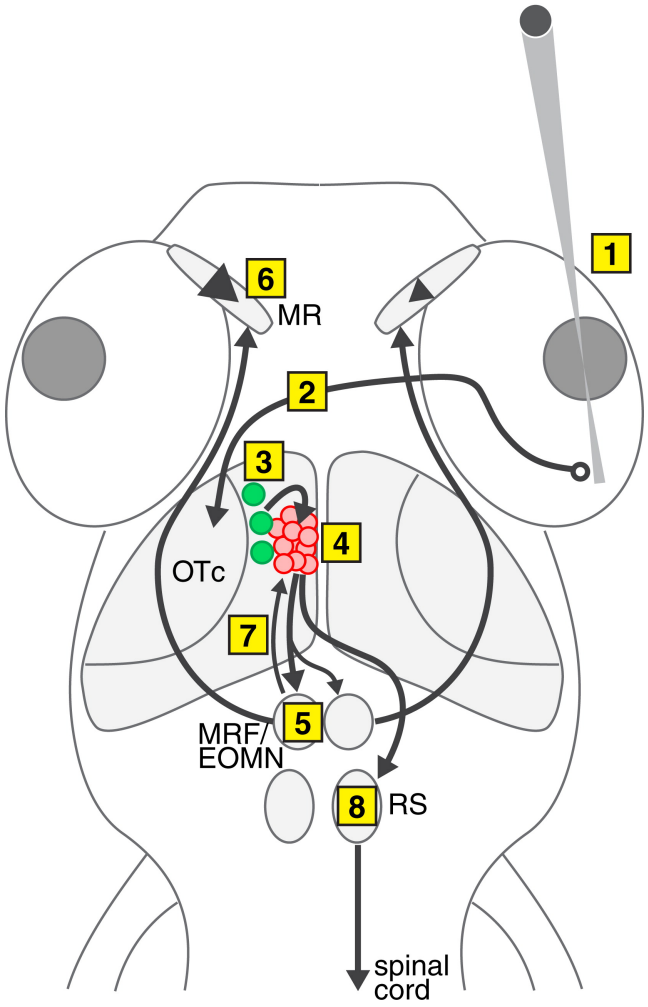

Figure 1.4: Proposed circuit model for prey detection and initiation of hunting behaviour. (1) The image of a prey-like visual stimulus is sensed in the retina by RGCs. (2) Visual information is transmitted to RGC arborization fields (AFs) in the contralateral brain hemisphere. (3) Non-linear mixed selectivity neurons (NLMS, green cells), selective for combinations of visual features that characterize optimal prey-like stimuli, are activated at corresponding locations in the tectum. (4) NLMS neurons recruit the activity of tectal assemblies (red cells). (5) Correlated bursting of tectal assemblies activate circuits in the mesencephalic reticular formation (MRF), which control a saccadic motor program involving activation of extraocular medial rectus motoneurons (EOMNs) in the oculomotor nucleus. OTc efferents project to the MRF with an ipsilateral bias, responsible for convergence asymmetry. (6) EOMNs control the ipsilateral medial rectus to produce a convergent saccade. (7) Reciprocal connections from the MRF to the tectum may provide a saccadic efference copy to mediate saccadic suppression, enabling the external stimuli to be distinguished from reafferent signals generated during gaze shifts. (8) Tectal assemblies activate reticulospinal (RS) neurons, which, in turn, recruit spinal circuits to produce an orienting turn toward the visual target. Adapted from (Bianco and Engert, 2015).

tion towards target stimuli when multiple targets are present. If so, where is this computed in the brain? One clue comes from an experiment where activity in the larva's OT was recorded when one or two competing small spots of light were presented to one eye. Both stimulus conditions elicit neuronal responses in the contralateral tectum when presented individually, however, when both spots are presented, the responses do not represent the linear summation of single responses, but rather a winner-take-all response where the activity corresponds to one or the other stimulus is present, suggesting the existence of competitive dynamics in the larval OT (Romano et al., 2015). Whether this competition arises solely through local tectal lateral inhibition or is mediated by other brain populations, such as the NI, is still unknown.

1.4 Aims of this thesis

How animals are able to sustain a targeted sequence of sensory-motor transformations towards relevant cues in their environment is a long-standing question in neuroethology. As we have seen, evidence supports the idea that in many vertebrate species, from fish to mammals, the OT/SC and its connected NI/PBG, act to select and prioritize these cues in the nervous system. However, it is still unclear how this information is used to drive and sustain goal-oriented behaviour. In this thesis, I aimed to explore this by investigating the circuit connections of the larval zebrafish's Nucleus isthmi and its role in mediating goal-oriented visually-guided behaviour, with a focus on hunting behaviour. Specifically, I aimed to address the following questions:

- Do young zebrafish larvae already possess developed NI circuit connections?
- Is the larval NI involved in mediating the sustained hunting routines of zebrafish larvae?
- Which specific sensory-motor transformations during complex goal-oriented behaviours is the NI involved in?

Using a combination of whole-brain gene expression analysis and circuit tracing, I uncovered two distinct populations of NI neurons in the larval zebrafish (Chapters 2 and 3). Then, using high-speed behavioural tracking and analysis in freely swimming larvae after bilateral NI ablations, I have uncovered the role of the NI in sustaining, but not initiating, hunting routines (Chapter 4). A closed-loop virtual reality assay with simultaneous monitoring of NI neuronal activity further revealed that the NI is especially triggered by the initiation hunting routines (Chapter 5).

Chapter 2

The Nucleus Isthmus of zebrafish larvae

2.1 Characterization of the zebrafish larva Nucleus isthmi

The Nucleus isthmi (NI) of vertebrates has long been characterized as a cholinergic population of neurons in the isthmic region of the midbrain tegmentum (Constantine-Paton and Ferrari-Eastman, 1981; Dunn-Meynell and Sharma, 1984; Glasser and Ingle, 1978; Graybiel, 1978; Grobstein et al., 1978; Gruberg and Lettvin, 1980; Sakamoto et al., 1981; Méndez-Otero et al., 1980; Udin and Fisher, 1985; Caine and Gruberg, 1985). In zebrafish, while the anatomical location of the NI has been characterized for adult brains (Mueller et al., 2004; Castro et al., 2006), not much information exists for the larval stages.

The great advantage of zebrafish as a model organism in systems neuroscience comes from its small size, transparency, and behavioural repertoire present at these early stages. Thus, if one is to understand how the NI might mediate such behaviours, it is necessary to investigate its anatomical, neurochemical and morphological characteristics during these developmental stages. This is likely to help formulate mechanistic models of the NI's role in modulating sensory processing in vertebrates, but also how these might differ across species, reflecting different ecological requirements. To that extent, it is still

unknown if the NI of teleosts is excitatory, inhibitory, or if it might be subdivided into separate sub-populations with different neurochemical and morphological identities, as is the case of the bird/reptilian NI.

To localize and characterize the larval zebrafish's NI, mRNA or protein expression of several neurotransmitters and genetic markers was analysed in the brains of 6 dpf larval fish.

2.2 Whole brain registration of expression patterns

The small size of the larval brain (≈ 700x350x350 µm) confers the advantage that standard confocal or 2-photon microscopy can be used to image a whole brain at a cellular resolution in a relatively small amount of time. Indeed, several recent studies have made an effort to build a whole-brain atlas of the 6 dpf larval brain that includes gene and transgene expression, along with manually (Marquart et al., 2015; Randlett et al., 2015) or semi-automatic (Ronneberger et al., 2012) curated anatomical labels. The advent of these tools is incredibly powerful in that it allows experimenters to statistically quantify, compare and share anatomical and expression data in a systematic way. In this study, an extensive use was made of the recently published ZBB atlas (Marquart et al., 2015, 2017) to register single 6 dpf larval whole-brain expression patterns of several genes, proteins and transgenes (Figure 2.1). To do this, whole or partial brain 3D image stacks of a registration marker (e.g., MAPK), typically called the "floating" image, were registered onto a whole-brain 3D image stack from the reference atlas expressing the same marker, the "fixed" image. This registration is composed of a set of linear and non-linear transformations, computed using image statistics and applied to the floating brain in order to spatially map each of its voxels to those of the reference fixed brain. Several algorithms and packages designed to register brain image volumes have been previously applied to larval zebrafish datasets (Randlett et al., 2015; Marquart et al., 2017; Allalou et al., 2017). Here, SyN non-linear registration using the

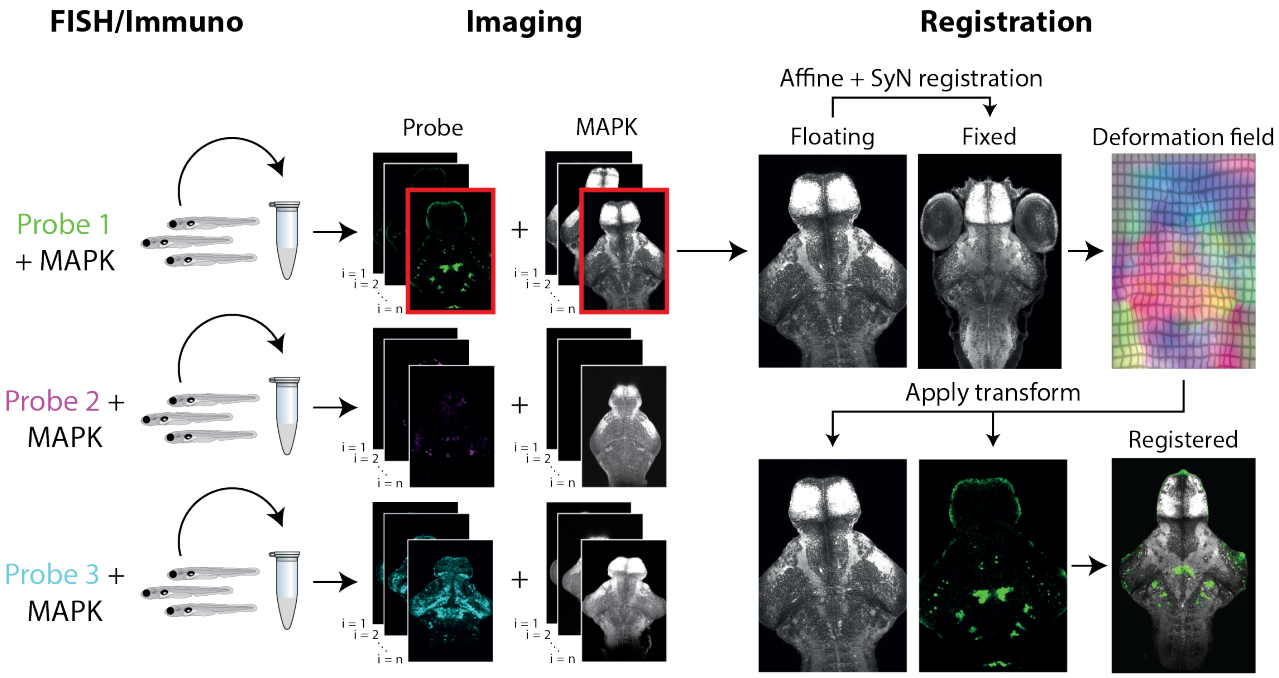

Figure 2.1: Whole-brain registration pipeline. Fixed zebrafish larvae are subjected to a fluorescent in-situ hybridization for a target mRNA probe combined with immunohistochemistry for MAPK on a separate fluorescent channel. Whole brains are then imaged for both the probe and MAPK using 2-photon or confocal microscopy. For each brain, the MAPK 3D imaging stack is used for registration onto the reference ZBB atlas, using as a template an already registered brain expressing the same marker. To do this, linear (affine) and non-linear (SyN) transformations are computed using the ANTs package, producing a deformation field which is then applied to both the probe and MAPK 3D imaging stacks, registering them in the same reference frame of the atlas.

ANTs package (Avants et al., 2011), which has been shown lead to more biologically plausible image deformations (Marquart et al., 2017), was used for all registration procedures (Figure 2.1, Methods).

2.3 The cholinergic NI of zebrafish larvae

Due to the cholinergic identity of most NI neurons across vertebrates, the expression of genes that identify cholinergic neurons in the CNS was performed in the brain of 6 dpf zebrafish larvae.

The *chat* gene encodes for the choline acetyltransferase enzyme (ChAT), which catalyses the synthesis of acetylcholine (ACh) from choline and acetyl

CoA (Nachmansohn and Machado, 1943). The presence of this enzyme in neurons is usually used to classify it as "cholinergic" (Wu and Hersh, 1994). ACh is then loaded into secretory vesicles by the vesicular acetylcholine transporter VAChT (Liu et al., 1999), which following vesicle fusion, allows ACh to be released into the synaptic cleft. The high-affinity choline transporter ChT, which in zebrafish is encoded by the *hact* genes (Hong et al., 2013), mediates the uptake of choline into the presynaptic terminal, and is specifically expressed in cholinergic neurons (Okuda et al., 2000). The *chat* and *vacht* genes are known to share the same genetic locus and regulatory elements in several species (Eiden, 1998) and in zebrafish, this locus is duplicated (Hong et al., 2013), a common feature of the zebrafish genome due to a teleost-specific whole-genome duplication around $\approx$ 100 mya (Postlethwait et al., 2000). These two loci can thus be separated by Ch-A (expressing chata and vachta), and Ch-B (expressing chatb and vachtb), which are expressed in different regions of the brain (Hong et al., 2013). Thus, to investigate if the larval NI can be described by one, or a combination of cholinergic genes, I investigated the expression of *chata*, *vachta*, *chatb*, *vachtb*, *hacta* and *hactb* genes in the larval brain by fluorescent in-situ hybridization. 3D imaging volumes were subsequently registered onto the ZBB atlas and compared in-silico. An attempt was also made to characterize the protein expression of ChAT, but was unsuccessful.

Whole-brain analysis of registered single gene expression patterns showed that the *chata* (n = 4) and *vachta* (n = 4) expression patterns largely overlapped across the larval zebrafish brain, mainly in the oculomotor nuclei (nIII), dorsal and ventral trigeminal nuclei (nVd/v), and in the isthmus (Ist) (Figure 2.2A-C"), while *chatb* (n = 3) and *vachtb* (n = 4) were mainly localized to the isthmus, pre-optic area and the right habenula (not shown) (Figure 2.2D-F"). *chata*/*vachta* expression was largely segregated from *chatb*/*vachtb* expression across the brain, especially in the isthmic region, where little to no overlap is observed between expression domains (Figure 2.2G-I"). Here, *chatb*/*vachtb* expressing neurons are located medial and dorsal to *chata*/*vachta* express-

ing neurons (Figure 2.2H-I"). Double FISH for *chata* and *vachtb* in the same brain shows that neurons in the isthmus largely express one or the other gene, confirming the *in-silico* results (Figure 2.3). This was further quantified by computing the voxelwise Pearson's correlation coefficient of the image intensities within the isthmic region across fish with different gene expressions (Figure 2.4). As can be observed, *chata* and *vachta* show a larger correlation with each other ($\rho = 0.14 \pm 0.03$) than with either *chatb* ($\rho = 0.03 \pm 0.04$) or *vachtb* ($\rho = 0.02 \pm 0.05$). Conversely, *chatb* and *vachtb* are also more correlated with each other than with other genes ($\rho = 0.09 \pm 0.04$). As this extends the previous accounts of the relatively similar expression patterns of genes within the Ch-A and Ch-B genetic loci to the isthmic brain region, *chata*/*vachta* and *chatb*/*vachtb* expressions will from now be referred to as cholinergic A (Ch-A) and B (Ch-B) domains, respectively. The expression of *hacta* was localized to both Ch-A and Ch-B regions while *hactb* was not expressed in the isthmic region and was not further investigated (data not shown).

These results suggest that either Ch-A, Ch-B, or both expression domains could represent the prospective larval NI. However, because in the adult brain, another cholinergic neuronal population, the Secondary Gustatory Nucleus (SGN), is located proximally to the NI (Mueller 2004), it is possible that Ch-A and Ch-B expression clusters could represent these two populations. To test this hypothesis, Calretinin (n = 6) and *reelin* (n = 4) expression was analysed. While Calretinin has been shown to be expressed in the adult zebrafish SGN, but not in the NI (Castro 2006), *reelin* expression has been characterized to colocalize in the adult (Costagli et al., 2002) and larval (Volkmann et al., 2010) NI.

Indeed, Calretinin positive neurons in the larval isthmus were found to colocalize with a small proportion of Ch-B, but not with Ch-A neurons (Figure 2.5D-D", Figure 2.4). Moreover, *reelin* expression preferentially colocalizes with Ch-A, but not Ch-B neurons (Figure 2.5E-E", Figure 2.4). These results suggest that Ch-B neurons mark a proportion of the putative larval SGN, while

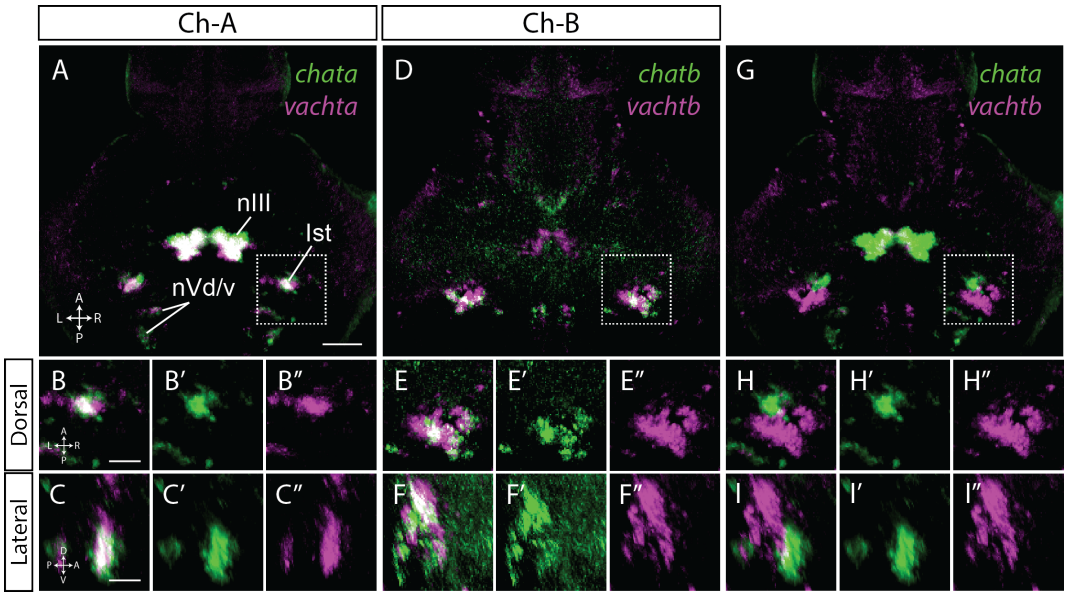

Figure 2.2: Expression of cholinergic genes in the zebrafish larval brain. (A) Expression of *chata* (green) and *vachta* (magenta) across the brain. Scale bar, 50 µm. (A'-A"') Close-up in the right isthmic region showing colocalization of both genes. Scale bar, 25 μm. (B) Expression of *chatb* and *vachtb* across the brain. (B'-B"') Close-up in the right isthmic region showing colocalization of both genes. (C) Expression of *chata* and *vachtb* across the brain. (C'-C"') Close-up in the right isthmic region that expression of both genes is largely segregated. All images represent a median volume across several fish (*chata*: n = 4; *chatb*: n = 3; *vachta*: n = 4; *vachtb*: n = 4) and are displayed as a maximum intensity z projection across a depth encompassing the entire expression of all genes in the isthmus (90 μm of total depth). nIII, Oculomotor nucleus; nVd/v, dorsal and ventral trigeminal nuclei; Ist, Isthmus.

Ch-A gene expression likely defines the majority of the larval NI. The Ch-A expression domain also appeared to be separable into an anterior (aCh-A) and posterior (pCh-A) zone by the lateral crossing of a large fascicle originating in the cerebellum, suggesting these could represent distinct subpopulations (Figure 2.5C', white arrow). This argument will be further supported in the following sections.

2.4 Excitatory nature of the larval NI

Along with their cholinergic identity, NI Ipc and SLu neuronal subpopulations in birds have been found to coexpress the vesicular glutamate transporter 2 (VGluT2) mRNA, raising the hypothesis that both ACh and Glutamate

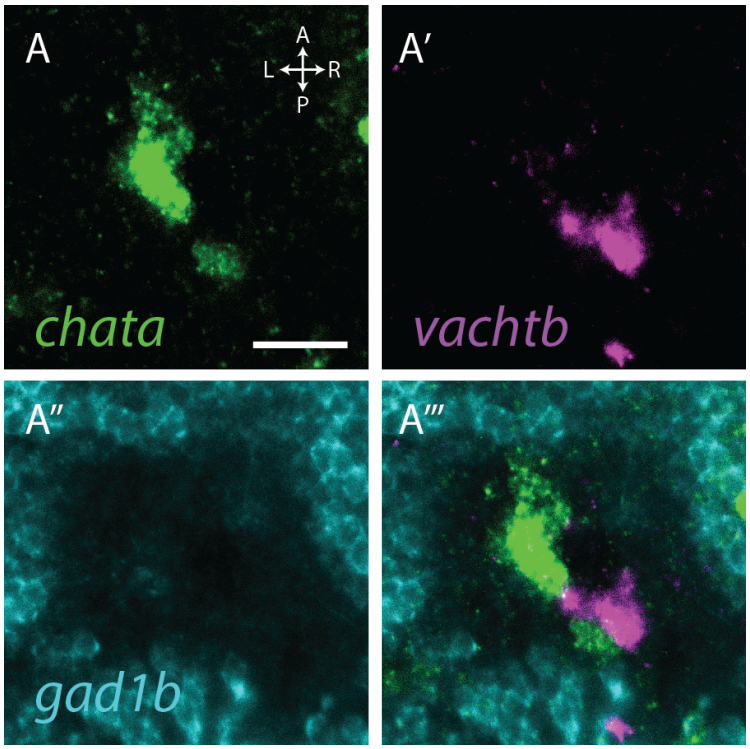

Figure 2.3: In-situ expression of cholinergic gene isoforms. (A-A"') Single confocal image of a triple fluorescent in situ of a 6 dpf larval brain coexpressing *chata*, *vachtb* and *gad1b* mRNA in the right isthmus. Scale bar, 25 μm.

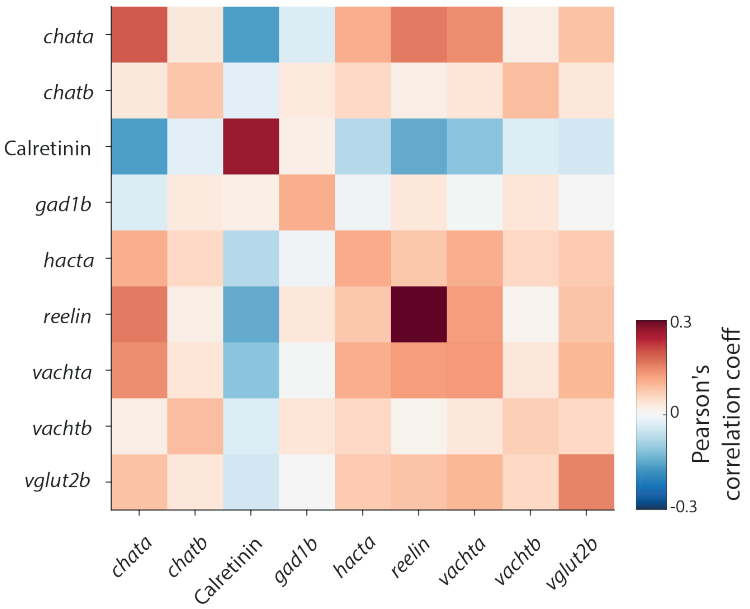

Figure 2.4: In-silico correlation analysis of gene expression. (A) Pearson's correlation coefficient across registered brains for all tested markers in the isthmic region. Values represent the mean across fish for each expression marker.

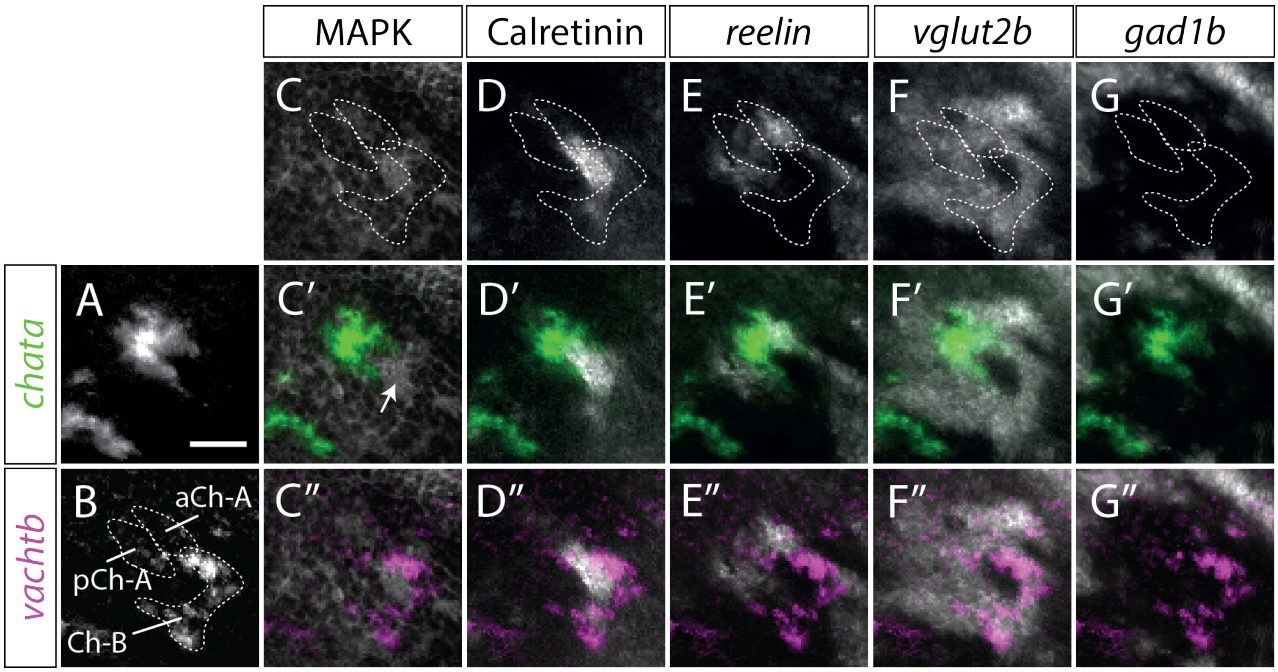

Figure 2.5: Molecular and neurotransmitter identity of the larval NI. (A-G") in-silico colocalization of various neurotransmitter and molecular marker genes in the isthmus. Dotted lines denote the boundaries of the anterior and posterior expression domains of *chata* and of *vachtb*. White arrow in C" denotes the fascicle of axons originating in the cerebellum. Scale bar, 25 μm.

might be coreleased by these neurons (González-Cabrera et al., 2015). At the same time, as was previously noted, birds and reptiles possess an inhibitory GABAergic NI subpopulation, the Imc (Domenici et al., 1988; Wang et al., 2004). Since the characterization of the neurotransmitter identity of NI neurons would have strong implications on the functional properties of the circuitry in which they're involved, the expression of *vglut2b* (n = 4) and *gad1b* (n = 4) in the isthmus was analysed (Figure 2.5F-G").

Both Ch-A and Ch-B expression domains were found to extensively colocalize with *vglut2b* expression (Figure 2.5F-F"), while no colocalization was observed with *gad1b* (5G-G"). Indeed, most neurons in the isthmic region are devoid of *gad1b* expression, suggesting that a population homologous to the Imc of birds and reptiles might not be present in zebrafish larvae. These findings support the conclusion that the larval NI might be excitatory and co-release both ACh and Glutamate to its post-synaptic partners.

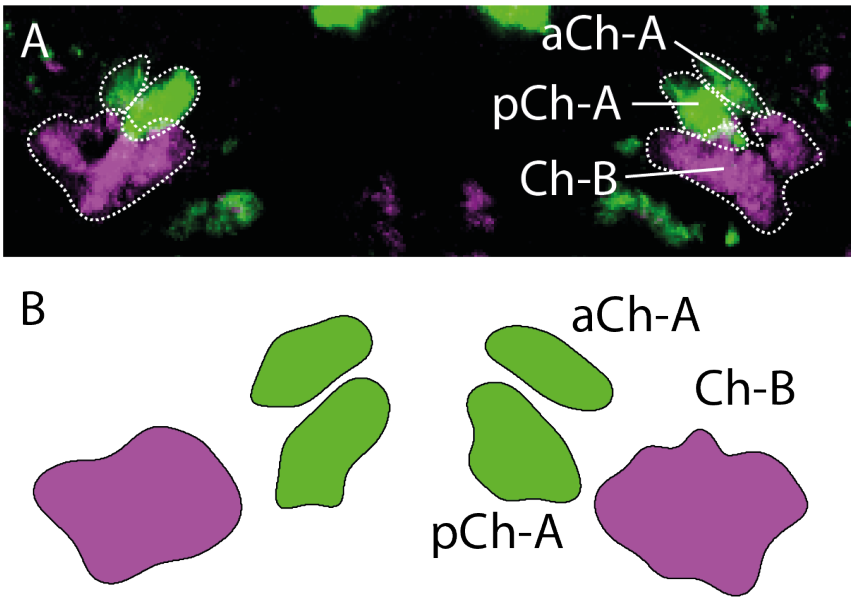

Figure 2.6: Schematic representation the larval isthmus. (A) Brain registered expression of *chata* and *vachtb* (B) Schematic representation the isthmic expression domains. Boundaries were draw by creating a binary mask of a sum z-projection of the Ch-A and Ch-B expressions in registered brains, and calculating the convex hull of the resulting mask in the isthmic area. The boundary between aCh-A and pCh-A was drawn manually based on the section where both areas appeared to be linked by the narrowest expression margin.

2.5 Discussion

Young zebrafish larvae possess a cholinergic Nucleus isthmi

A cholinergic nucleus isthmi has been characterized for a number of vertebrate species, however, no systematic effort had been done to characterize its anatomical structure and molecular identity in the early stage of development of any animal. Here, a detail characterization of the young (6 dpf) zebrafish larva's nucleus isthmi was performed in order to localize the NI in the larval brain and to investigate its neurochemical, genetic and morphological identity.

It was found that the larval NI is likely to the composed of a small population of neurons ($\approx$ 100 cells on each side) expressing Ch-A genes (*chata*/*vachta*) in the isthmic region, near the midbrain-hindbrain boundary. Several lines of

evidence lead to this conclusion. First, Ch-A positive neurons coexpress *reelin*, similarly to what has been described in the adult zebrafish NI. Second, although another cholinergic population expressing Ch-B genes is present in the isthmus, the part co-localization of Calretinin in these neurons makes it likely to correspond, at least in part, to the Secondary Gustatory Nucleus (SGN).

Another possibility is that Ch-A and some Ch-B expressing neurons could represent different subpopulations of the zebrafish NI. Indeed, in the bird NI, differential expression of cholinergic genes is found in the Ipc and SLu subnuclei: where VAChT transcripts are only observed in the SLu, ChAT transcripts are highly expressed in the somata of SLu neurons, but only moderately in the Ipc (González-Cabrera et al., 2015). CHT1, the bird homolog of the zebrafish *hact* gene, is highly expressed in both populations. In Chapter 3, further evidence will be provided that suggests that the Ch-B region is likely to contain both NI and SGN neurons. It would however be interesting to investigate the expression of Ch-A and Ch-B genes in adult brain section, allowing the comparison with the previously identified NI population in the adult brain, examine if this domain segregation is still present, and compare it to the more anatomically recognizable SGN neurons (Castro et al., 2006; Mueller et al., 2004).

What might be the functional differences between Ch-A and Ch-B expressing neurons? While in zebrafish no study has investigated the differences between Ch-A and Ch-B isoforms, different ChAT transcripts have been shown to differ in their catalytic rate, which is likely to impact ACh transmission (Bellier and Kimura, 2011). In the bird Ipc/SLu, a dual ACh release mechanism has been proposed, which would be vesicular-mediatd in SLu axons, but act in a non-quantal way in the Ipc, possibly through Ca^{2+} dependent transport by CHT1 (González-Cabrera et al., 2015). As reported here, hacta transcripts can be found across all NI neurons, including those expressing Ch-B, and all neurons express at least one isoform of the chat and *vacht* gene, making it unlikely that such a mechanism is true in the zebrafish NI. Electrophysiological

recordings of Ch-A and Ch-B expressing neurons and its downstream targets might help clarify the functional difference between these two types.

The NI of zebrafish larvae probably excitatory

Acetylcholine has been found to be co-released with both GABA and Glutamate in several different neuronal populations (Granger et al., 2016; Higley et al., 2011). In the NI, however, the only reports of a possible co-release of neurotransmitters has come from birds, which have shown that VGluT2 is also expressed in the cholinergic Ipc and SLu subpopulations (Islam and Atoji, 2008; González-Cabrera et al., 2015). In agreement with this, I have found that the larval zebrafish cholinergic NI co-expresses *vglut2b*, but not *gad1b*, suggesting that zebrafish NI neurons co-release Glutamate and ACh to their post-synaptic targets.

A clearly defined GABAergic population of neurons in the isthmus, similar to the bird/reptile Imc, was not observed in the larval brain, suggesting that a Imc homolog might not exist in zebrafish. Indeed, to date, the only report of a GABAergic population of neurons in the NI in a non-reptilian specie was shown in the frog (Li and Fite, 2001), thought more studies are likely to be required to confirm this observation. Thus, although it is still possible that a similar subpopulation is found in zebrafish or other teleost species, it seems more plausible that it might represent a reptilian specialization.

Chapter 3

Nucleus isthmi efferent circuitry

The most conserved efferent target of the NI is the ipsilateral OT, in which the connections has been established for all vertebrate species studied so far (Gruberg et al., 2006). Thus, if cholinergic neurons in the zebrafish larval isthmus project to the OT, this would provide strong evidence that they belong to the NI. NI neurons also project to pretectal nuclei in adult zebrafish (Yáñez et al., 2018), but it is still unknown if these belong to a different type than those projecting to the OT, or if the same neuron projects to both structures. Revealing the projection morphologies of NI neurons in larval zebrafish, especially considering the large amount of functional and behavioural studies of tectal and pretectal areas at this age (Orger, 2016), might inform hypothesis of NI function in larval zebrafish.

In Chapter 2, we observed that the larva isthmus has two different cholinergic expression domains, Ch-A and Ch-B. We also observed that Ch-A might be further subdivided into an anterior (aCh-A) and posterior (pCh-A) region. Do neurons in these different areas have different projection patterns? For example, one expectation is that neurons in the Ch-B domain belonging to the SGN would project to the lateral hypothalamus. There is also evidence for a segregation of ipsilateral and contralateral isthmotectal projections in the NI of frogs (Dudkin et al., 2007) and pleiotropic salamanders (Wiggers, 1998), while bilateral projections in teleost have been recently hinted to exist too (Johnson et al., 2013). To investigate these issues, focal electroporation of a

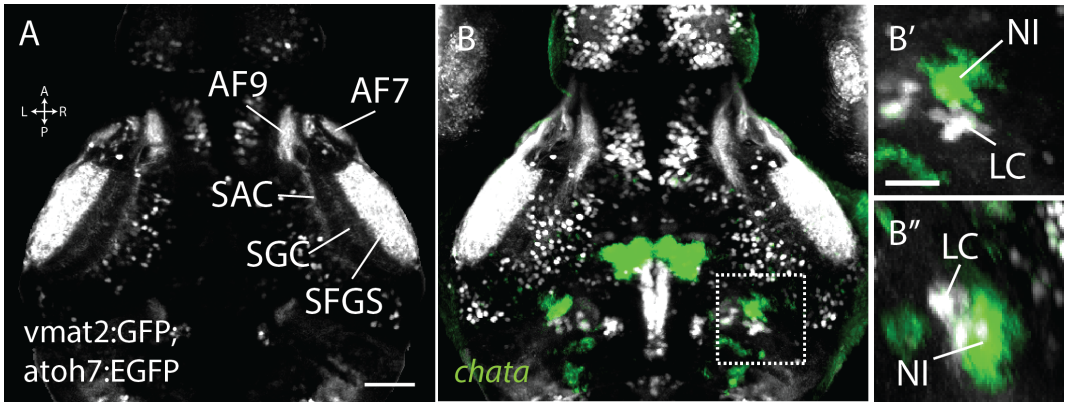

Figure 3.1: Transgenic labelling of RGCs and Locus coeruleus neurons in Tg(vmat2:GFP; atoh7:EGFP) fish. (A) Section through the brain of a registered fish showing GFP expression in several retinocipient layers of the OT neuropil and arborizations fields (AFs). (B) Same brain as in A overlaid with a median imaged of the registered chata expression. Image is a maximum projection through the slices containing chata expression in the isthmus. (B') Dorsal zoomed in region in the right isthmus showing Locus coeruleus (LC) neurons adjacent to the chata expression in the larval NI. Scale bar, 25 μm. (B") Sagittal projection through the isthmus.

fluorescently labelled dextran conjugate was used to visualize the morphology of single NI axonal projections.

Single neurons in the isthmic region of 4 dpf larvae transgenic for Tg[vmat2:GFP] and Tg[atoh7:EGFP] were electroporated and labelled cells were imaged at 6 dpf (Figure 3.1). vmat2 expression in the Locus coeruleus (LC), which is in close proximity with the NI (Costagli et al., 2002), helped to target NI neurons for electroporation (Figure 3.1B). At the same time, atoh7 expression in RGCs, which labels the retinorecipient neuropil layers of the OT, allowed the precise localization of NI axonal processes in these layers (Figure 3.1A). The transgenic expression patterns of these genes were further used to register all brains to the ZBB atlas, allowing the localization of labelled cell bodies with respect to the isthmic Ch-A and Ch-B expression domains, as well as comparative analysis of the labelled processes. Using this technique, several isthmic neuronal projection morphologies were observed.

3.1 NI Type I neurons

3.1.1 Morphology

The first class of labelled neurons, here classified as NI Type I neurons, sent an axonal projection that moved anteriorly from the location of the soma towards the pretectum, possibly through the isthmo-pretectal tract (Figure 3.2, Yáñez et al. (2018). At the pretectum, an axon collateral extends towards the AF7 pretectal neuropil and densely wraps around it (Figure 3.2A'). Although this innervation covers a large proportion of the AF7 neuropil, it does not cover it entirely, rather seemingly to localize to a particular area. From here, an axonal collateral ascends dorsally and posteriorly towards the anterior portion of the OT, where multiple fibres branch off and terminate (Figure 3.2A"). Indeed, this anterior localization of OT arbours was consistent across fish, covering the first half of the OT neuropil (0.07 ± 0.06 to 0.48 ± 0.09 of the OT neuropil A-P bounds; means ± s.d.), and but varying in depth (0.29 ± 0.15 to 0.70 ± 0.14 of the OT neuropil D-V bounds; means ± s.d.) (Figure 3.3A-D').

It was not easy to establish whether this OT projection branches off before or after the axon enters the AF7. In one case, a collateral process clearly branches of towards the OT before the AF7 innervation, while in two other cases this seems to stem from the dense AF7 arbors. A larger number of example morphologies and with higher resolution might help resolve this issue.

The dendrite of NI type I neurons always protrudes from the soma posterior and laterally, and its processes are small and dense, terminating in a neuropil region in the lateral hindbrain (Figure 3.2A"'). A total of 6 neurons were labelled with this type of morphology, but only 4 fish had single labelled neurons with high intense labelling to allow them to be traced (Figure 3.3).

Registration to the reference atlas further revealed that all labelled somata were located within the Ch-A expression domain of the Isthmus, and that were evenly distributed between the anterior and posterior NI (aCh-A and pCh-A: 50%; n = 4; Figure 3.12).

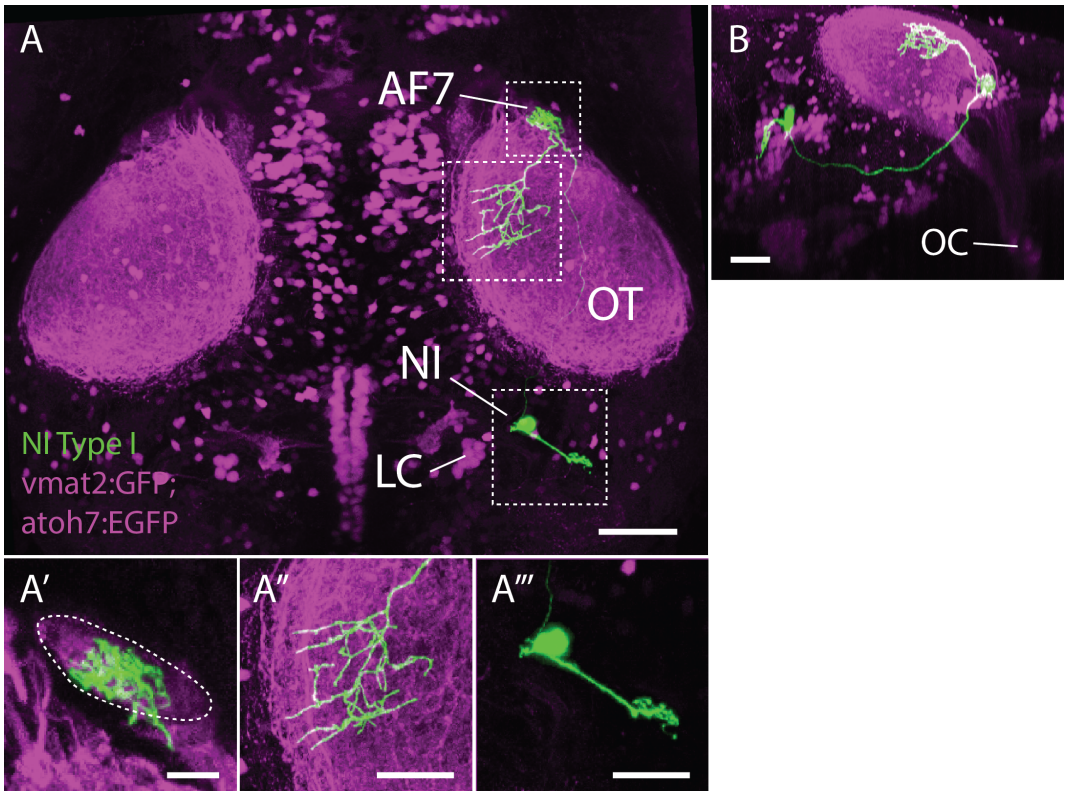

Figure 3.2: NI Type I projection morphology. (A) Dorsal view of an example unregistered larval brain where one NI Type I neuron was labelled with a fluorescent dextran using single cell electroporation. Image is a maximum projection through all imaging slices (264 μm). Scalebar, 50 μm. (A') Zoom in of the AF7 innervation. Scalebar, 10 μm. (A") Zoom in of the arbours innervating the anterior OT. Scale bar, 25 μm (A"') Zoom in of the soma and dendritic process. Scale bar, 25 μm. (B) Sagittal projection through the brain showing the specific anterior-dorsal innervation of the OT. Scale bar, 50 μm. OC, Optic Chiasm. LC, Locus Coeruleus.

3.1.2 OT layer innervation

To precisely localize the axon terminal arbors of these neurons within the OT neuropil, a rotated projection of the OT was used to better visualize its retinocipient layers (Figure 3.3A"'-D"'). This revealed that the axonal arbours of NI type I neurons were primarily localised to the most superficial laminae in the SO and SFGS layers, which was consistent across all labelled neurons. A clear inspection of these projections shows that, although some processes pass through the SO layer, some them run in between the SO and SFGS layers, with branches stemming from these and crossing transversally through the

SFGS in a columnar fashion (Figure 3.3C"', white arrowheads). This suggests that these arbors might not synapse with processes in the SO layer, but rather with either only at the SFGS layers or also with non-retinal processes at the SO-SFGS boundary.

These results show, for the first time, that a single NI neuron projects to both the pretectum and tectum and reveals a dedicated patterning of these projections towards the anterior portion of the OT neuropil, which is known to represent the anterior visual field (Niell and Smith, 2005).

3.1.3 AF7 retrograde labelling with lipophilic tracer dyes

Because the number of electroporated NI Type I neurons was small, it remained unclear to what extent is the larval NI composed of this type of neurons. This also made it difficult to confidently determine if they these neurons are equally spread between the aCh-A and pCh-A domain, as the location of electroporated soma suggests, or if there might be a preferential localization one of the cholinergic sub-domains characterized in Chapter 2.

To investigate this, a retrograde lipophilic dye (DiI) was locally applied to the AF7 of fixed transgenic 6 dpf larval brains expressing nuclear localized GCaMP6s (Tg[elavl3:GCaMP6s-H2B]) using iontophoresis. The dye was then left to diffuse through the cell membranes for 1 week before the whole brain of labelled fish were imaged and retrogradely labelled somata were manually marked in the isthmic region (Figure 3.4). Because of the small size of the AF7 neuropil, the majority, if not the entire arborization was likely labelled by the dye application, thus potentially back-labelling the large majority of its afferent projections.

Retrogradely labelled cell bodies could be found throughout the ipsilateral tectal PVN cell body layer, especially in the most anterior portion, and in the thalamus (data not shown). Very few, if any cell bodies were ever found on the side contralateral to the application. As expected, a prominent cluster of retrogradely labelled cell bodies was found in the ipsilateral isthmus (Figure 3.4C).

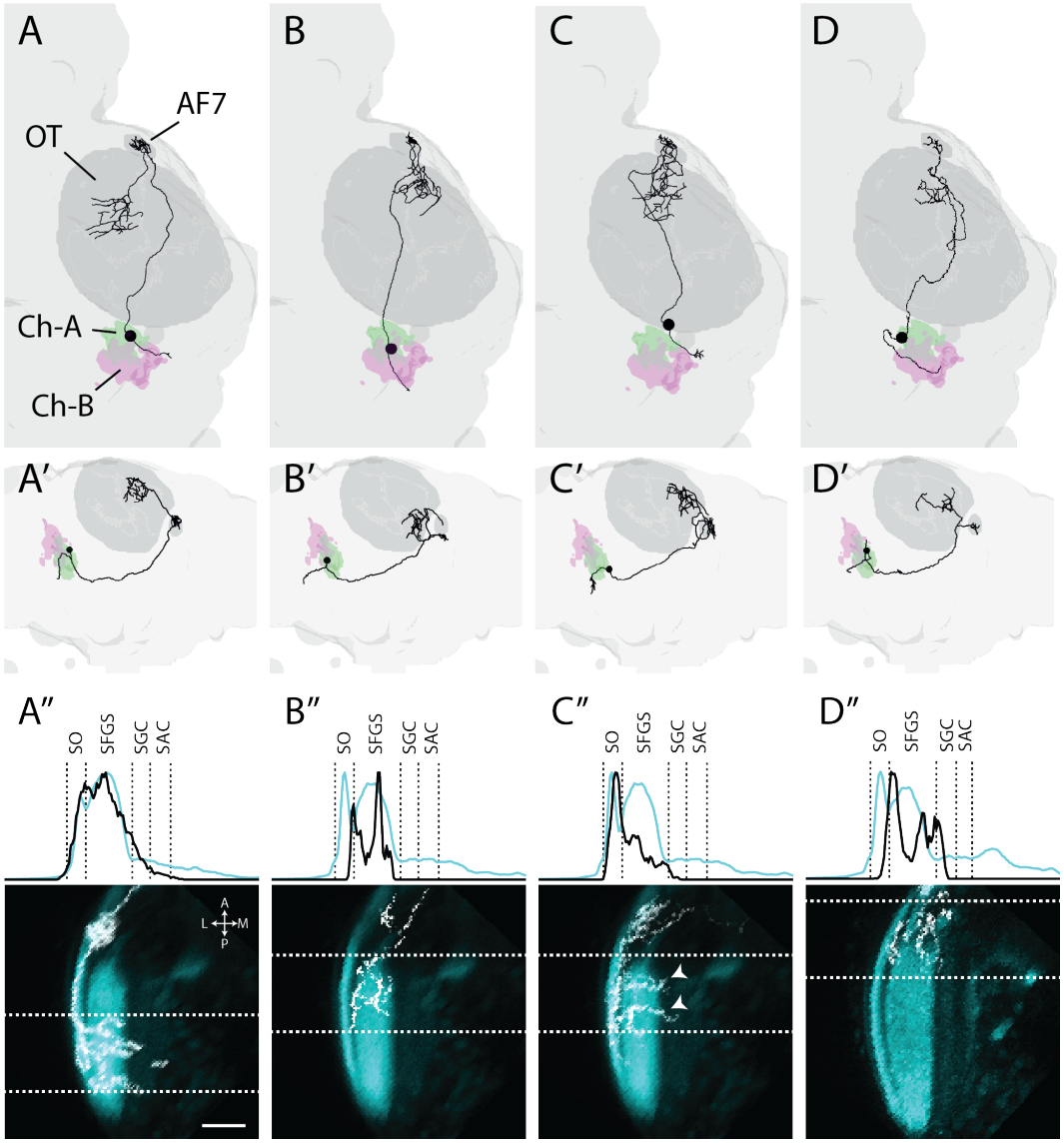

Figure 3.3: NI Type I innervation through the Optic Tectum layers. (A-D) Registered tracing dorsal projections from multiple labelled NI Type I neurons. Tracings are plotted overlaid with surface renderings of relevant atlas's masks. (A'- D') Sagittal projections of upper panels. (A"-D") NI Type I arbours (gray) in the OT neuropil layers (cyan). To produce these images, the atoh7:GFP 3D imaging volume that was used as a template for registration was rotated rightwards in the A-P axis around 30 deg and then leftwards in the L-R axis by around 40 deg. This has the effect of aligning the layers in the D-V axis. A mean projection across the OT neuropil was then taken over a volume that encapsulates most of the projection arbours for each type (60 μm depth). Dotted while lines delineate the area used to compute the arbour density profiles on top (normalized to maximum). Dotted black lines mark the separation of the different retinocipient OT neuropil layers. White arrowheads in C" point to the columnar processes running transversally through the SFGS layer. Scale bar, 25 μm.

A set of fibres are seen stemming from isthmic cell bodies laterally (Figure 3.4C'). This area was the same region where the dendrites of electroporated NI Type I neurons were seen extending towards, indicating that it is likely composed of the dendrites of labelled cell bodies in the isthmus. Indeed, this organization is reminiscent of the cell body "shell" and neuropil "core" seen in the NI of adult teleosts (Ito et al., 1982), suggesting that this organization is already apparent in the young larval stage of zebrafish.

To localize the labelled cell bodies to the cholinergic isthmic domains, the imaged larval brains were registered onto the atlas and the coordinates of marked cells transformed to its reference frame. Interestingly, labelled cells were almost exclusively and consistently found in the ipsilateral aCh-A domain, with very few cells located in the pCh-A and Ch-B regions (Figure 3.4D-F). This strongly indicates that NI type I neurons are distinctly segregated in the aCh-A and suggests that aCh-A and pCh-A might represent distinct subpopulations with different connectivity profiles.

3.2 NI Type II neurons

3.2.1 Morphology

The second class of neurons labelled in the larval isthmus, here classified as NI Type II neurons, innervate the OT bilaterally (Figure 3.5). These processes were clearly distinct from the previous Type I morphology. From the soma, the axon extends anteriorly towards the ipsilateral tectum, following a path that was located more medially than that of Type I neurons. At the anterior edge of the tectum, an axonal collateral moves laterally, running through the same path as a set of retino-tectal fascicles that seems to innervate the deeper layers of the OT. This axon collateral then branches off to extensively innervate the ipsilateral tectal neuropil across a large portion of its A-P axis (Figure 3.5A; 0.15 ± 0.09 to 0.66 ± 0.11 of the OT neuropil A-P bounds; means $\pm$ s.d.). The main axon dives ventrally and crosses to the contralateral side through the post-optic-commissure (poc) (Figure 3.5A'). It then extends dorsally and

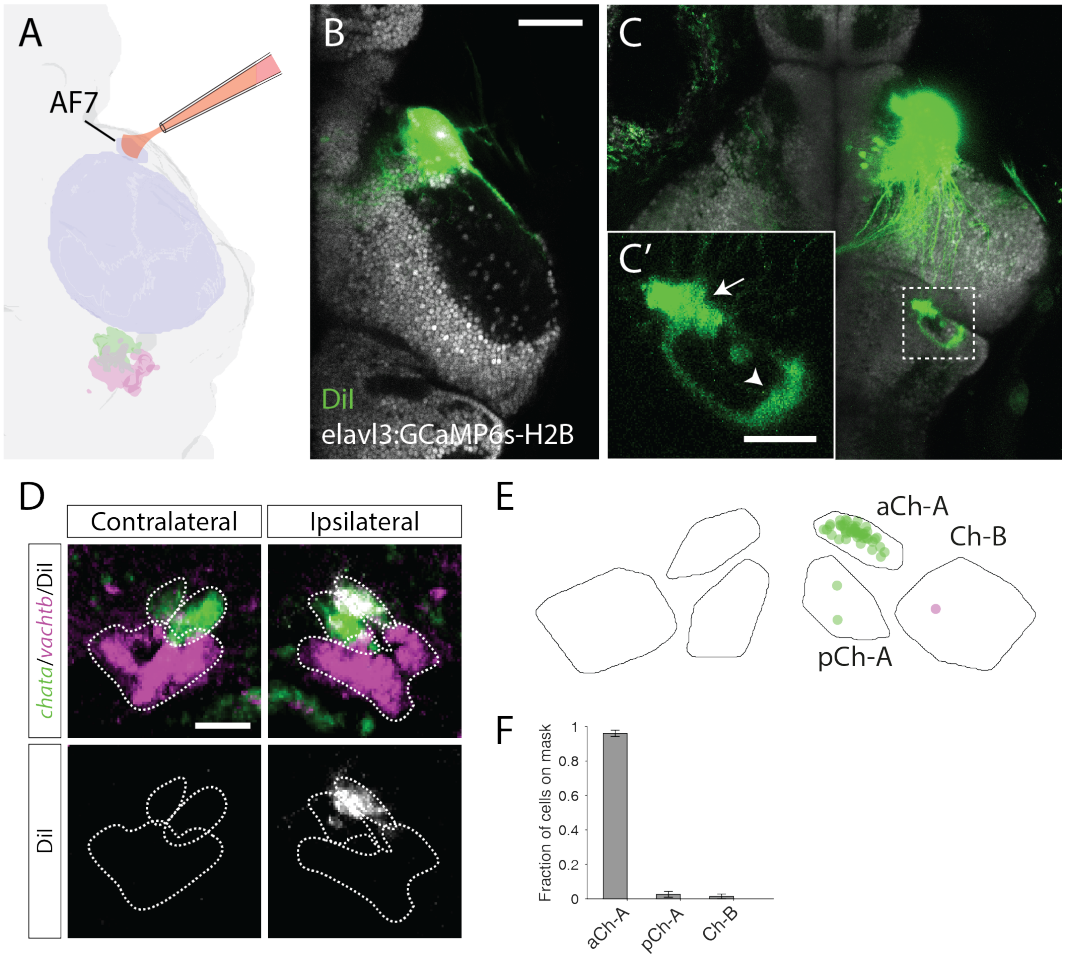

Figure 3.4: Retrograde labelling of NI neurons from AF7 DiI application. (A) Schematic representation of the local application of DiI into the AF7 thorough iontophoresis. (B) Example application showing the localized fluorescence originating from AF7 in elavl3:GCaMP6s-H2B. Scale bar, 50 μm. (C) Same fish as in B showing retrogradely labelled cells at the level of the larval isthmus. (C') Zoom in in the isthmic region. White arrow, labelled perikarya. White arrowhead, labelled neuropil fibres stemming from the isthmic labelled perikarya. Scale bar, 25 μm. (D) Isthmus of the same brain as in B and C registered onto the atlas and overlaid with *chata* and *vachtb* expression patterns, showing the specific colocalization of retrogradely labelled perikarya to the anterior *chata* expression domain. Scale bar, 25 μm. (E) Scatter plot of the registered location of all labelled perikarya (n = 90) in the isthmus from multiple experiments (n = 6). For illustration purposes, the distances between isthmic domains have been changed and do not correspond to the correct distances, but distances within each domain are correct. (F) Mean fraction of cells that fell into the 3 cholinergic domains. Error bars show standard error of the mean (SEM).

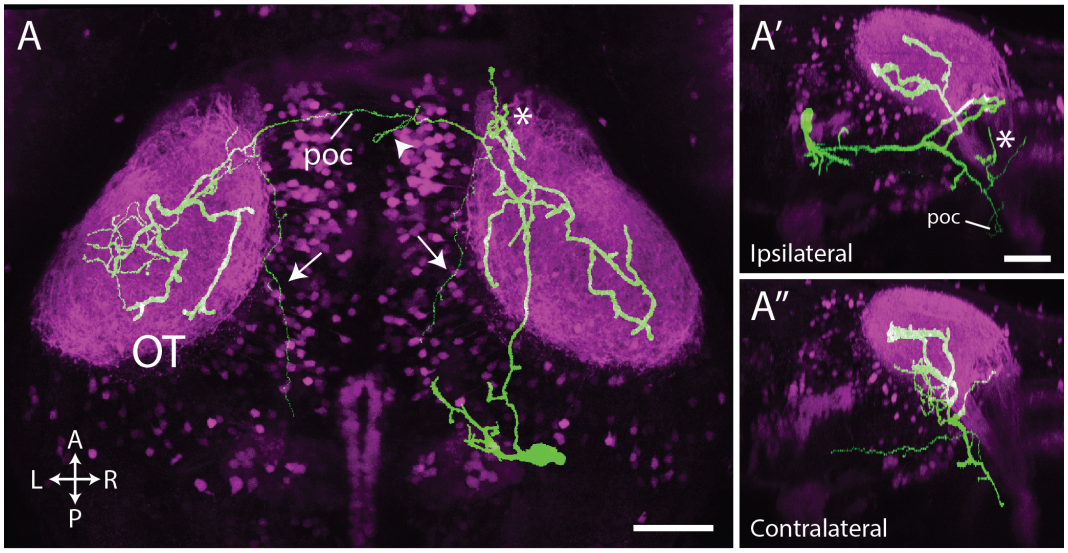

Figure 3.5: NI Type II projection morphology. (A) Dorsal view of an example unregistered larval brain where one NI Type II neurons was labelled with a fluorescent dextran using single cell electroporation. Image is a maximum projection through all imaging slices (292 μm). Scalebar, 50 μm. White arrows, collaterals directed towards the tegmentum. White arrowhead, branching process in the post-optic-commissure (poc) crossing. White asterisk represents branches that spur before the poc crossing. (A') Sagittal projection through the ipsilateral side of the cell body. Scale bar, 50 μm. (A") Sagittal projection through the contralateral side.

innervates the contralateral tectal neuropil, extending through its A-P axis in a similar fashion to the ipsilateral side (0.15 ± 0.07 to 0.67 ± 0.13 of the OT neuropil A-P bounds; means $\pm$ s.d.). The dendritic processes of these neurons were very stereotyped, extending several branches towards the anterior, ventral and medial position of the cell body towards a highly dense neuropil region in the midbrain tegmentum (data not shown)

A total of 17 neurons were labelled with this type of morphology, of which 10 were traceable. Unlike NI Type I neurons, however, the morphology of NI Type II neurons showed more variability in terms of their innervation pattern. For example, some small branches were sometimes observed to terminate near other retinal arborization fields on both sides of the brain but did not seem to innervate them (Figure 3.5A, white asterisk). Similarly, one or two branches are also sometimes seen stemming from the main axon at the poc (Figure 3.5A,

white arrowhead). Two labelled neurons were also seen sending deep collateral projections on both sides, on one case towards the midbrain tegmentum (Figure 3.5A, white arrows) and on the other towards the hindbrain (data not shown). Furthermore, the contralateral OT projection appeared sometimes to be formed of very few, or even a single axonal branch, in one case resembling a growth cone (Figure 3.6C and data not shown). These observations suggest that these neurons might not have yet achieved their final innervation pattern. Despite this, the clear bilateral OT innervation, contralateral crossing through the poc and stereotypic dendritic processes are good indications for them to belong to the same class.

Registration of labelled brains revealed that Type II labelled soma populated the aCh-A, pCh-A and Ch-B regions with similar proportions (aCh-A: 42%, pCh-A: 29%, Ch-B: 29%; Figure 3.12), indicating that this population of neurons are more evenly distributed in the larval isthmus, and suggesting that some portions of the Ch-B domain contain NI neurons.

3.2.2 OT layer innervation

As with Type I neurons, the laminar innervation of NI Type II processes in the OT neuropil was inspected. The previously mentioned innervation variability of these neurons was also translated into which OT layers they innervated. However, the majority of projections innervated the deeper laminae of the OT, such as the deep SFGS layers, SGC and SAC (Figure 3.6). Moreover, the location of the maximum arbour density was found to be mildly correlated between the ipsilateral and contralateral sides (Figure 3.7), suggesting that despite the variability in the innervation of OT layers across fish, arbours on the left and right side might modulate similar neuronal populations by innervating the same OT layers.

3.2.3 OT retrograde labelling with lipophilic tracer dyes

To get a better insight on the distribution of NI Type II neurons across the isthmic cholinergic domains, DiI was locally applied to one side of the OT

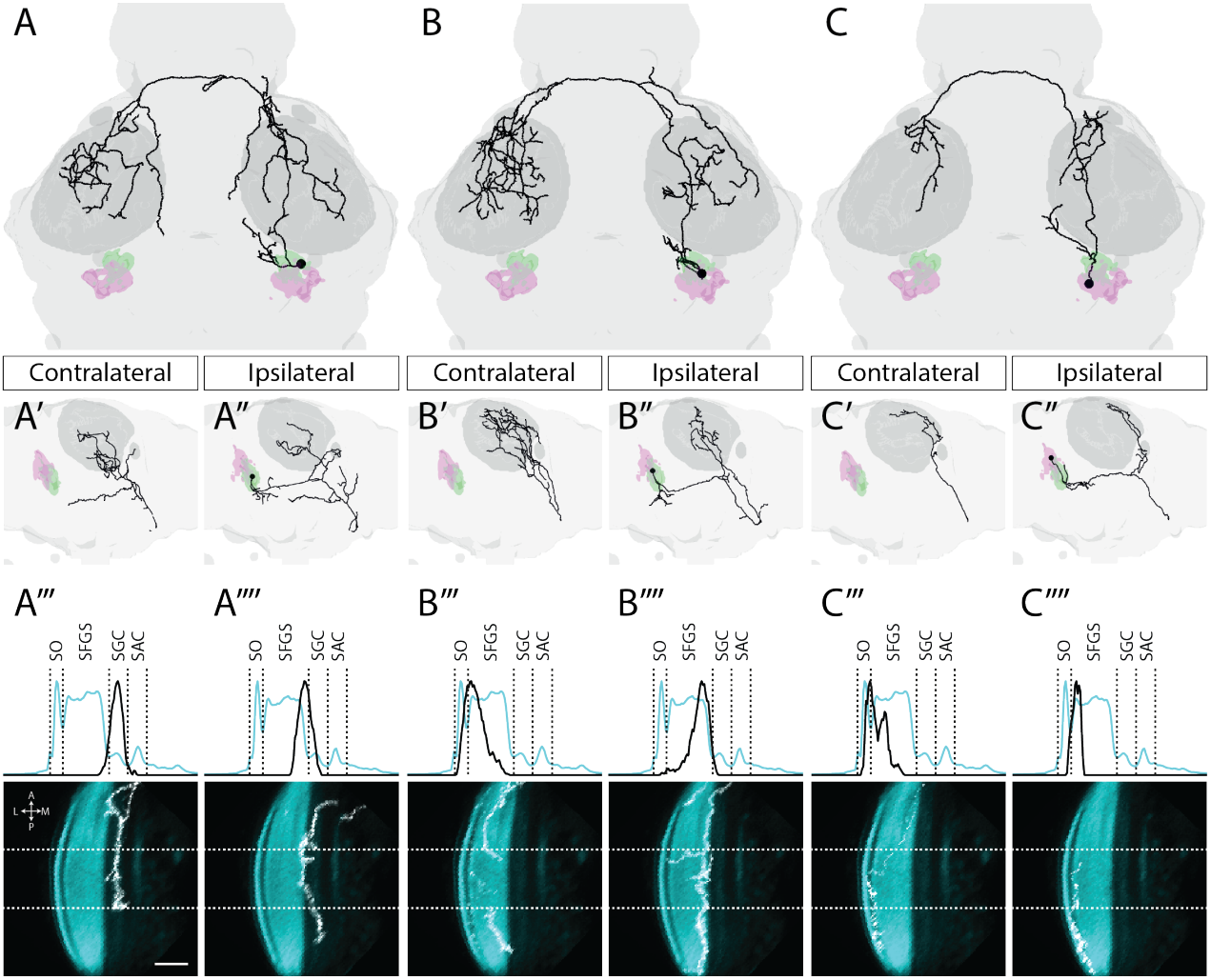

Figure 3.6: NI Type II innervation through the Optic Tectum layers. (A-D) Registered tracing dorsal projections from 3 examples of labelled NI Type II neurons. Tracings are plotted overlaid with surface renderings of relevant atlas' masks. (A'- C") Lateral projections of upper panels for both ipsilateral and contralateral sides of the brain. (A"'-C"") NI Type II arbours (gray) in the OT neuropil layers (cyan). Images were produced as in Figure 3.3. Dotted while lines delineate the area used to compute the arbour density profiles on top (normalized to maximum). Dotted black lines mark the separation of the different retinocipient OT neuropil layers. Scale bar, 25 μm.

neuropil. This experiment will inevitably label Type II arbours on the ipsilateral side, and thus retrogradely labelled cells in the ipsilateral isthmus will represent a mixture of Type I and Type II cells. However, due to the bilateral innervation of Type II neurons, labelled perikarya on the side contralateral to the dye application should only represent Type II neurons.

In agreement with this a large proportion of cells were retrogradely labelled in the aCh-A domain ipsilateral to the dye application (Figure 3.8C,D-F). On the contralateral side, however, few cells are seen in the aCh-A domain, but rather evenly distributed on both pCh-A and Ch-B domains (Figure 3.8D-F). These results indicate that, as opposed to NI Type I neurons, Type II neurons more densely populate pCh-A and Ch-B expression domains, suggesting that a part of the zebrafish NI expresses Ch-B genes.

3.3 NI-OT topographical space map

The topographical mapping of NI-OT reciprocal projections is a hallmark of their connectivity, having been observed on all species where it's been carefully analysed. To assess if this mapping was also present in zebrafish larvae, the registered centroid positions of NI Type I and II cell bodies were compared to the centroid location computed from all points belonging to the segments of the traced axonal branches that terminated within the OT neuropil, for both NI Type I and Type II neurons, and also in the AF7, in the case of NI Type I neurons (Figure 3.9).

3.3.1 NI Type I neurons

Despite the small number of examples, a prominent anticorrelation exists between the soma dorsal-ventral position and the OT arbours anterior-posterior location, such that the ventral NI projects to more anterior location in the OT neuropil (Figure 3.9B). A positive correlation also exists between the anterior-posterior location of the AF7 arbours and both the anterior-posterior and lateral-medial position of the soma (Figure 3.9C). In terms of the relation between the OT and AF7 arbours, a prominent negative correlation exists be-

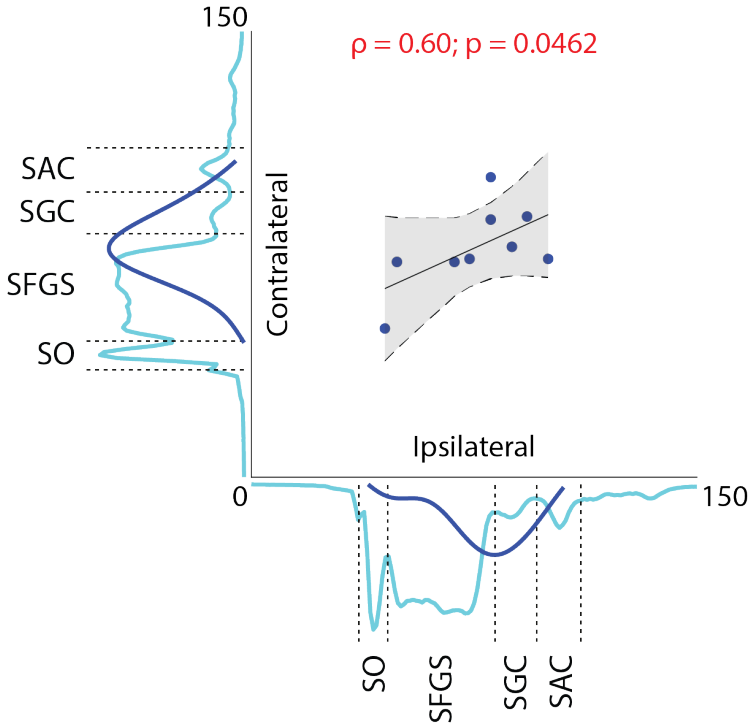

Figure 3.7: Ipsilateral and contralateral correlation of NI Type II OT layer innervation. Correlation between the ipsilateral and contralateral location of the peak arbour density through the OT laminae, as per the profiles on Figure 3.6. Solid blue lines represent the distribution of peaks for each side. Solid cyan lines represent the mean intensity profile of the RGC terminals in the OT, which reveal the different laminae, showed bounded by the dotted black lines. Solid black line through the data points shows the linear fit to the data and shaded gray region denotes the 95% confidence bounds of the fitted line. Units are in microns.

tween the OT lateral-medial axis and AF7's dorsal-ventral axis, as well as a positive correlation between both OT and AF7's dorsal-ventral axis (Figure 3.9D).

These results suggest that NI Type I neurons are topographically mapped with both the OT and AF7's space map, although it is not entirely clear the relationship between the OT and the AF7 maps: while for the OT it is the NI's dorsal-ventral position that appears to show topography, for AF7 it is most predominantly the NI's anterior-posterior axis. More examples might help clarify this issue.

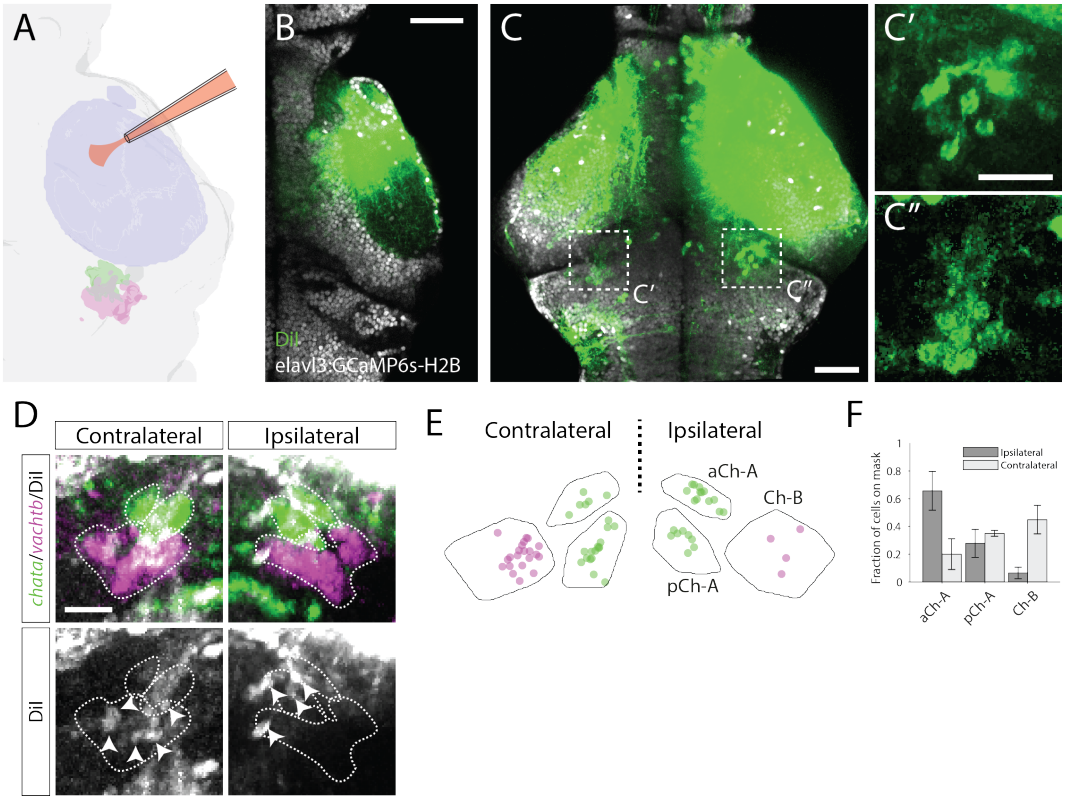

Figure 3.8: Retrograde labelling of NI neurons from OT DiI application. (A) Schematic representation of the local application of DiI into the OT neuropil thorough iontophoresis. (B) Example application showing the localized labelling of the anterior portion of the right OT neuropil in elavl3:GCaMP6s-H2B. Scale bar, 50 μm. (C) Same fish as in B showing retrogradely labelled cells at the level of the larval isthmus on both ipsilateral and contralateral sides of the brain. Scale bar, 50 μm. (C') Zoom in in the isthmic region contralateral (left) to the dye application showing labelled perikarya. Scale bar, 25 μm. (C") Zoom in in the isthmic region ipsilateral (right) to the dye application. (D) Isthmus of the same brain as in B and C registered onto the atlas and overlaid with chata and vachtb expression patterns, showing labelled perikarya in all cholinergic domains (white arrowheads). Cells might appear slightly distorted due to the registration procedure. Scale bar, 25 μm. (E) Scatter plot of the registered location of all labelled perikarya (ipsi: n = 67; contra: n = 67) in the isthmus from multiple experiments (n = 11). For illustration purposes, the distances between isthmic domains have been changed and do not correspond to the correct distances, but distances within each domain are correct. (F) Mean fraction of cells that fell into the 3 cholinergic domains. Error bars show standard error of the mean (SEM).

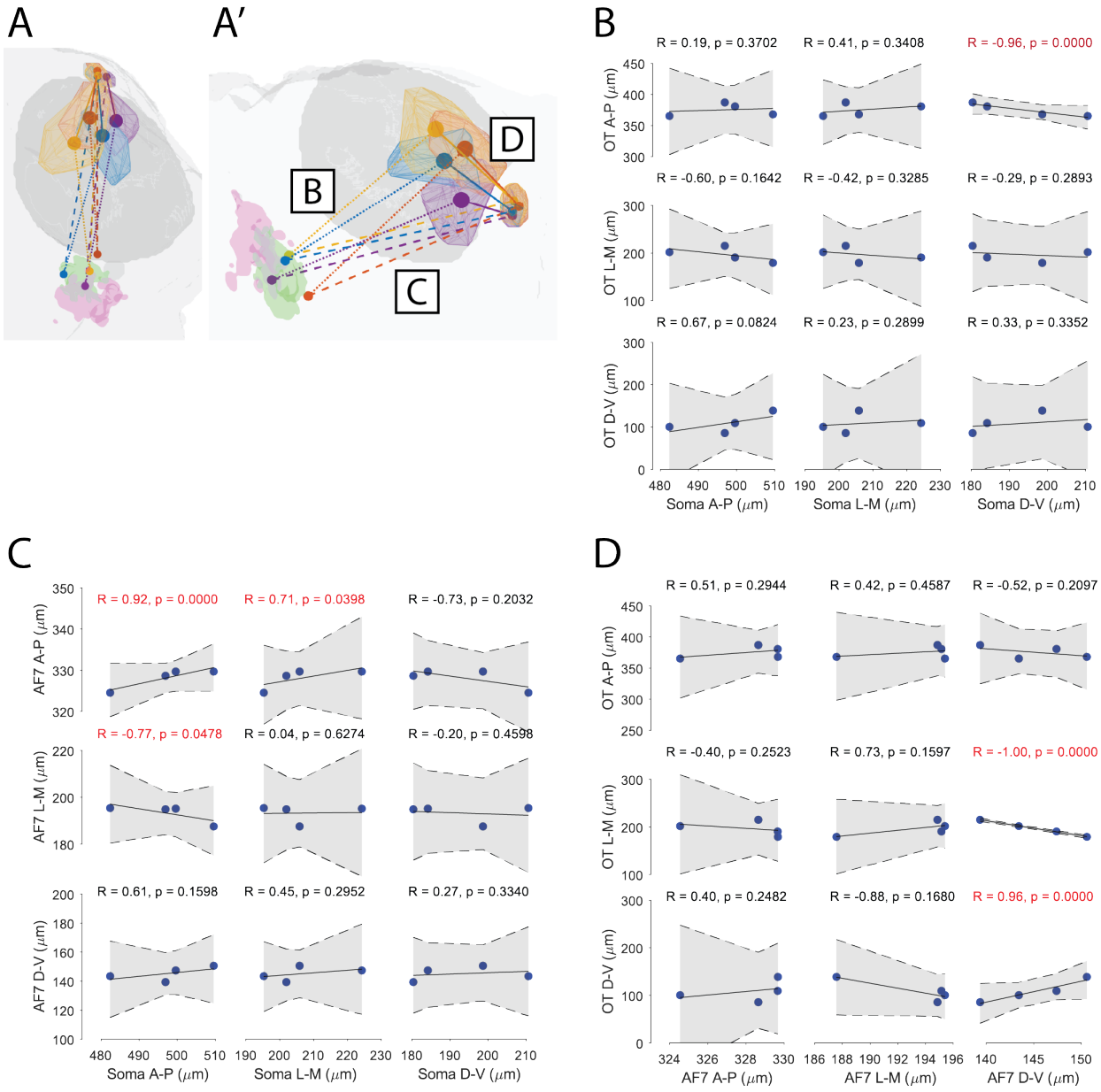

Figure 3.9: Topographical organization of NI Type I neurons. (A) Dorsal brain rendering showing the correlated positions in B-D. Each colour represents an individual traced NI type I neuron. Smaller dots represent the registered location of the cell body in the isthmus. Larger dots represent the computed centroid position of the ipsilateral OT and AF7 arbours. Overlaid in the schematic are shown Delaunay triangulations of the traced arbor segments that fell within the OT neuropil for each fish. (A') Sagittal projection of A. (B) Correlations between all 3 axis of the cell body location and the corresponding OT arbour centroids. (C) Correlations between the cell body location and the corresponding AF7 arbour centroids. (D) Correlations between the AF7 and OT arbour centroids. For all plots, values denote positions in the reference ZBB atlas. Solid black line through the data points shows the linear fit to the data and shaded gray region denotes the 95% confidence bounds of the fitted line. R indicates Pearson's correlation coefficient and p the bootstrapped p-value of the correlation (See methods).

3.3.2 NI Type II neurons

The ipsilateral OT projection of NI Type II neurons shows prominent evidences of topography throughout the OT map. In summary, as the soma location moves towards the NI's posterior, ventral and medial positions, their arbours innervate the ipsilateral tectum at more anterior, ventral and medial locations (Figure 3.10B). On the contralateral size, however, the highest correlation is between the soma's dorsal-ventral position and the arbours lateral-medial position, though this is not particularly strong (Figure 3.10C). It is possible that this apparent lack of a strong contralateral topography is a consequence of these arbours still being in "development". It would be interesting to analyse the morphology of these cells at later stages of development to clarify this issue.

The dorsal-ventral position of the ipsilateral arbours also seems to be positively and negatively correlated with the contralateral dorsal-ventral and lateral-medial axis, respectively (Figure 3.10D). This is likely to be related to the laminae positions which these arbours innervate on both sides, as was observed previously (Figure 3.7), which are highly correlated to the dorsal-ventral and medial-lateral axis due to the OT's "cup-like" structure.

In summary, these results indicate that NI Type II neurons are topographically mapped to the ipsilateral tectal space map, and to a lesser extent to the contralateral one, giving further support that these neurons belong to the larval NI.

3.4 Hypothalamic projections

Electroporation isthmic neurons also labelled another class of projection morphology. From the soma of these neurons, a process is seen descending and then branching in two. One of these processes moves posteriorly and arborizes soon after into several ramifications, likely representing the dendritic tree. The other moves anteriorly and then sharply descends to profusely innervate the ipsilateral lateral hypothalamus (Figure 3.11A'), which can be observed by

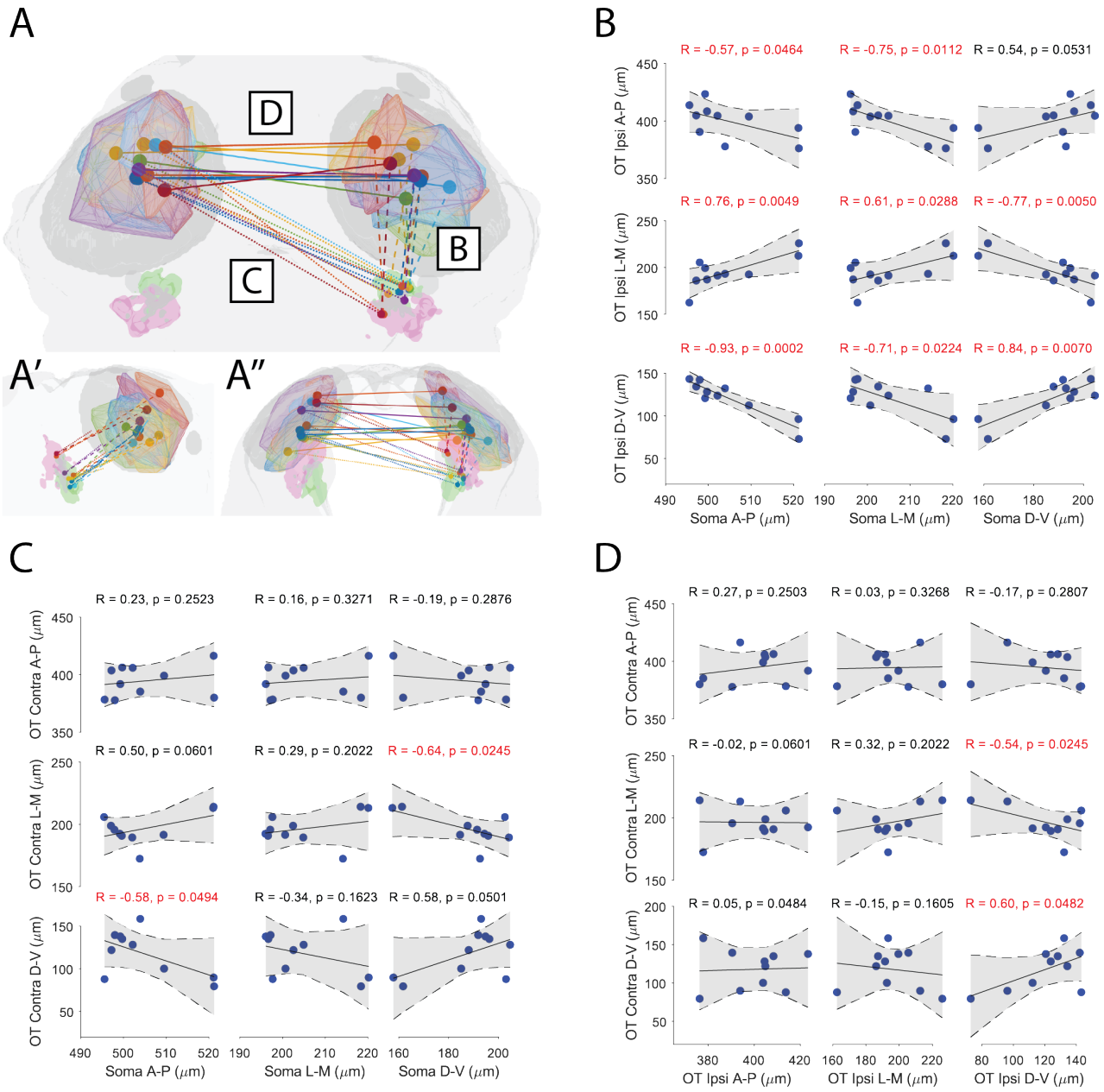

Figure 3.10: Topographical organization of NI Type II neurons. (A) Dorsal brain rendering showing the correlated positions in B-D. Each colour represents an individual traced NI type II neuron. Smaller dots represent the registered location of the cell body in the isthmus. Larger dots represent the computed centroid position of the ipsilateral and contralateral OT arbours. Overlaid in the schematic are shown Delaunay triangulations of the traced arbor segments that fell within the OT neuropil for each fish. (A') Sagittal projection of A. (A") Transverse projection of A. (B) Correlations between all 3 axes of the cell body location and the corresponding ipsilateral OT arbour centroids. (C) Correlations between the cell body location and the corresponding contralateral OT arbour centroids. (D) Correlations between the ipsilateral and contralateral OT arbour centroids. For all plots, values denote positions in the reference ZBB atlas. Solid black line through the data points shows the linear fit to the data and shaded gray region denotes the 95% confidence bounds of the fitted line. R indicates Pearson's correlation coefficient and p the bootstrapped p-value of the correlation (See methods).

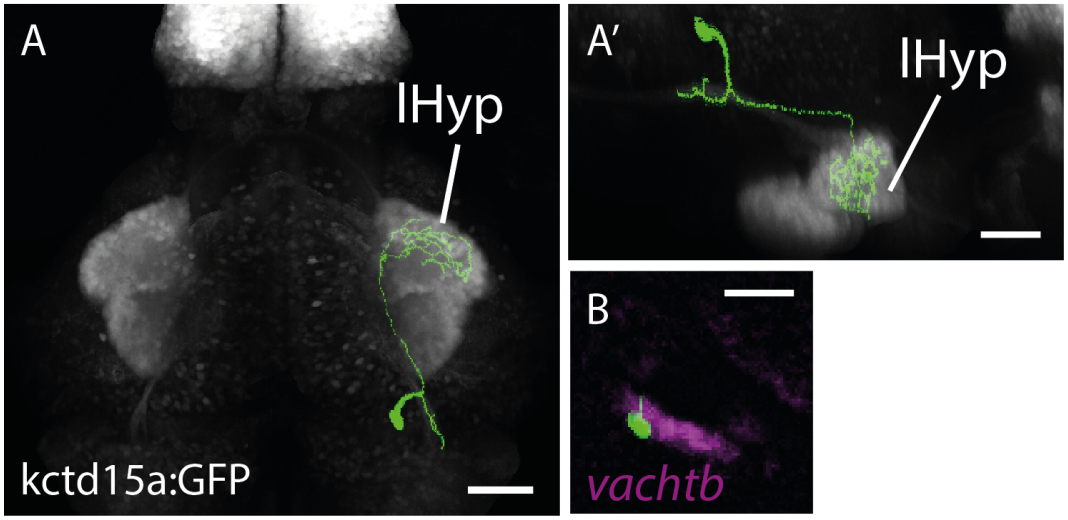

Figure 3.11: Hypothalamic projecting neurons in the larval isthmus. (A) Dorsal maximum projection of a registered electroporated neuron in the isthmus projecting to the lateral hypothalamus, evidenced by the transgenic expression of Tg(kctd15a:GFP). Scale bar, 50 μm. (A') Lateral projection of A. Scale bar, 50 μm. (B) Colocalization of the electroporated soma with the expression of vachtb. Scale bar, 25 μm.

transgenic expression of Tg(kctd15a:GFP) (Heffer et al., 2017). A total of 3 neurons were labelled with an almost identical morphology. Due to their specific projection to the lateral hypothalamus, these cells likely belong to the zebrafish larval SGN, which is known to project to this area in adult zebrafish (Yáñez et al., 2017). The soma of these electroporated neurons was also found to localize exclusively to the Ch-B isthmic domain, particularly in its most dorsal region (Figure 3.11B, Figure 3.12), further suggesting that the Ch-B domain contains neurons of both SGN and NI in the larval fish.

3.5 Discussion

Using targeted single-cell electroporation of neurons in the larval isthmus, this study provides the first clear evidence for two types of projection neurons in the NI of a vertebrate.

NI Type I neurons

The projection from NI Type I neurons innervates ipsilaterally the anterior

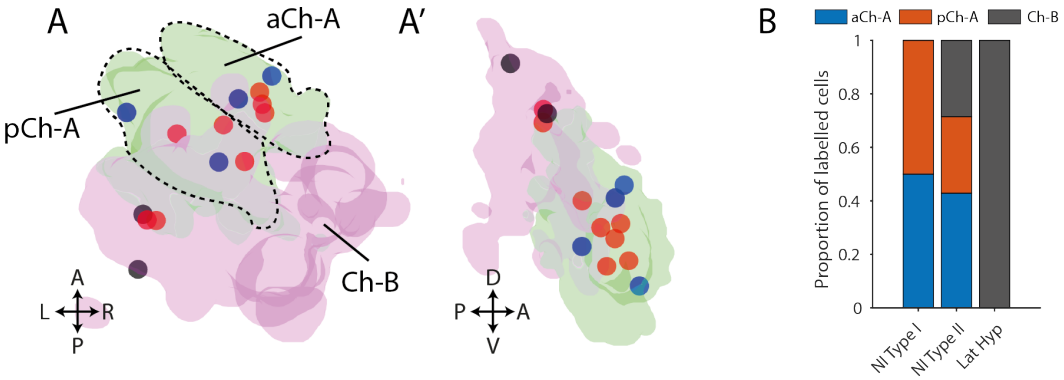

Figure 3.12: Localization of electroporated cell bodies in the isthmus. (A) Dorsal rendering of the Ch-A and Ch-B expression domains with scatter plot of the registered cell body locations belonging to all 3 electroporated cell morphologies found in the larval zebrafish isthmus. (A') Lateral view of A. (B) Proportion of neurons of each of the 3 types of morphology that fell in the different cholinergic expression domains.

tectum and the AF7. Previous studies have found that the NI projects to the pretectal nuclei in several teleost species (Yáñez et al., 2018; Folgueira et al., 2008), but not in other vertebrates, suggesting that the isthmo-pretectal connection might be a teleost specialization. This is, however, to the best of my knowledge, the first evidence that shows that the same neuron project to both the ipsilateral tectum and pretectum.

In adult zebrafish, the application of DiI crystals to the NI reveals a bundle of labelled terminals in the rostral part of the pretectal PSp nucleus, while application to the PSp reveals stained perikarya in the ipsilateral NI, but not in the adjacent SGN (Yáñez et al., 2018). Although the direct correspondence between retinorecipient arborization fields and their post-synaptic pretectal nuclei is not known, this would suggest that NI type I neurons are presynaptic to pretectal PSp neurons. Indeed, based on a comparison of the location of the larval AFs and pretectal nuclei in the adult, the PSp was considered a likely candidate to receive input from AF7 (Burrill and Easter Jr, 1994). Interestingly, the adult NI also projects to another pretectal nucleus, the APN. In the results presented here, it was not observed any other clear projection from the NI to an arborization field besides the tectum and AF7, although it was noted

that NI Type II neurons seem to branch off several arbours near some other AFs. It is possible that these projections are not yet fully realized in the 6 dpf larval brain, and so it is difficult to conclude if NI type II neurons will innervate another AF further in the development, which might perhaps be presynaptic to the APN. Another hypothesis is that both PSp and APN receive input from the AF7. To clarify these issues, it would be important to understand the correspondence between the described larval AFs and their postsynaptic pretectal targets. One possibility would be to use variegated transgenic labelling of RGCs (using for example the Tg(atoh7:GFP) line), which could be used to identify single projections to specific AFs in the larva (Robles et al., 2014) and follow up by analysing the expression in the adult.

Functional considerations

The specific arborization of NI Type I neurons in the anterior OT and AF7 provides some hints on te possible function of these neurons. As previously mentioned, the anterior portion of the OT receives retinal inputs from the anterior part of the visual field (Niell and Smith, 2005). Similarly, AF7 receives preferential innervation from the temporal retina, which also maps to the anterior visual field of the larva (Robles et al., 2014). This area is of crucial importance for hunting behaviour in zebrafish larvae, as during hunting routines, larvae consistently orient themselves towards prey by bringing its image near the centre of their visual field (McElligott and OMalley, 2005; Trivedi and Bollmann, 2013). Moreover, the location in the retina that represents this portion of the visual field is specifically enriched with UV-sensitive photoreceptors, which are postulated to allow larvae to better discriminate UV scattering prey (Zimmermann et al., 2018). On a similar note, Semmelhack et al. observed that the AF7, but not the adjacent AF9, is specifically activated by prey-like visual stimuli, and ablation of the AF7 reduces hunting responses in tethered fish (Semmelhack et al., 2014). These observations seem to converge on the hypothesis NI Type I neurons might play a role in modulating

neuronal circuits that control hunting behaviour.

On a similar note, both the AF7 and OT arbours of NI Type I neurons seem to be topographically mapped with respect to their soma location. Indeed, spatial topography is a defining characteristic of isthmo-tectal connections, present in all vertebrate species examined. In birds, this is thought to provide a focal facilitation of OT responses towards salient stimuli (Knudsen, 2018), and in frogs, local NI ablations suppress behavioural responses to stimuli presented at locations of the visual space that map to the ablation site (Gruberg et al., 1991). Together, these results suggest that NI Type I neurons might provide local facilitation of sensory responses towards moving target prey during hunting. Indeed, the specific innervation of these neurons in the most superficial layers of the OT neuropil, which receive abundant retinal input, could indicate that these neurons provide facilitation of retino-tectal transmission, similar to what has been observed frogs and teleosts (King and Schmidt, 1991). The causal relation of the NI in hunting behaviour of larval zebrafish is investigated in the following chapters.

NI Type II neurons

The second class of NI neurons discovered here, NI Type II neurons, project bilaterally to the OT neuropil. In most vertebrate species, including amphibians (Wang, 2003), reptiles (Wang et al., 1983), mammals (Graybiel, 1979) and teleosts (Johnson et al., 2013), the NI or its homolog structure, the Parabigeminal nucleus, has been shown to project both ipsilaterally and contralaterally to the OT. Birds are the most notable exception, where only ipsilateral isthmo-tectal projections have been observed (Wang et al., 2006). However, because these studies have mostly used the application of retrograde tracers to map isthmo-tectal connections, it remained unknown if single NI neurons projected to both tectal hemispheres, or if there existed separate ipsilateral and contralateral projecting NI neurons. In one noteworthy exception, single NI biocytin labelled neurons in plethodontid salamanders were found

to project either ipsilaterally or bilaterally to the OT (Wiggers, 1998). The results provided in this study together with these observations suggests that bilateral NI projections might exist in other species too.

These results are also in agreement with the observation in several species that contralaterally projecting neurons can be anatomically distinguished from ipsilateral ones, with the former populating more ventral and caudal regions of the NI (Dudkin et al., 2007). Indeed, DiI application in larval OT revealed that the majority of NI labelled cells on the side contralateral to the application were found in the posterior Ch-A and Ch-B domains. This is in contrast with the location of retrogradely labelled cells from AF7 dye application, which are almost exclusively found in the anterior portion of the Ch-A expression domain. This strongly indicates that NI Type I and Type II neurons form anatomically and molecularly distinct subpopulations of the larval NI. It would be interesting to know if Ch-B and Ch-A expressing NI Type II neurons have slightly different projection morphologies, perhaps to modulate different tectal output circuits. From the limited set of electroporated neurons reported here, there did not seem to be any observable difference between neurons whose soma localized with Ch-A or Ch-B expression domains. However, it should be noted that registration errors combined with the small volume of the larval NI could have resulted in the incorrect assignment of labelled soma to the cholinergic expression domains. More example morphologies combined with in-situ expression of cholinergic markers and a more detained morphological analysis would be required to resolve this issue.

Functional considerations

The bilateral innervation of the OT by NI Type II neurons, indicates that these neurons relay information from one side of the visual field, though ipsilateral tecto-isthmic projection, to both tectal hemispheres. What could be the functional implications of this?

One possibility is that might be involved in binocularity processing in the

OT. Indeed, if the contralateral isthmotectal projection is severed by cutting the posterior optic chiasm in frogs, these lose the ability to respond to prey in the contralateral binocular field, which would still be present without input from the contralateral eye (Weber et al., 1996). This suggests that the contralateral isthmotectal projection is required for frogs to reach behavioural threshold to induce prey-capture in the binocular visual field. However, the projection pattern of Type II neurons, which although seemingly topographic, still encompasses a great proportion of the tectal space map, which extends way beyond the larval binocular visual field. Thus, while it is unlikely that these neurons might provide response facilitation in the binocular zone during hunting initiation in larval zebrafish, it is still possible that them might do so during hunting responses, when larval have their eyes converged, and thus a large increase in their binocular zone (from 12% to 36% according to Bianco et al. (2011)). As we will see in Chapter 3, however, this is unlikely to be the case for the zebrafish larva.

Another hypothesis is that instead of being required for localization or perception of objects, these neurons might instead modulate a generalized arousal state. In argument of this, NI Type II tectal arbours, although topographically mapped, are more widely distributed across the OT neuropil than those of NI Type I neurons. Furthermore, their innervation pattern towards the deeper layers of the OT suggests that they might modulate non-sensory input signals, such as pre-motor or multi-sensory or other state-related information. Indeed, in zebrafish, these deeper tectal layers have been shown to receive input from the rostral hypothalamus (Heap et al., 2018), including Orexin/Hypocretin positive neurons in adults (Kaslin et al., 2004) and in larvae (Supperpool A., Personal communication), and serotonergic positive neurons in the dorsal raphe (Yokogawa et al., 2012). It is thus possible that NI type II projections might provide response facilitation of these systems in responses to spatially precise visual stimulation. As opposed to NI Type I neurons, which seem well positioned to mediate hunting behaviour, NI Type II could potentially me-

diate global attentional states to threatening visual stimuli, such as looming spots, by facilitating responses to both sensory and global arousal circuits in the tectum through their superficial and deep tectal projections, respectively.

Both NI type I and type II neurons colocalise to isthmic cholinergic region, and so it is likely that they will express and release ACh to their post-synaptic partners. Indeed, although not exclusively to this neuromodulator, there is plenty of evidence that ACh mediates both local and global states of attention though tonic and phasic release mechanisms (Sarter et al., 2014; Thiele and Bellgrove, 2018). It is possible that NI Type I neurons might provide phasic facilitation on tectal transmission during goal-orienting tasks, while tonic sustained ACh release across the tectum might modulate global states. Thus far, no information exists on the ACh release mechanisms of NI neurons, though novel genetically encoded ACh fluorescent indicators show a promising tool to monitor ACh release in the tectum following NI activation during behavior (Jing et al., 2018). Moreover, it would be interesting to dissect the 1^{st} and 2^{nd} order post-synaptic targets of NI neurons to better understand their role in mediating different system. Transsynaptic labelling tools might offer a good approach to this issue (Beier et al., 2016).

It is worth pointing out that in this study I did not investigate the reciprocal projection from tectum to the larval NI, although preliminary results show that photoactivation of tectal PVN neurons in the anterior portion of the OT result in axonal projections labelled in the ipsilateral, but not contralateral NI. In the future, I will use a similar electroporation technique to label single cells in the tectum PVN layer and map their projections to the NI. Due to the opposing dendritic trees of NI Type I and type II neurons, it might be possible to discern if different cell types in the OT project back to different NI neurons. If true, this might provide insights on which circuits in the tectum might activate differentially activate NI neurons and postulate their behavioural implications.

Chapter 4

The Nucleus isthmi mediates sustained hunting behaviour

The previous chapter established that the larval zebrafish NI, due to its projection pattern to the OT and AF7 regions, might have a role in modulating hunting behaviour. Indeed, unilateral NI ablation in frogs severely impacts their ability to catch worms in the contralateral visual field (Caine and Gruberg, 1985; Gruberg et al., 1991). However, responses to visual threats are also impaired after NI ablations (Caine and Gruberg, 1985), suggesting a more complex role in visually guided behaviour. As we have discussed, this might instead be mediated through NI Type II neurons. These previous studies have gone to directly implicate the NI in mediating visuo-motor behaviour, but one important question is which visuo-motor transformations that happen during these complex behaviours is the NI involved in mediating? Do NI neurons participate in the initial prey detection stages, perhaps by tuning tectal responses to specific features? Are they involved in the activating specific pre-motor neurons in the OT important for initiation of behaviour? Or are they responsible to allocate attention to relevant parts of the visual field during goal-oriented behaviour?

In this chapter, I will investigate these questions through loss-of-function experiments of the NI, combined with high spatial and temporal tracking of visual-guided behaviours in freely swimming zebrafish larvae.

4.1 NI cell ablation

To explore if the NI is involved in visually guided behaviour, a loss-of-function experiment was performed by ablating NI cells bilaterally using a pulsed infrared laser. Since some proportion of Ch-B positive neurons are likely to belong to the larval SGN, an attempt was made to specifically target only the Ch-A expressing neuron population, on both its anterior and posterior domains. As per the results in Chapter 1 and 2, this is likely to result in ablation of the majority of NI Type I and a small proportion of NI Type II neurons.

Well-fed larvae of 5 dpf (n = 8) were tested in the behavioural assay (explained bellow) for 1h and were then anesthetised and mounted in an agarose slide for NI cell ablations. Control larvae (n = 8) were mounted alongside test larvae and submitted to the same manipulation except for laser targeting. Because at the time of these experiments, there existed no transgenic zebrafish line for ChAT with expression in the isthmus, the task of targeting this population of neurons was made somewhat more difficult. Nevertheless, as previously mentioned, some anatomical features of the area surrounding Ch-A expressing neurons, e.g. being at the midbrain-hindbrain boundary and localized around a large fascicle of axons from the cerebellum, allowed them to be targeted using the elavl3:H2B-GCaMP6s expression (Figure 4.1A,B). Post-hoc imaging was also used to record the auto-fluorescent "scar" resulted from the ablation, which after registration to the atlas allowed the precise localization of the damage to specific brain regions (Figure 4.1C-E, see Methods). This revealed that the NI on both sides was accurately targeted to the Ch-A domain (Figure 4.1C), with minimal off-target damage to either Ch-B expressing neurons, or adjacent areas such as the Locus Coeruleus and the Cerebellum (Figure 4.1D-E).

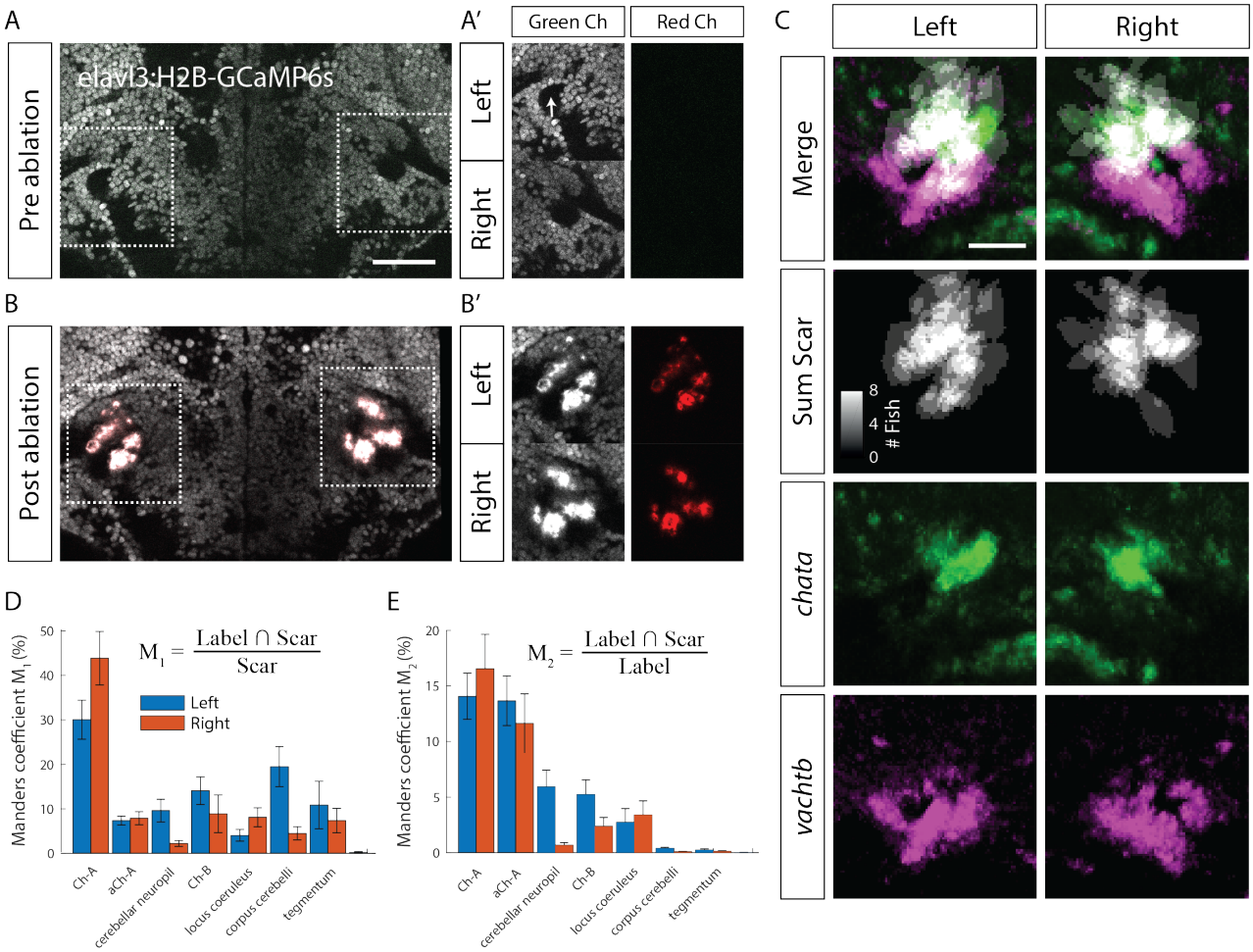

Figure 4.1: Bilateral ablation of the Nucleus Isthmi. (A) 2-photon pre-ablation image of a 6 dpf transgenic Tg(elavl3:H2B-GCaMP6s) larval zebrafish brain at the level of the NI. White dotted boxes show the location of the isthmus on both sides of the brain which are shown on the right. Scale bar, 50 μm. (A') Segregation of green and red channels showing no autofluorescence on the red channel. White arrow points to the location of the cerebellar fascicle that can be used to locate the larval NI. (B) Post-ablation image of the same brain. (B') Green and red channel images of the isthmus of the post ablated brain. The autofluorescent ablation scar that results from laser ablations can be seen on both green and red image channels. (C) Sum of the registered binary masks of each fish's ablation scar overlaid with with chata a vachtb expressions in the isthmus. Scale bar, 25 μm. (D-E) Ranked Manders coefficients of ablation scars with anatomical masks. M1 represents the percentage of voxels in the ablation scar mask that colocalize with the anatomical label. M2 represents the percentage of voxels in the ZBB atlas' label that colocalizes with the ablation scar.

4.2 High-speed behavioural monitoring of visual-guided behaviour

Zebrafish larvae display a variety of visually-guided behaviours (Portugues and Engert, 2009) which have motor kinematics ranging from slow orienting J-turns of hunting routines (Patterson et al., 2013) to incredibly fast (escape manoeuvres evoked by looming and mechano-acoustic stimuli (Budick and O'Malley, 2000; Burgess and Granato, 2007; Dunn et al., 2016). Thus, to be able to accurately measure motor kinematics and avoid errors of sampling frequency (Harper and Blake, 1989), it is imperative to record behaviour at high enough speed. Here, to test the impact of NI ablations on several visuomotor behaviours of zebrafish larvae, an experimental setup was developed to track freely swimming larvae at high frame rates (700 Hz). Images at this rate were acquired as a square window (length: 7.25 mm, 24.8 px/mm) centred of the fish's body centroid, allowing the entire body of the fish to be recorded at any orientation. This allowed the analysis of eye and tail motor kinematics in great spatial and temporal resolution (Figure 4.2).

To elicit visually guided behaviours, various computer generated visual stimuli were presented to the larvae at 90 s intervals and in random order. Looming spots of varying contrast evoked directional escape responses (Figure 4.2B). These stimuli were shown on either the left or right side of the larvae in a fixed egocentric reference frame (see also Dunn et al. (2016)). To test the optomotor response (OMR), left or right drifting gratings were presented (Figure 4.2C). Also, live paramecia, a natural prey of zebrafish larvae that vehemently elicit hunting behaviour, were added to the behavioural arena at the beginning of the experiment (Figure 4.2D). Finally, mechano-acoustic "tap" stimuli were introduced in the final 10 minutes of the experiment to induce startle responses (Figure 4.2E, Kimmel et al. (1974)). NI ablated larvae and control fish were tested in this experimental setup 24h after the procedure. As mentioned above, all larvae were pre-tested at 5 dpf using the same setup and at similar time during the day to use as internal control for developmental de-

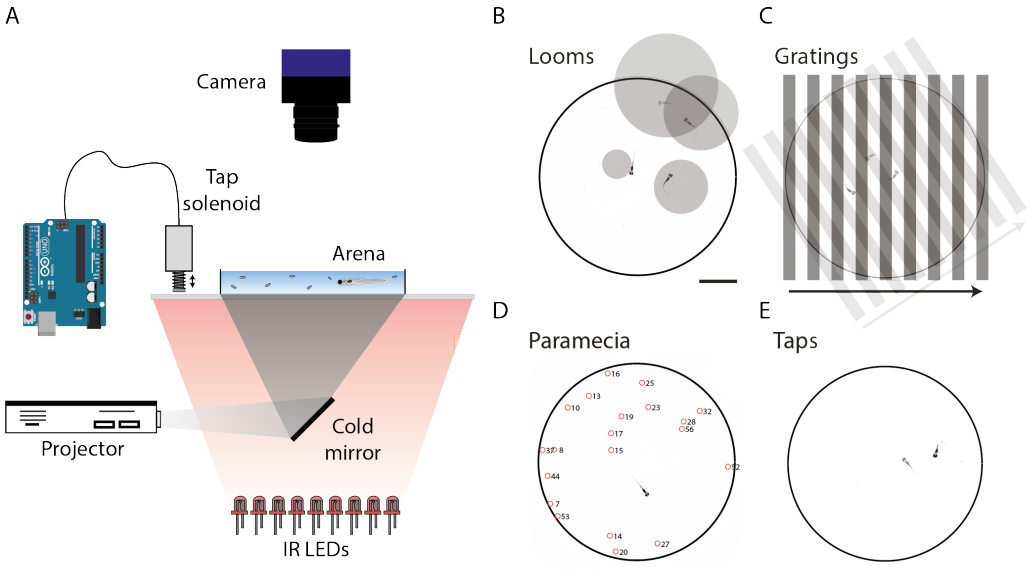

Figure 4.2: High-speed tracking of free-swimming behaviour in larval zebrafish. (A) Schematic of the experimental setup used for tracking larval free-swimming behaviour. (B-E) Examples of stimuli presented to the larvae overlaid with video frames of real behavioural responses. Scale bar, 3 mm. Numbered red circles in D represent tracked paramecia locations.

lays. As the behaviour of larvae at this age is more variable (data not shown), all analysis here described is of 6 dpf post-procedure larvae, although all larvae displayed "normal" behaviour at 5 dpf.

4.2.1 Hunting

As described in detail in Chapter 1, zebrafish larvae use specialised tail and eye movements during hunting behaviour (Figure 4.3). Upon detection of a target prey, larvae initiate hunting with a convergent saccade (both eyes converge towards the centre) (Figure 4.3B,C; Bianco et al. (2011)). Lateralized J-turns with amplitude proportional to prey azimuth are then used to orient towards the target and subsequent goal directed swim bouts gradually position the prey directly in front of the fish (Figure 4.3D,E, Trivedi and Bollmann (2013); Patterson et al. (2013)). Finally, larvae attempt to consume their prey using either a capture swim or, less often, a suction strike (Figure 4.3B").

4.2.1.1 Hunting metrics

Predator-prey interactions can help reveal specific aspects of the visuomotor transformations during naturalistic behaviour (Mischiati et al., 2015). Thus, to measure fish-target kinematics during hunting routines, lower framerate movies (17 Hz) of the whole arena were acquired in order to track paramecia using an offline algorithm. These tracks were then used to semi-automatically determine the fish's target prey for each hunting epoch and automatically measure fish-target parameters across the epoch. Vergence angle, as defined by the sum of the angles between each eye and the body axis, was used to define the beginning and end of hunting epochs (see Methods section). Tail angle was calculated by the cumulative angle between 9 segments along its body axis. Fish-target distance was measured as the Euclidean distance between the centre of the eyes and the target centroid and fish-target angle as defined as the azimuth between the vector from eye centre and the target and the fish's body axis vector (Figure 4.3A).

To identify target paramecia, a principled and conservative criterion was used. At the beginning of a hunting routine, as defined by eye convergence, if one paramecia was observed being pursued by the larva for more than one successive swim bout, that paramecia was manually labelled as a prospective target. If several paramecia were in the field of view and no clear identifiable target could be discerned (at the experimenter's discretion), the epoch was labelled as "target unidentified". Then, for each swim bout in the hunting routine, which ends by divergence of the eyes, the fish-target distance-gain and orientation-gain were computed as the fraction of distance or orientation between fish and prey that was eliminated by the bout (Figure 4.3A). Prospective targets were only defined as "target" if at the beginning of the epoch they were located within the larva's reaction zone (6 mm from the centre of the eyes and $< 120°$ from each side of the body axis, following roughly the metrics observed in (McElligott and OMalley, 2005; Patterson et al., 2013; Trivedi and Bollmann, 2013) and the distance-gain and orientation-gain for the first two

bouts of a hunting sequence were positive (orienting towards and approaching the prey, Figure 4.3A,D,E, see Methods).

One limitation of this approach is that some true targets will be discarded as it might not be expected that the fish will only target paramecia within these bounds (although Trivedi and Bollmann (2013); Patterson et al. (2013); McElligott and OMalley (2005)) report fish-target distances and orientations at hunting initiation well within the limits imposed here), and the fish might not always have positive distance and orientation gains for the two first bouts. An obvious observation would also be that NI ablation would impair larvae to correctly turn towards its target, which would inevitably lead to a larger fraction of "unidentified targets" in the NI ablated fish. However, this is not the case, as a similar fraction of these epochs was observed between control and NI ablated groups (Controls: 0.50 ± 0.13, Ablated: 0.46 ± 0.11, $p = 0.3823$). These relatively high numbers (half of epochs are discarded), might represent either spontaneous convergence epochs, or convergences that were triggered by stimuli unaware to the experimenter.

Routines were also manually labelled based on their outcome, e.g., if the fish captured or not its target, and if so, which type of swim bout was used (ram or suction). Interestingly, it was observed that not all hunting routines progress as far as the final attempt to consume prey, but instead may be aborted (Figure 4.3C-C",E). Such events were previously reported for young zebrafish larvae (Westphal and OMalley, 2013), although it is not known why larvae choose to abort routines midway. Nevertheless, such events might give insights on the animals hunting state.

4.2.1.2 Analysis of hunting routines

Analysis of hunting performance revealed that NI ablated larvae captured prey at lower rates than controls (Figure 4.4A,B). This reduced capture rate was not due to differences in prey availability, as the number of paramecia added to the arena was not different between groups (Figure 4.4C). Moreover, both control and ablated larvae started to swim at the centre of the arena and to

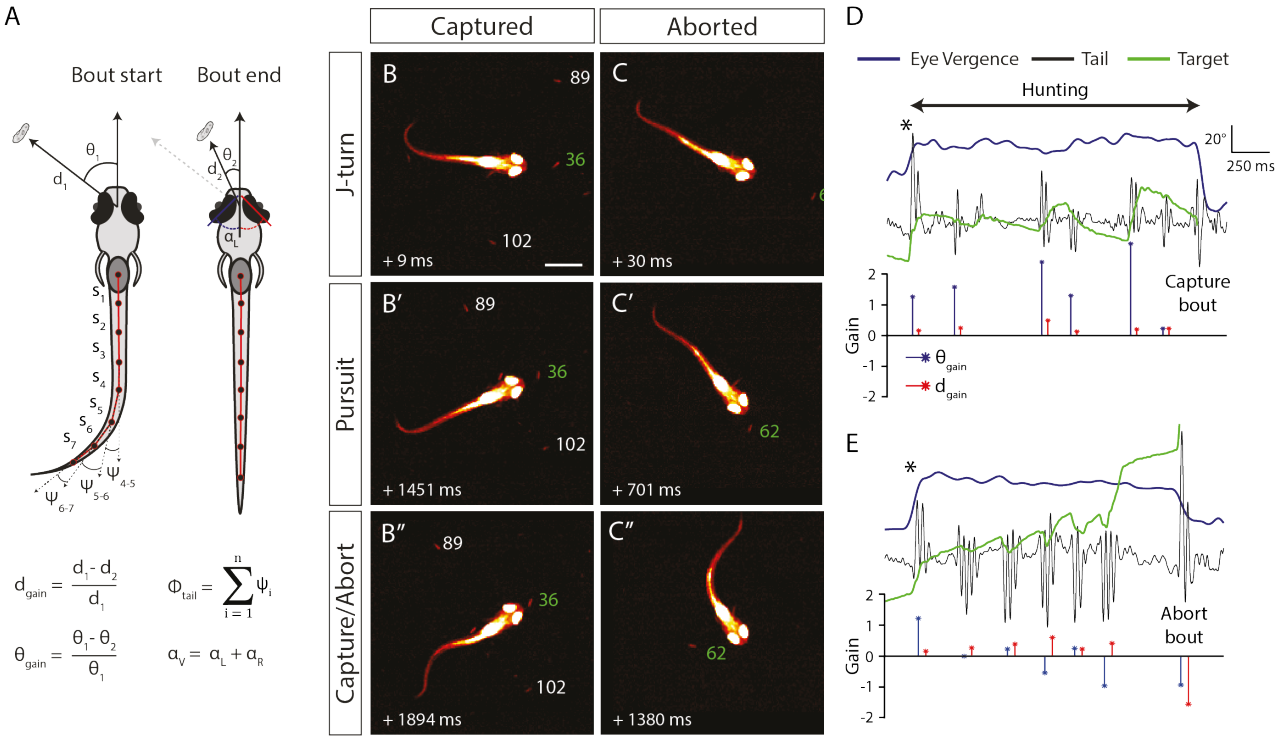

Figure 4.3: Quantification of hunting behaviour. (A) Schematic illustration of the calculations of fish-target orientation/distance gains and tail and eye angles used to analyse predator-prey interactions during hunting routines. Circles along the fish's tail represent the tracked tail segments, which are used to compute the cumulative tail angle, used for assessment of swim bouts and displayed in D and E panels. (B-C") Examples image frames of hunting routines that ended up in a capture (B-B") or abort (C-C"). Numbers represent tracked paramecia of which the green one represents the target. Timepoints represent elapsed time since convergence event. Scale bar, 1 mm. (D,E) Tracked parameters of the hunting routines in B and C, respectively. Black asterisk represents the start of the hunting routine identified by convergence of both eyes. Notice in E, the abort bout displayed negative distance and orientation gains.

hunt soon after the beginning of the experiment (Figure 4.4A), excluding the hypothesis of a difference in adaptation to the arena.

To determine whether NI ablated fish have defects in prey perception or reduced motivation to feed, the rate of initiation of hunting behaviour, quantified by occurrence of saccadic eye convergences, was examined. This revealed no difference in convergence rate between groups, which remained steady throughout the experiments (Figure 4.4E, Figure 4.5J). Likewise, the location of target prey at the onset of hunting routines and at the time of initiation of capture swims was indistinguishable from those of control fish (Figure 4.5A-D), arguing against defects in prey detection or depth perception.

To understand why NI ablated larvae captured fewer prey than controls, despite normal rates of hunting initiation, the probabilities of the outcomes of hunting routines was examined. This revealed a remarkably specific defect: NI ablated larvae displayed a significantly higher probability of aborting hunting routines compared to control fish (Figure 4.4D-I, Controls: 0.52 ± 0.12; Ablated: 0.76 ± 0.09. $p = 0.001$). Notably, other aspects of hunting routines were unaffected, namely probabilities of capture type (ram vs suction) and capture success rates (Figure 4.4G-I).

One hypothesis for why NI ablated fish might abort hunting routines more often is that after the initial target-directed manoeuvre, larvae fail to reduce their distance and/or orientation towards the target by enough amount to allow the deployment of a capture swim. However, both orientation gain and distance gain were found to be unaffected compared to controls during pursuit swims, further suggesting that the phenotype cannot be explained by an inability of NI ablated fish to correctly localize the prey's azimuth, to perceive its distance to the target or to track their movement (Figure 4.5H-I).

Arguably, a fish might stop pursuing a target before eye divergence, which could indicate a drop in attention towards target prey without the release of the hunting state. Taking this into account, an "abort bout" was defined by the first bout in the routine with a negative orientation-gain and distance-

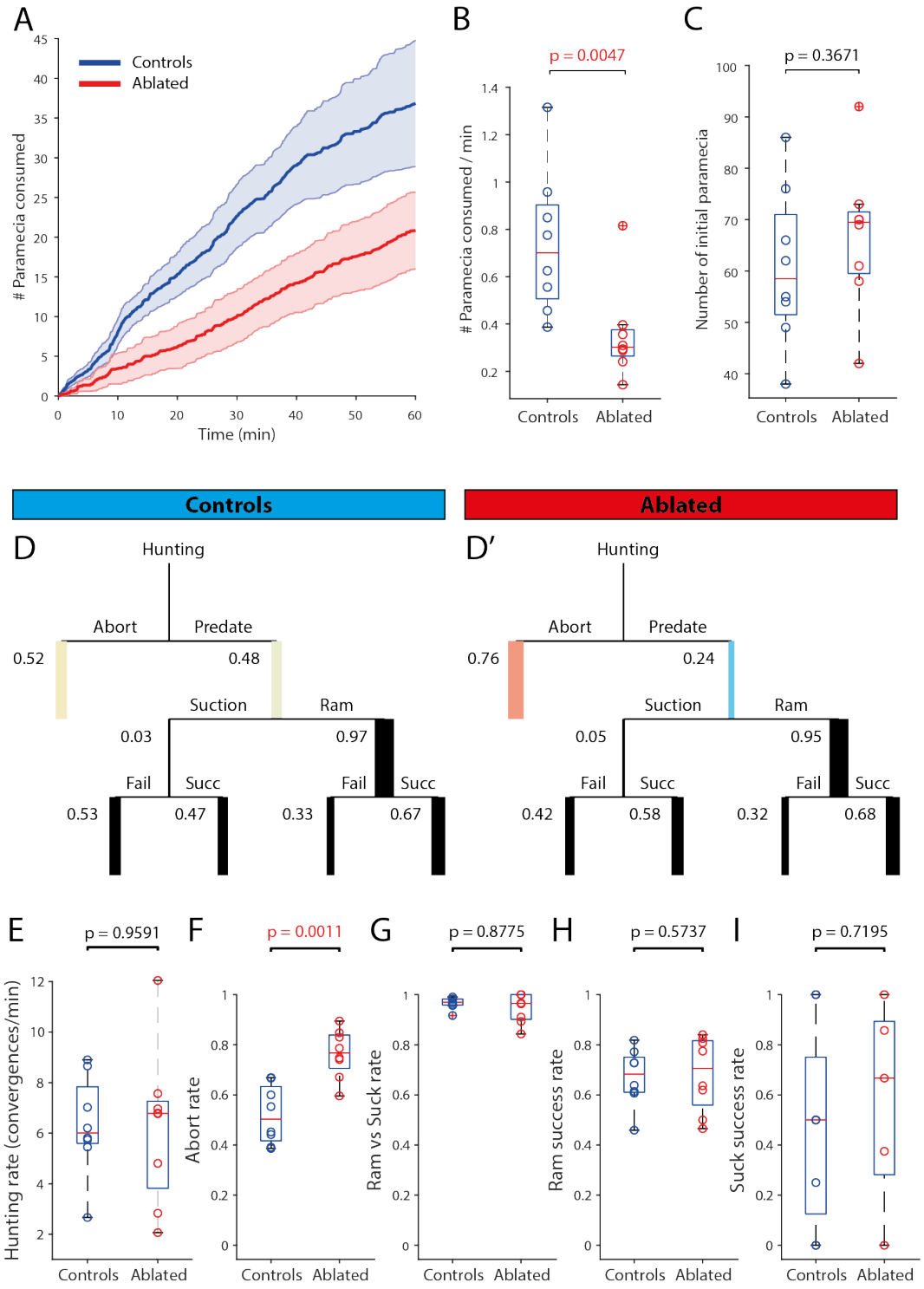

Figure 4.4: Behavioural quantification of hunting responses following NI ablation. (A) Cumulative number of paramecia consumed for NI ablated (n = 8) and control (n = 8) larvae. (B-C) Paramecia consumption rates and numbers of initial paramecia for both control and NI ablated groups. (D-D') Ethograms of hunting routines for NI ablated and control larvae showing the difference in capture versus abort rates, but not in capture type or success rates. The thickness of the branches is scaled to each probability, also showed to their left. (E-I) Quantification of the different hunting routine scoring categories between groups.

gain. The duration between the abort bout and eye divergence (post-abort duration) was, however, not different between groups (Figure 4.5L). Similarly, the pursuit duration, as defined by the amount of time the hunting lasts until an abort or capture swim, was also found not to be different between groups and outcomes (Figure 4.5K).

Because NI ablation leads to a higher probability of aborting a hunting routine, but as far as was measured here, with the same characteristics of "normal" aborted events, it leads to the conclusion that the NI has a specific role in sustaining hunting routines towards target prey.

4.2.1.3 Paramecia density

Could this abort phenotype be explained by an inability of NI ablated larvae to deal with competing stimuli? In other words, if the NI in larval fish is involved in selective attention towards target stimuli by mediating a winner-take-all computation, it's possible that NI ablated larvae are "distracted" by competing stimuli in their visual field, such as other paramecia.

To test this, I analysed the number of paramecia present within the larva's "trigger zone" (<= 120° on each side of the body axis and <= 6 mm distance) present at the timing of the bout that precedes the last bout of the routine (abort bout or capture bout for capture routines). This timing was chosen to allow for a better comparison between outcome conditions, as during capture bouts paramecia sometimes are difficult to track due to the proximity to the fish. However, values at the beginning of the last routine bout and an average across the entire routine was also analysed, yielding similar results. The mean values for each fish were then compared between groups and hunting outcomes.

Contrary to expectation, larvae tend to be surrounded by a smaller number of paramecia during aborted routines than during capture routines, an effect that was consistent among groups (Figure 4.5M). To test if aborted routines tend to occur for hunting routines where a smaller paramecia density exists to begin with, I compared the same values but for the first bout in a hunting routine. Indeed, the same effect is observed at hunting start and con-

sistent across groups (Figure 4.5N), indicating that low density of paramecia in the larva's visual field is predictive of the routine being aborted.

Why would this true? One possibility for this is that routines tend to be aborted at locations closer to the edge of the arena, where higher paramecia densities tend to occur (personal observation, as paramecia at the edges of the arena are difficult to track due to image distortions). Although NI ablated larvae tended to terminate routines at distances further from the centre of the arena compared to control fish (Figure 4.5O), aborted bouts seem to be terminated at relatively closer distances in both groups, making it unlikely to explain the effect. Further investigation will be required to underpin the cause of this observation.

4.2.1.4 General swim statistics

Zebrafish larvae have been shown to have impaired feeding when exposed to a stressor (such as high NaCl concentration in the water), but also increased locomotion at high stressor conditions (De Marco et al., 2014). However, larvae of both control and NI ablated groups spent the majority of the experiment at the centre of the arena, although ablated fish tended to distribute more uniformly and also occupied the outer edges of the "middle ring" (Figure 4.6A). Also, both groups swam at similar average speeds (Figure 4.6B-C), suggesting that control and NI ablated larvae did not showed stress related signs or an impairment in their foraging ability.

To better understand if NI ablations generated a specific motor deficit related to the larvae's swim ability, several swim bout kinematics were extracted. Swim bouts used in hunting pursuits and those in which no stimulus was being presented and the larvae were not engaging in hunting routines were compared across groups. This revealed no significant difference in bout duration, inter-bout-interval, tail-beat-frequency, mean bout angle or mean bout velocity (Figure 4.6D-H). This indicates that the NI is not involved in directly modulating swim-bout kinematics, and that off-target effects, if present, did not significantly impacted the larva's swim repertoire.

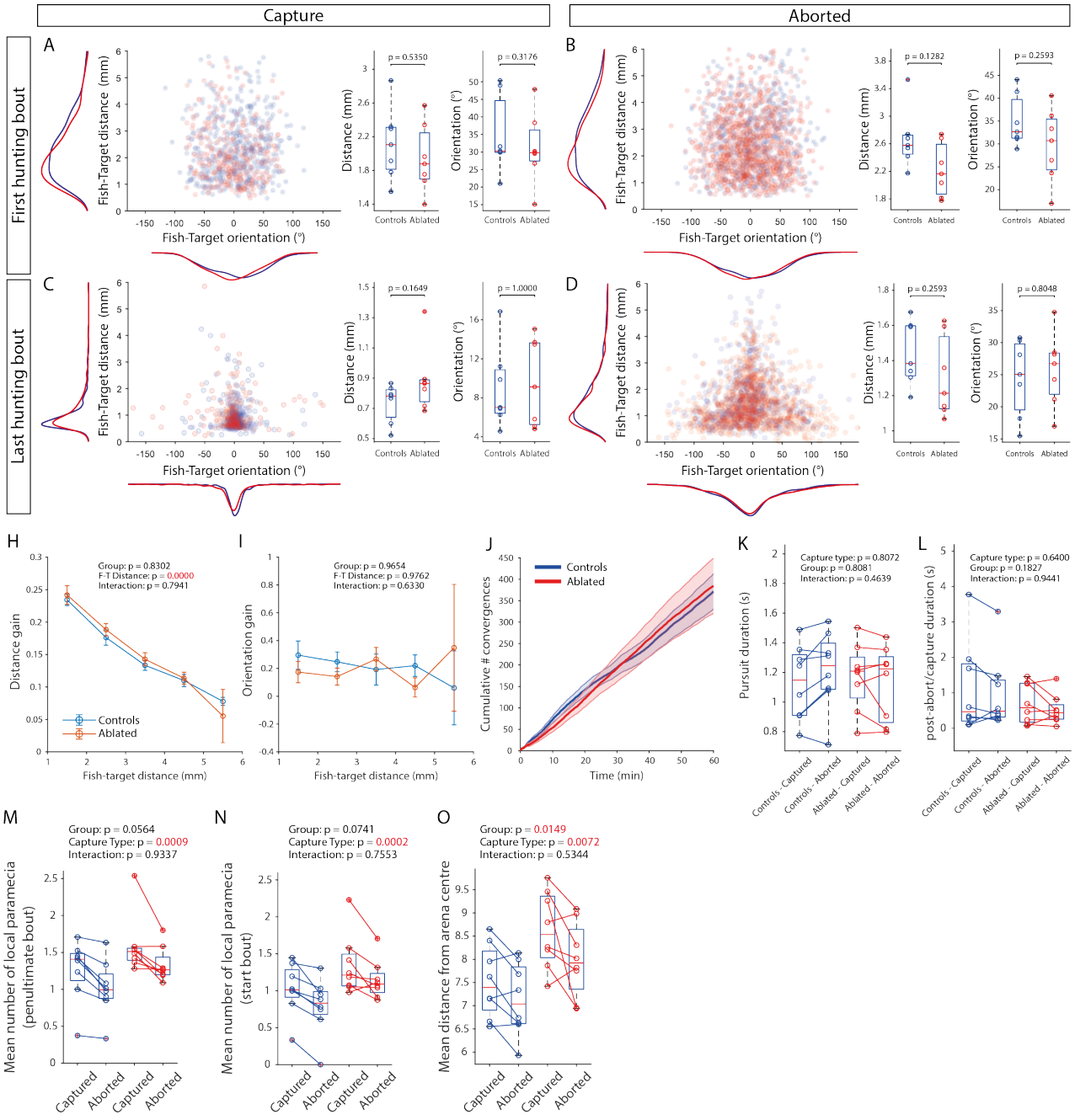

Figure 4.5: Quantification of predator-prey parameters during hunting routines. (A-B) Orientation and distance at which larvae encounter target prey at initiation of hunting routines for (A) captured and (B) aborted routines. (C-D) Same parameters for the last hunting bout, which in capture routines equates to the capture bout and in aborted routines the abort bout. (H-I) Mean distance and orientation gains across groups (of medians across fish) during pursuit bouts, binned by the distance at which the target was located at the beginning of the bout. (J) Cumulative number of convergences across groups for the length of each experiment. (K-L) Pursuit and post-abort/capture durations across groups. (M-N) Paramecia density quantification. (O) Mean distance from centre of the arena where each routine type terminated.

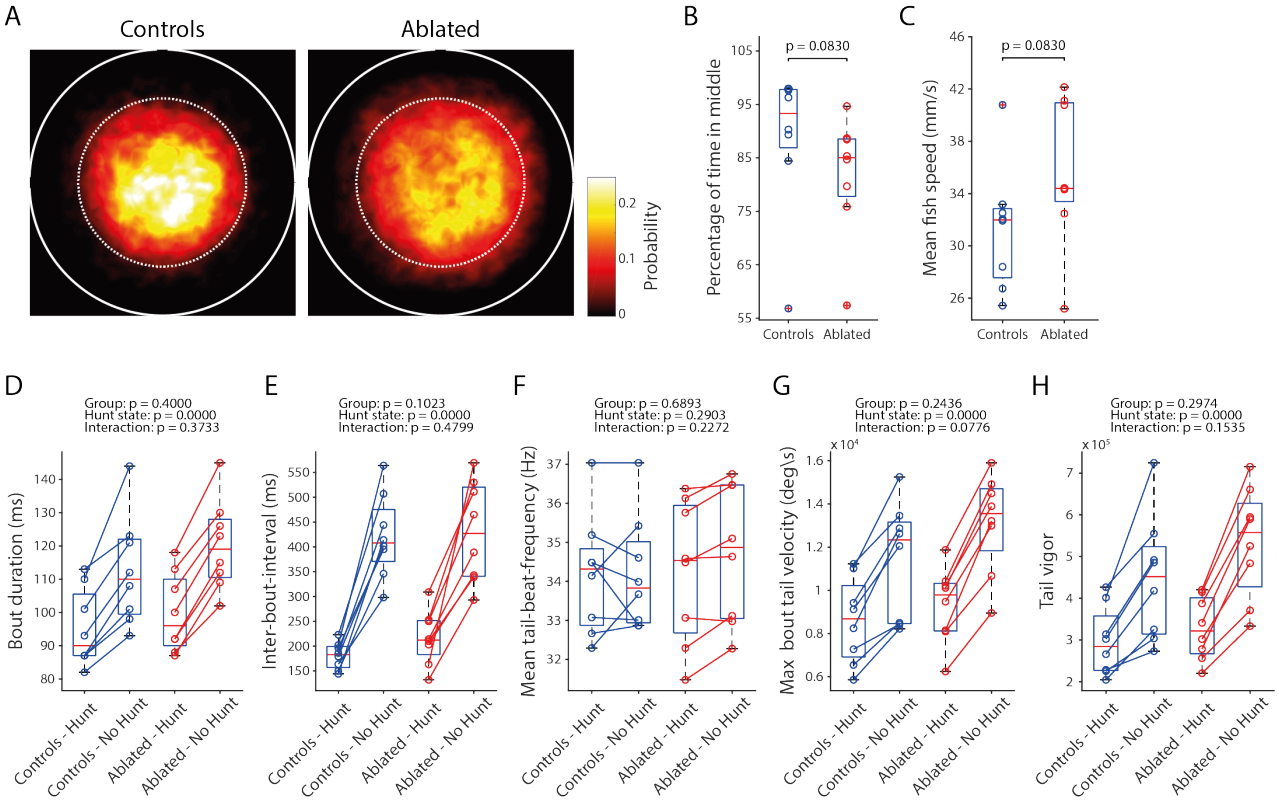

Figure 4.6: General swim statistics. (A-A') Mean location probability of larvae in the behaviour arena for NI ablated and control larvae. Outer while ring represents the edge of the arena. Inner dotted while ring represents the area in which the larvae were considered "in middle" and where stimuli were allowed to be presented. (B) Percentage of time of larvae in the middle of the arena. (C) Mean speed of the larvae for the duration of the experiments. (D-H) Quantification of several bout and tail kinematics across groups grouped by hunting or not hunting (and no stimulus presentation) bouts.

4.2.1.5 Looming escape

When presented with looming disks, zebrafish larvae reliably respond by escaping with a high-angle tail bout, mainly directed away from the location of the stimulus (Dunn et al., 2016; Temizer et al., 2015). This response is present in many vertebrate and invertebrate species (Sun and Frost, 1998; Ewert et al., 2001; von Reyn et al., 2017) and the probability of escaping a looming stimulus has been shown to increase with the stimulus contrast level (Evans et al., 2018). Previous studies in birds have pinpointed NI cholinergic Ipc neurons to modulate both contrast gain and response gain of OT responses to loom-

ing stimuli, as inactivation of Ipc neurons shifts the contrast-response curve of these neurons towards the right and downwards (Asadollahi and Knudsen, 2016). Thus, it is possible that if the zebrafish larval NI has a similar role, it could act to modulate behavioural responses to looming stimuli. To test this, looming stimuli of 5 different contrast levels were presented to either the left or right side of the fish (Figure 4.2B, Figure 4.7).

A similar effect was observed for larval zebrafish (Figure 4.7A). These escape-response probabilities can be well fitted with a psychometric logistic function, which allows the analysis of contrast-response curves across both groups. Three free parameters (threshold, slope and lapse-rate) were fitted to the response probabilities of each fish. The lower asymptote, or "guess-rate", was fixed to 0, as spontaneous escape responses were very rare. Comparison of the fitted parameters across groups revealed a significant shift of the function towards the right in NI ablated fish, corresponding to an increase in the contrast-gain (Figure 4.7A,B). Although in birds, Ipc blockade also resulted in downwards shift of the contrast-response functions of OT units, there was no evidence of any change in either the slope or the lapse-rate of the fitted curves (Figure 4.7C-D), indicating that the NI might not be involved in modulating looming response-gain in larval fish.

Larval fish decide when to escape to a looming threat when it reaches a specified size threshold in the retina, independently of the stimulus velocity (Dunn et al., 2016; Temizer et al., 2015). Consistently with this, larvae of both control and NI ablated groups reliably escaped when the presented stimulus reached a specific size threshold (Controls: 48.2 ± 23.8°, Ablated: 48.5 ± 22.2°), which was independent of stimulus contrast (Figure 4.7E). This indicates that the NI doesn't play a role in the size-threshold computation of looming stimuli. Moreover, both groups displayed similar response laterality across all contrasts (Figure 4.7F), indicating that even at low contrast levels, larvae can accurately identify the laterality of looming stimuli, and that the NI is not involved in this computation.

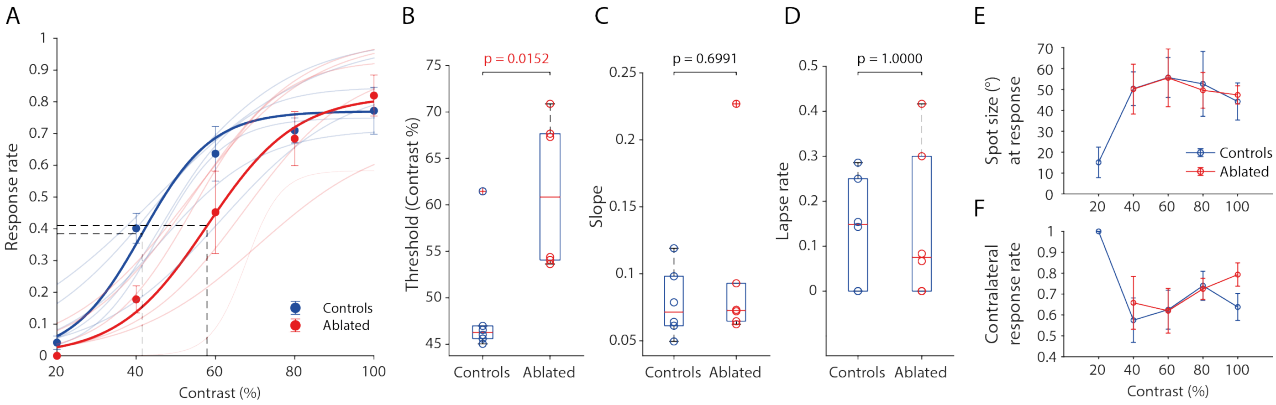

Figure 4.7: Behavioural responses to looming stimuli. (A) Contrast-response psychometric fits to looming stimuli for control and ablated larvae. Background curves correspond to the fits of individual fish. Foreground curves correspond to the fits to the mean response rates for each group, which are displayed as solid points (B-D) Quantification of psychometric fit parameters for each fish on each group. (E) Mean spot sizes to which fish perform an escape in response to looming stimuli. (F) Response rate to which fish escape to the contralateral side to where the stimulus was presented. Lack of data at 20% contrast in the ablated group is due to the fact that no fish in this group responded to this contrast level, as can be seen in panel A.

These results are consistent with the function conservation of the NI across vertebrates, which in zebrafish larvae seems to be involved in increasing the contrast-response sensitivity to looming threats, improving performance to low contrast stimuli.

4.2.1.6 Optomotor response

When visually presented with whole-field moving stimuli, such as directional moving gratings, fish will move in the direction of the perceived motion, in what's called the optomotor response (OMR) (Neuhauss et al., 1999; Orger et al., 2008). In the real world, such whole-field motion would occur, for example, if the fish was being dragged by a water current, in which case the response acts to stabilize the fish's position in the water. Here, OMR responses were tested to assess the larva's ability to perceive whole-field motion and to swim in response to it.

Egocentric left- and rightwards moving gratings readily elicited OMR responses in both control and NI ablated fish, whose responses followed the

correct direction of the stimulus and produced swims that ended up producing similar total angular turns (Figure 4.8A-C), suggesting than neither whole-field motion detection nor motor ability was impaired in NI ablated larvae.

4.2.1.7 Mechano-acoustic escape responses

Zebrafish larvae display a stereotypic C-start escape manoeuvre, or "startle" behaviour, when presented with mechano-acoustic stimulation (Kimmel et al., 1974; Burgess and Granato, 2007). The brain circuits involved in startle responses have been well characterized, involving the large Mauthner neuron of the reticulospinal system, which receives direct excitatory input from the ear through VIIIth cranial nerve (Zottoli et al., 1995), and is modulated by caudal hypothalamic and hindbrain neurons in rhombomere 4 (Mu et al., 2012). Although not immediately intuitive, it is still possible that NI neurons might indirectly modulate startle responses, either by modulating caudal hypothalamic afferent projections (though NI Type II neurons) or another mechanism. Thus, larvae were subjected to mechano-acoustic "tap" stimuli at the end of each experiment.

Responses to tap stimuli were variable, but both groups responded with the same probability on average (Figure 4.8D). Similarly, Both the response latency and the laterality of the responses were not different between NI ablated and control fish (Figure 4.8E-F), indicating that the NI does not modulate startle response circuitry.

4.3 Discussion

Using a high-speed behaviour tracking setup, combined with detailed analysis of behavioural kinematics during several visually-guided and mechano-acoustic stimuli following bilateral loss-of-function of the NI in zebrafish larvae, this study was able find a specific but strong phenotype: NI ablated larvae fail to sustain hunting responses to target prey.

The NI has been previously studied in the context of hunting behaviour, particularly in amphibians (Ewert et al., 2001). Indeed, where the NI has

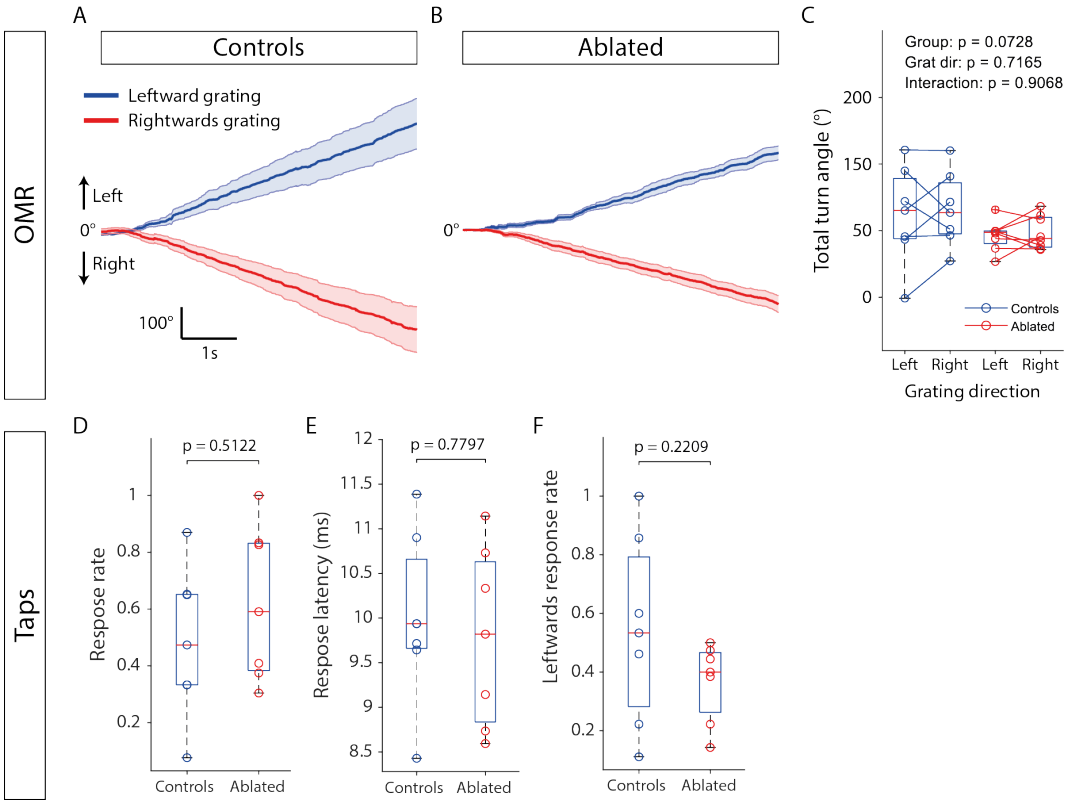

Figure 4.8: Responses to directional gratings and mechano-acoustic tap stimuli. (A-B) Cumulative delta angle of fish in response to leftwards or rightwards moving gratings in control and ablated fish. Errors are SEM across fish means. (C) Quantification of mean total angle turn between groups. (D) Response rate, (E) response latency and (F) Leftwards response rates for tap stimuli.

been unilaterally ablated in frogs, studies have found a marked suppression of both hunting and avoidance behaviours in the contralateral visual hemifield, likened to the appearance of a scotoma, which is topographically mapped to the ablation site (Caine and Gruberg, 1985; Gruberg et al., 1991). Here, a scotoma-like effect does not seem to occur when the entire Ch-A NI domain is ablated in zebrafish larvae, as responses to prey and looming stimuli can still be readily evoked. What could be the reason for these discrepancies?

It is possible that the NI in frogs has evolved to meet different ecological and biological differences between the two species. In frogs, the NI seems to mediate binocularity in responses to prey (Gruberg et al., 1989; Weber et al., 1996). Differently to zebrafish larvae, the frog strategy to hunt for prey (mov-

ing mealworms) is a sit and wait strategy where responses are elicited when a stimulus with the correct visual features invades its visual field (with a preference for the rostral (binocular) portion and is ballistic. On the other hand, zebrafish larvae actively pursue their prey during sustained hunting routines with discrete events (swim bouts) where the target is consistently approached. These goal-oriented pursuits might require more dedicated attentional mechanisms, as not only is the probability of other competing stimuli interfere with the pursuit higher, there is likely a selective pressure to successfully conclude such pursuits in the shortage amount of time.

These results also do not support the hypothesis that the NI mediates the correct detection of prey, as NI ablated fish respond to prey at similar rates and located at similar distances and azimuths than control fish, both at the start of the hunting routine as with successive hunting bouts. Rather, these results seem to indicate that NI neurons are required to facilitate continuous responses toward target prey. Rather, given that the strongest phenotype observed relates to an inability of ablated larvae to sustain a hunting routine towards a target prey, it seems more likely that the larval NI has a prominent role in modulating sustained attention to relevant target stimuli. Indeed, the NI has been extensively studies in the context of selective visual attention in birds, where cholinergic Ipc/SLu and GABAergic Imc isthmic nuclei are thought to function as a mechanism for a winner-take-all computation to arise in the OT, selecting responses towards the most salient visual objects (Knudsen, 2018). In the larval zebrafish, it is possible that a similar mechanism is implemented by the NI. Although no evidence yet exists of a homologous population to the Imc in zebrafish, it is possible that NI neurons might recruit the activity of wide-field tectal interneurons to supress off-target responses in a similar fashion. One possible population of neurons are the GABAergic superficial interneurons (SINs) found in the neuropil of the OT (Del Bene et al., 2010; Barker and Baier, 2013). The dendritic tree of these neurons is monostratified, targeting the most superficial tectal layers, albeit with varying

depth (Preuss et al., 2014), making them a good candidate to be targeted by NI Type I or Type II neurons. Moreover, their branches extend widely in the anterior-posterior direction of the OT, which could provide lateral inhibition to adjacent tectal areas to suppress responses to competing visual cues. SINs seem to be tuned to the size of visual objects depending on the layer in which their dendrites stratify, with size tuning increasing with layer depth, and SIN ablation impairs the ability of larvae to feed on paramecia (Del Bene et al., 2010; Preuss et al., 2014), suggesting a role in object detection and/or classification (small vs large), although a careful analysis of behaviour after SIN loss-of-function could better elucidate their role in hunting. To test if NI targets the SIN population, one possibility would be to stimulate NI activity, either optogenetically (Mohamed et al., 2017), using a Gal4 transgenic line or by current injection, while recording activity in SIN neurons. Transgenic lines that label the SIN population of neurons already exist (Barker and Baier, 2015), which combined with genetically encoded Ca^{2+} indicators would make this experiment feasible.

Nevertheless, this experimental paradigm did not explicitly test for selective attention. To test this, it would be required to assess if responses to competing stimuli anywhere else in the visual field could be elicited more often than NI non-ablated controls. Here, due to the low prey density, an arguable requisite to allow unbiased identification of target prey during hunts, does not permit to test this hypothesis. One idea would be to use a tethered virtual-reality assay where multiple competing prey-like visual stimuli could be presented to the larvae (see Bianco and Engert (2015)). Such preparations are, however, difficult to implement, as hunting responses in tethered larvae are severely suppressed compared to free-swimming conditions (Bianco et al., 2011; Bianco and Engert, 2015; Semmelhack et al., 2014), this Thesis), especially sustained responses (author's personal experience). Understanding why this suppression of feeding behaviour exists in tethered conditions and developing methods to overcome it is thus required.

Whatever the mechanism, one hypothesis is that after NI ablation, failure to facilitate responses in the anterior OT to target prey in the frontal visual field might result in sensory or internal cues to win over the fish's attention, resulting in the termination of the hunting state and an aborted routine. The most obvious candidate projection to allow this modulation is NI Type I neurons, which specifically project to the anterior-dorsal tectum. In these experiments, it is likely that the majority of NI Type I neurons were ablated on both sides, as the Ch-A area was specifically targeted for ablation. Indeed, due to the fact that, as was observed in Chapter 3, the majority of NI Type II neurons is in the Ch-B domain, which some also populating the pCh-A region, it seems plausible that a significant portion of the NI Type II population remained intact. This might explain why the main phenotype observed here was related to hunting routines.

The second observation of these experiments was that the contrast-response curve for looming escape responses was shifted to the right in NI ablated fish, indicating an effect in contrast sensitivity. Such an effect is also observed in the response of deep OT units after Ipc inactivation birds (Asadollahi and Knudsen, 2016), although that study also found that the response gain (lapse rate) of these responses was also shifted down, which was not observed for behavioural responses here. Moreover, other aspects of looming responses, such as the size threshold to which responses occur, nor the response laterality were perturbed by NI ablation. This reveals that the NI has a specific effect of changing the contrast sensitivity of tectal neurons in the larval NI. Such an effect might be mediated through NI Type II neurons. Indeed, the broader projection pattern across the tectal lamina in these neurons suggests that it might have a more global arousal function across the visual field, as opposed to the specificity of NI Type I neurons to the anterior visual field. It would be interesting to test this hypothesis by presenting looming stimuli from both nasal and temporal locations of the visual field and assess if contrast sensitivity differs between these locations in NI ablated fish.

These observations, along with the findings of Chapters 2 and 3 leads to two general hypotheses. First, NI Type I neurons in the aCh-A domain might mediate sustained hunting responses towards target prey. Second, NI Type II neurons in pCh-A and Ch-B domains might mediate contrast gain responses to looming stimuli. From these, we might expect that NI Type I neurons might fire in response to prey stimuli and during hunting routines, and that NI Type II neurons might respond to looming stimuli. In the next Chapter, I will attempt to test these hypothesis by optically recording NI neurons during presentation of prey-like and looming stimuli in a closed-loop experimental paradigm for tethered larvae.

Chapter 5

The Nucleus Isthmi is active during hunting routines

The anatomical and behavioural results presented in the previous chapters strongly indicate that the zebrafish NI plays a role in hunting, and specifically, that it acts to sustain the fish's continuous engagement towards target prey during hunting routines. Given these observations, the first expectation is that NI neurons are recruited at hunting initiation. Then, if the NI are responsible to facilitate responses to targets during hunting routines, one might also expect that these neurons continue to be active during sustained hunting routines. We also observed that NI ablation decreases the contrast-gain of escape responses to looming stimuli. This indicates that NI neurons might also be recruited in response to looming stimuli.

To address these questions, experiments were conducted in a virtual-reality assay where neuronal responses in the NI of tethered larvae were recorded simultaneously with closed-loop hunting behaviour.

5.1 2-photon imaging of NI neurons during closed-loop behaviour

2-photon microscopy was used to image live, tethered zebrafish larvae (n = 9) expressing nuclear localized GCaMP6s (Tg(elavl3:H2B-GCaMP6s)), while simultaneously presenting moving prey-like visual stimuli (5° spots moving

CW or CCW at 30°/s) to induce hunting (see Bianco and Engert (2015) and Semmelhack et al. (2014)), as well as light or dark whole-field flashes as control for luminance changes (Figure 5.1). The stimuli were back-projected onto a diffusive screen in front of the fish. Importantly, fish were mounted such that both eyes and tail were free to move (Figure 5.1B), allowing them to behaviourally respond to visual cues. Tail and eye kinematics were tracked in real time at 430 Hz and 60 Hz, respectively (Figure 5.1B').

To allow for the larvae to continuously engage with a virtual prey, prey-like stimuli were presented in closed-loop conditions where the location of the stimulus was updated to the centre of the screen, initially in response to a convergence event and then following successive swim bouts, thus mimicking free-swimming hunting (Figure 5.1B'). Also, to get a better insight into the specific contribution of NI neurons during hunting responses in relation to other areas in the brain, neurons of the NI, OT and pretectal neurons around the AF7 (Griseum Tectale, Gt), were simultaneously imaged (Figure 5.1B").

5.1.1 NI neuronal responses to prey-like stimuli

To analyse visual sensory responses of imaged neurons across all experiments, a visual-responsive vector (VRV) was constructed for each cell by concatenating its mean normalized dF/F responses for each presented stimulus type (Figure 5.2A, see Methods). Then, an unsupervised 2-step agglomerative clustering methodology was used to find clusters of visually-responsive cells based on the similarity of their VRVs, as measured by their correlation (Bianco and Engert, 2015) (see methods). Briefly, in the first step, a stringent correlation threshold ($\rho \geqslant 0.9$) is used to find the main response archetypes present in the dataset, and in the second step, these archetypes are used as templates to cluster previously unassigned cells using a less stringent threshold ($\rho \geqslant 0.7$). This results in clusters that are "homogenous" with respect to VRVs of component cells (Figure 5.2A).

Clustered neuronal responses fell into 3 archetypes: (1) Whole-field luminance responsive (WF), (2) Direction-selective CW-moving prey-like spot

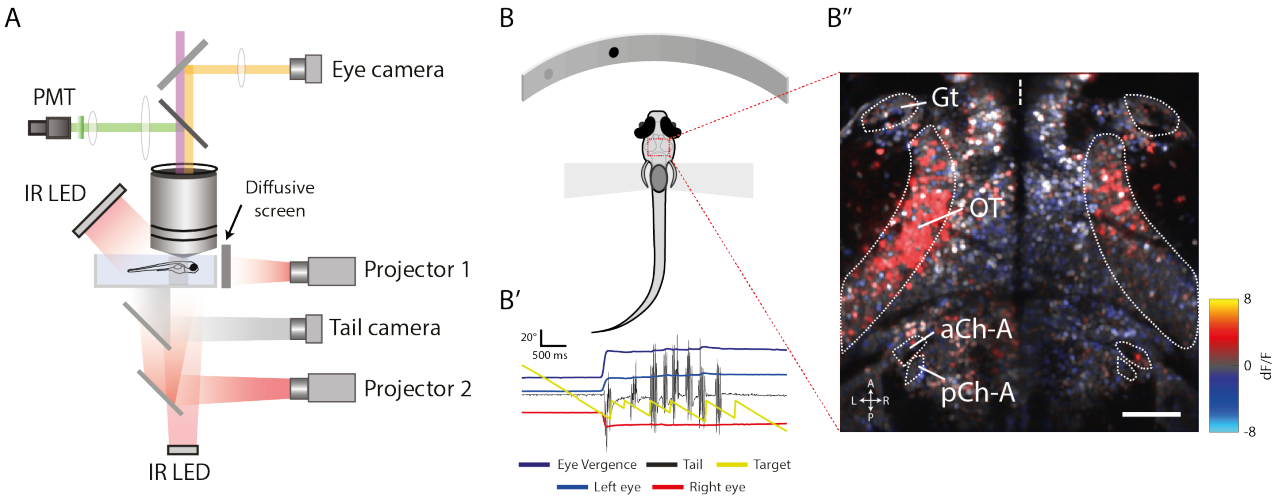

Figure 5.1: 2-photon imaging of NI neurons during closed-loop behaviour. (A) Schematic representation of the 2-photon virtual-reality setup to record neuronal activity simultaneously with behaviour in tethered larval zebrafish. In the experiments reported here, Projector 1 presents visual stimuli to the fish, while projector 2 also provides background light to the whole setup. Tail and eye kinematics are recorded through brightfield infrared (IR) illumination from bellow (eyes) and obliquely to the fish's body (tail). (B) Schematic representation of the mounting setup. Larvae are tethered by a block of agarose at the level of the swim bladder, while eyes and tail are free to move. (B') Tracked tail, eye and spot kinematics during a sustained hunting routine to the presentation of a prey-like spot. The spot is moved to the midline position when the fish converges its eyes and in follow-up tail swims. (B") Mean dF/F map of neuronal responses to a CCW moving prey-like spot within the imaging field-of-view. Scalebar 50 µm. Dotted lines mark several areas of the brain for which neuronal responses were recorded.

responsive (Spot CW) and (3) Directional CCW-moving prey-like spot responsive (Spot CCW) (Figure 5.2A). Most clustered neurons (N = 31980) fell into the WF class (84% versus 7% Spot CW and 9% Spot CCW, Figure 5.2B), which were widespread across the brain (Figure 5.2C). Prey-like responsive neurons were also found across the brain, but their distribution showed marked lateralization, particularly in the OT, where CW and CCW responsive neurons were more densely located in the right and left sides of the brain, respectively (Figure 5.D-E). In the NI, most neurons were not assigned to any of the cluster types (aCh-A: 77% , n = 139; pCh-A: 79%, n = 154; Ch-B: 88%, n = 108, unclustered, versus 60% across the entire dataset), suggesting

that most NI neuronal responses are not well explained by sensory responses to the tested visual stimuli. Of the clustered NI neurons, the large majority were WF responsive (Figure 5.2B, Figure 5.3D). However, a relatively large proportion of visually responsive aCh-A neurons were responsive to prey-like visual stimuli, as compared to other isthmic domains (aCh-A: 25%, pCh-A: 6%, Ch-B: 3%, Figure 5.3E,F). These cells also showed some evidence of being lateralized, particularly for CCW responsive cells, which were mainly localized to the right side of the brain (Figure 5.3F), although the small number of total cells included in spot-responsive clusters doesn't allow for a confident assessment of this lateralization. A quantification of the average response profiles of aCh-A neurons to CW and CCW moving spots in comparison to OT-SPV neurons revealed that aCh-A prey-responsive cells are activated to spots in the contralateral visual field, similarly to cells in the OT (Figure 5.3H,I). This suggests that aCh-A neurons receive ipsilateral input from the OT, as has been described in other species. Moreover, these responses begin when the spots are located at more central positions of the fish's visual field, as opposed to OT neurons which start responding at the beginning of the stimulus trajectory, which might suggest that the receptive field of aCh-A neurons is localized to more rostral regions of the visual field (Figure 5.3H,I).

These results strongly indicate that the activity of a small proportion NI neurons can be explained by sensory responses to prey-like and luminance visual stimuli. The localization of prey-like responses to the aCh-A indicates that this sub-population might be specialized in modulating hunting behaviour, which would fit with the previous finding indicating NI Type I neurons, which target the anterior OT and AF7 regions predominantly populating this domain.

5.1.2 NI neurons are specifically active during initiation of hunting

Since the activity of most NI neurons did not seem to be reliably sensory driven by the stimulus set presented here, perhaps they could be best explained by

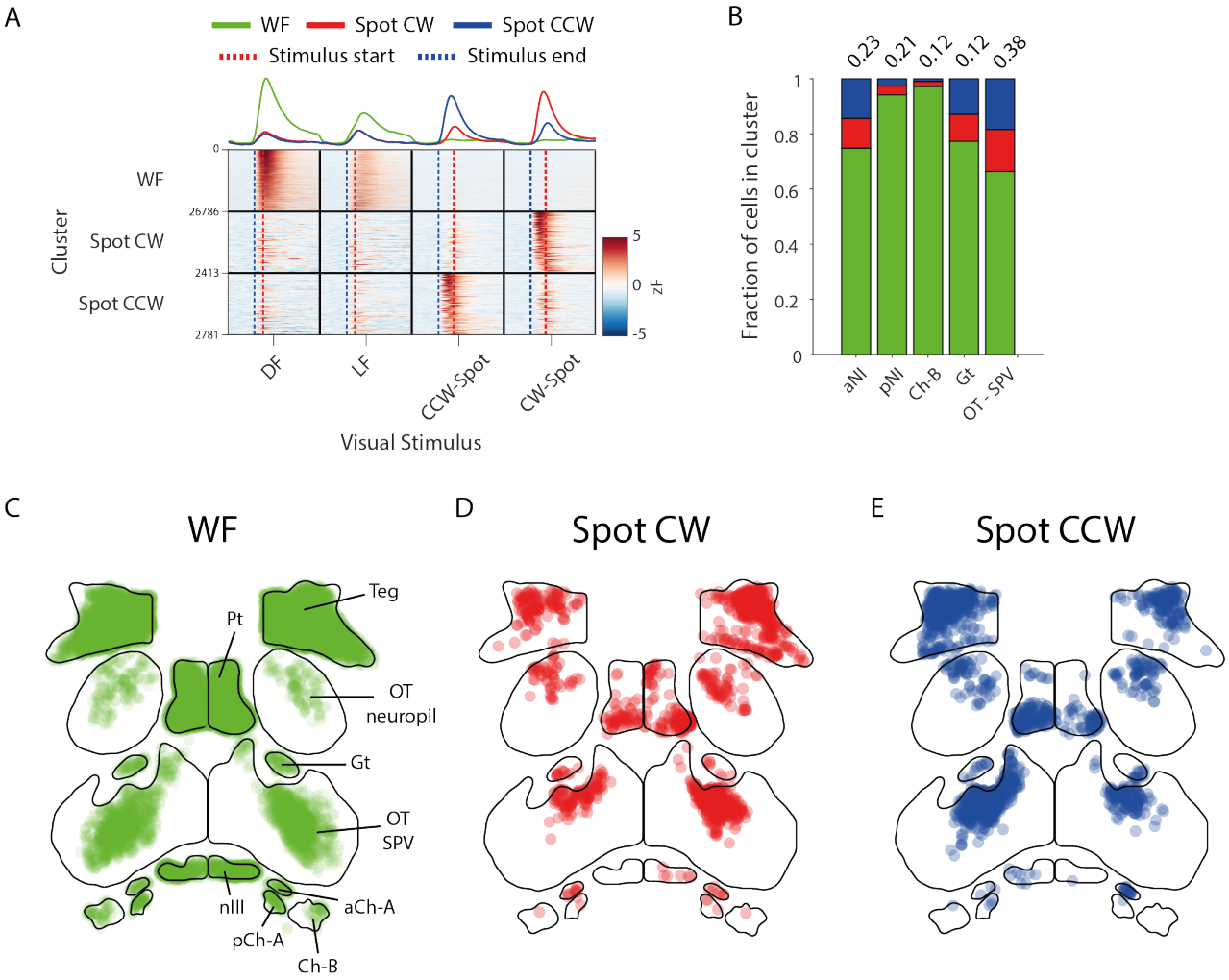

Figure 5.2: Visual responses to prey-like and luminance stimuli in the zebrafish midbrain and isthmus. (A) VRV clustered responses across all imaged ROIs. Top represents the average response of each cluster. Rows in the raster represent all ROI VRVs, separated by their cluster identity. Number on the left shown number of ROIs on each cluster (B) Fraction of cells in each clusters of representative brain areas. Numbers on top correspond to the total fraction of cells that were clustered. (C-E) Scatter plot of ROIs across several representative brain areas for each cluster type. For illustration purposes, distances between brain areas have been offset, but distances within each area are correct.

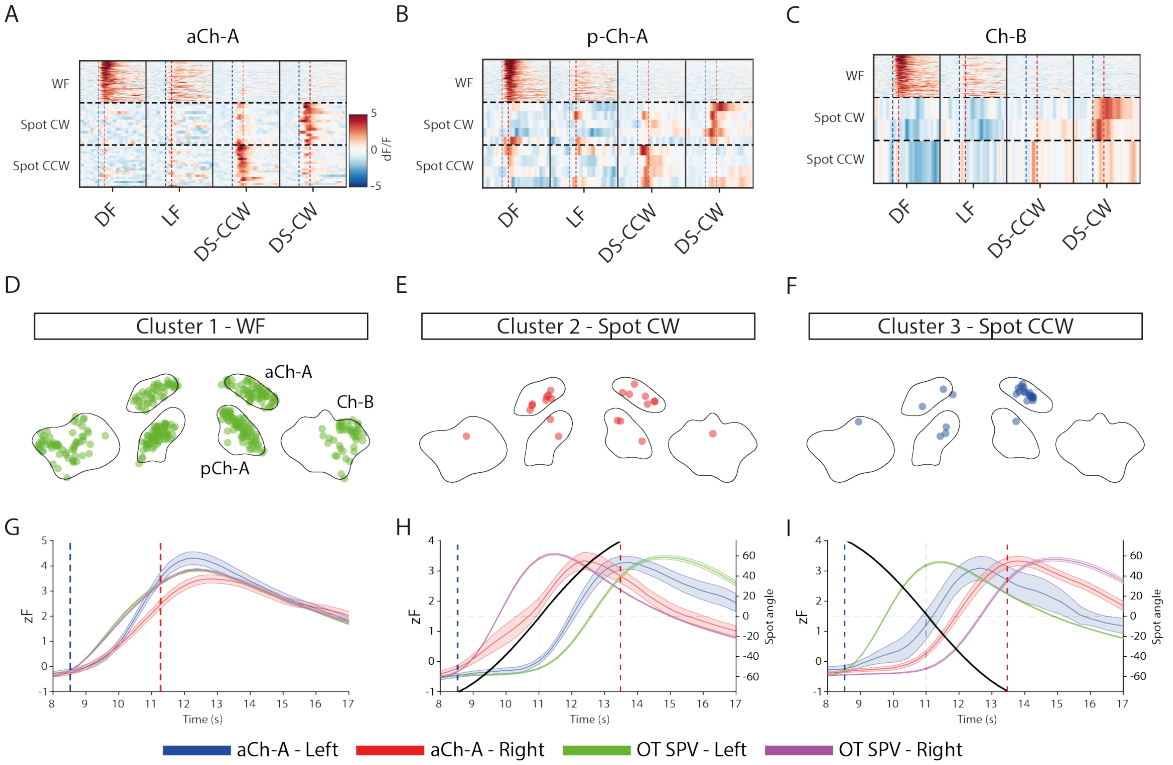

Figure 5.3: Visual responses in the larval zebrafish ithmus. (A-C) Clustered VRVs for aCh-A, pCh-A and Ch-B ROIs to visual stimuli. (D-F) Scatter plots of clustered isthmic ROIs. (G-I) Average response profiles of aCh-A and OT-SPV ROIs on both sides of the brain in response to visual stimuli. Blue and red dotted lines represent the start and finish of the stimulus presentation, respectively. Negative spot angles correspond to the left visual field of the fish.

motor variables related to hunting behaviours. Indeed, considering that NI ablation experiments strongly indicate that this population is involved in sustaining hunting responses, but produced no effect on prey perception, one tempting hypothesis is that NI neurons are activated at hunting initiation and throughout the routine. To examine hunting-specific motor-related activity, epochs were subdivided into those in which the fish engaged in hunting behaviour (defined by eye convergence) during the stimulus presentation window (GO epochs, n = 160, 5.8 ± 3.6%), versus epochs where no response occurred (NO-GO epochs, n = 2799, 94.2%). In addition, spontaneous convergences that occurred during the inter-stimulus interval were also analysed (n = 586, Figure 5.4).

Activity during convergences in the NI is relatively sparse, as only a small fraction of imaged cells is active (zF $>$ 2) during a 1 s window around the convergence event (aCh-A: 15 $\pm$ 11%, pCh-A: 12 $\pm$ 10%, Ch-B: 12 $\pm$ 11%), although it is likely that these values are not representative of the entire population, as only a small proportion of cells in each brain region is imaged at each z-position (aCh-A: 29 $\pm$ 7; pCh-A: 28 $\pm$ 11; Ch-B: 32 $\pm$ 14). Figure 5.4 shows the response of active isthmic, OT and Gt neurons during a GO epoch, and the activity of the same neurons during NO-GO and Spontaneous epochs. As can be observed, neurons in aCh-A, pCh-A and Gt are activated at the time of the convergence event, while activity in the OT seems to follow both visual and "pre-motor" activity, as a large fraction of neurons are active during stimulus presentation and preceding the convergence event. However, the same NI cells show little or no activity during a NO-GO or Spontaneous epoch, indicating these neurons don't reliably encode for sensory or motor related variables during hunting routines (Figure 5.4A'-C"). Rather, their activity might be sparse. In contrast, several Gt cells still respond during a spontaneous convergence, and these responses seem to be lateralized, suggesting that they are more reliably activated during convergence saccades, possibly encoding pre-motor commands related to hunting initiation (Figure 5.4C"')

To investigate and compare the population activity profile of isthmic neurons during convergence events, neuronal responses were aligned to the time of convergence and averaged. This revealed that both aCh-A and pCh-A neurons show increased activity at the time of convergence for both GO and Spontaneous events (Figure 5.5A,B). As can be observed, the responses are relatively small, which likely reflects that only a small proportion of neurons are active during convergence saccades. Ch-B neurons also show an increased activity at the time of convergence, but with smaller amplitude than the other isthmic populations (Figure 5.5C). Interestingly, while response amplitude seemed relatively similar for most neuronal populations, responses to GO epochs in aCh-A neurons showed a marked increased activity compared to spontaneous

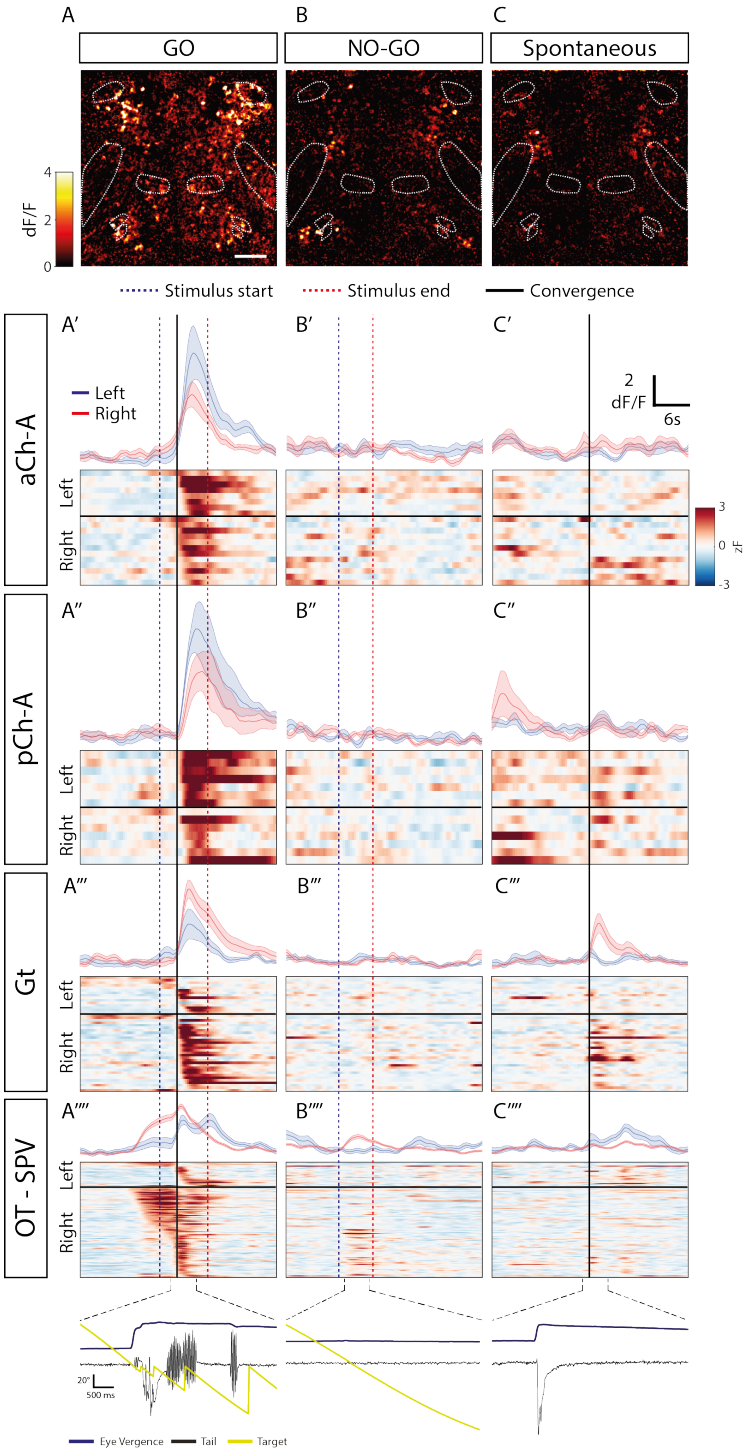

Figure 5.4: Convergence related activity in the NI. (A-C) Average zF responses of cells in the imaging field-of-view during a time windows around the convergence event (1s to each side) for GO, NO-GO and Spontaneous epochs. Scale bar, 50 µm. (A'-C"") Responses of the same cells selected by being active during a GO epoch (zF $>$ 2) across several representative brain areas during the same GO, NO-GO and Spontaneous epochs. Rasters represent activity traces for active cells during the convergence window. Plots on top are the mean across left and right active cells. Bottom traces represent the tracked tail and eye angles and the spot location during the epochs.

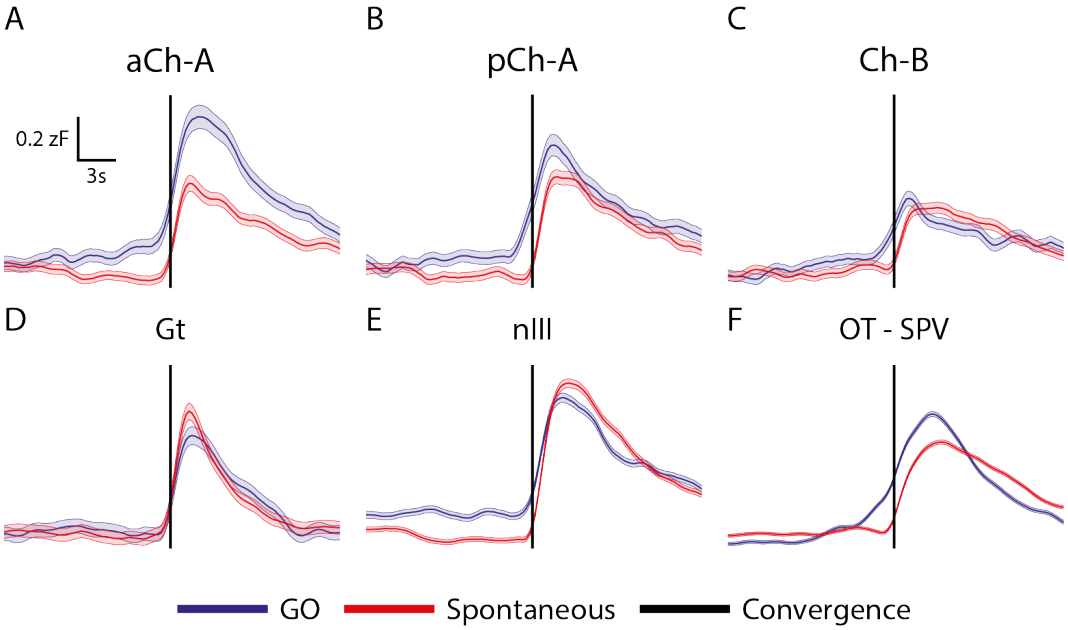

Figure 5.5: Response profiles of NI and other brain regions aligned to convergence events. (A-F) Average response profile of cells of representative brain regions aligned to convergence events in GO and Spontaneous epochs. Shaded region represents SEM across cells.

epochs (Figure 5.5A). Given the previous observation that several aCh-A neurons showed reliable sensory responses to prey-like visual stimuli, this increased activity compared to Spontaneous convergences is likely to represent a "contamination" of sensory responses. Indeed, all isthmic domains seem to show a small increased activity preceding the convergence event, indicating that this might be true for all domains. Alternatively, this activity increase might represent latent variables that do not represent the purely motor or visual components during convergent saccades, such as stimulus relevance.

5.1.3 aCh-A isthmic neurons encode convergence-related activity

To disentangle sensory versus motor-related components of neuronal responses during convergences, a metric was devised to compare neural activity in GO vs NO-GO trials (CZ-scores, see Methods). Briefly, for each hunting initiation event, a cell's mean response was measured during a time window surrounding the convergence event. This value was compared to the distribution of

responses measured at the same timepoint and for the same visual stimulus during NO-GO trials (Figure 5.6A). This ensures that neural activity is compared under equivalent sensory conditions (e.g., same stimulus at the same position in the visual field), to isolate the effect of the behavioural response. A similar metric was devised for Spontaneous responses, which compared spontaneous convergence activity with the "baseline" activity during no stimulus presentation periods (SpCZ-score, see Methods).

As convergences are generally lateralized, such that the change in position of one eye is usually larger than that of the other eye, and this is associated with the location of the stimulus (Bianco 2015), CZ-scores and SpCZ-scores were averaged within each cell based on whether the convergence involved higher change in angle of the left eye compared to the right, or vice-versa (Figure 5.6B-C). This allowed the investigation as to whether NI responses are lateralized with respect to convergence direction.

Comparing mean CZ-scores across several imaged brain areas reveals that aCh-A ranks as the area with the highest value (0.66 ± 0.34 for ipsilateral convergence) (Figure 5.6B,D). Indeed, these scores were comparable to those of the oculomotor nucleus (nIII), which are expected to be active during convergent saccades. Notably, high CZ-scores were also found in cells of the Gt and OT neuropil regions (Figure 5.6B-D), suggesting that these regions, along with aCh-A neurons, are triggered by hunting initiation. pCh-A and particularly Ch-B neurons did not have particularly high CZ- or SpCZ-scores, suggesting that their activity is not well explained by convergence events in general.

Interestingly, CZ-scores and SpCZ-scores also showed a marked lateralization with respect to convergence laterality in several brain regions, including in the aCh-A, OT neuropil, oculomotor and Gt, where higher values are seen in the side ipsilateral to the direction of the convergence (Figure 5.6B-D). This suggests that these regions might be act in synergy to modulate behaviour in a target-oriented fashion. Indeed, given the targeting of NI type I neurons, highly present in this region, to the OT neuropil and AF7, which is likely

presynaptic to neuron in the Gt, this highly suggests that NI Type I neurons mediate convergence related activity in the aCh-A region.

Taken together, these results strongly indicate that neurons of the NI, and particularly those belonging to the aCh-A domain, are activated in response to initiation of hunting behaviour, and point to their role in mediating visually evoked hunting routines towards prey-like stimuli.

5.1.4 NI neurons are responsive to looming stimuli

Following the observations that NI ablations seems to impair the contrast-gain during escape responses to looming stimuli, it seems likely that NI neurons would be activated by the presence of looming stimuli. Also, as we observed, hunting related activity seems to be more restricted to neurons in the aCh-A domain, which would fit with the hypothesis that these responses are mediated by NI Type I neurons. Are NI neuronal responses in the pCh-A and Ch-B domains better evoked by threatening stimuli such as looming spots? To test this, I recorded neuronal responses in a similar part of the brain as the experiment above, but in response to looming stimuli presented in front of the fish's visual field. As this represents only a preliminary dataset (n = 3 fish), I will only present results for sensory responses to looming stimuli, without considering how activity in the NI might relate to motor components of escape responses.

Looming stimuli as well as luminance control stimuli, which had similar intensity dynamics as the looms were presented to larvae in a similar setup as the experiment described above for hunting responses. ROI VRVs were computed in a similar fashion but were clustered using the K-means clustering algorithm (see Methods). Several types of visual responses were observed across the brain, of which two clusters showed clear responses to looming stimuli (Figure 5.7).

In the first cluster, neuronal responses ramp up at the beginning of the looming stimulus (Loom early) while in the second cluster, responses increase primarily at the end expansion stages of the stimulus (Loom late) (Figure

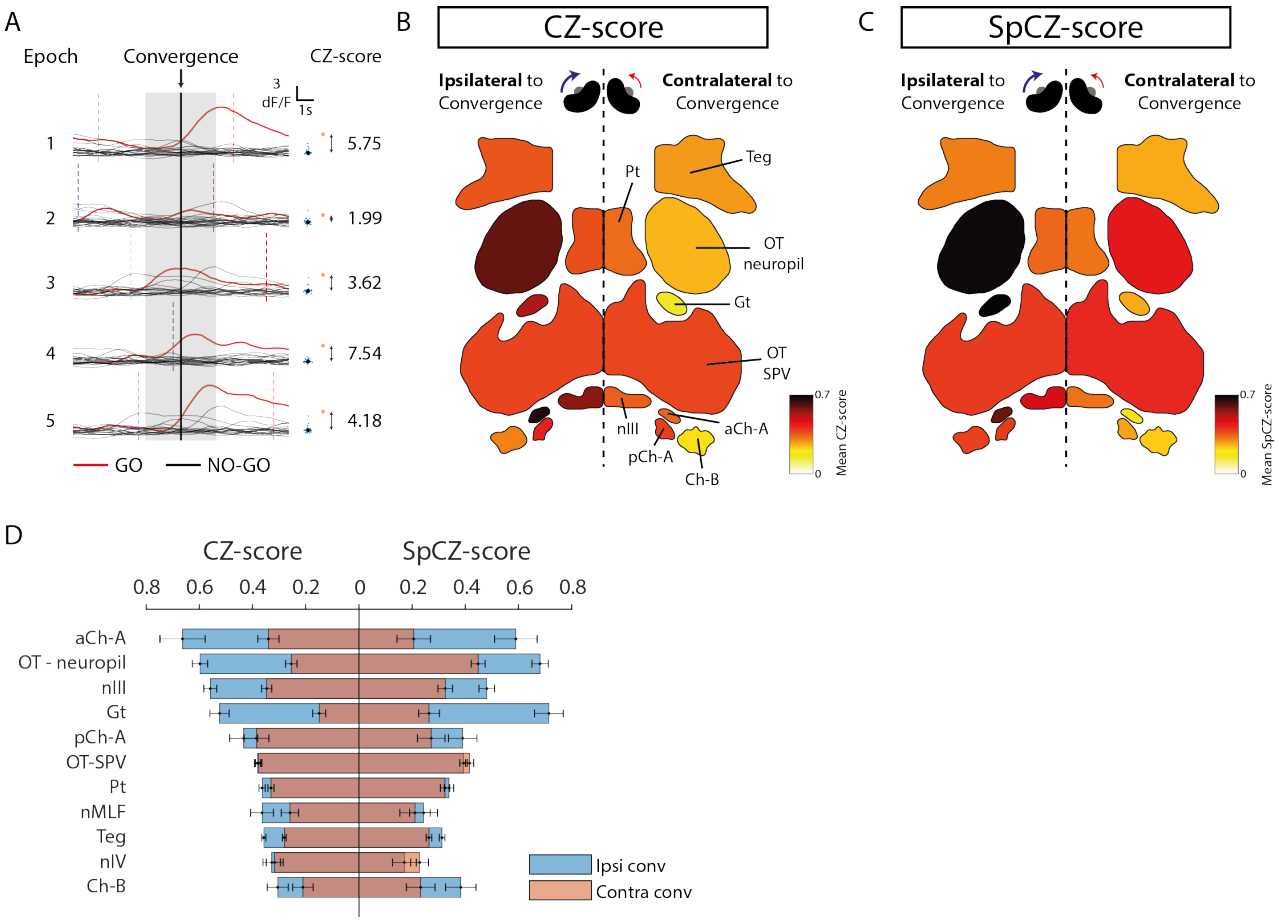

Figure 5.6: Convergence related activity in the Isthmic and other areas of the zebrafish larval brain. (A) CZ-Score calculation. For each cell, (one example cell is represented here) all epochs where a convergence event occurred during the stimulus ON time are taken. Then, for each epoch, a mean zF value is calculated across a convergence time window (shaded grey area), and compared with the distribution of mean values during NO-GO epochs at the same time where the convergence occurred in the GO trial. The CZ-Score is calculated as the distance between the GO value and the mean of the NO-GO distribution in units of its standard deviation. (B-C) Schematics of several brain areas coloured by their average CZ-score or SpCZ-score to ipsilateral or contralateral convergences. For illustration purposes, distances between brain areas have been offset. (D) Ranked mean CZ-score and SpCZ-score of several brain regions calculated based on brain and convergence laterality.

5.7). As can be observed, several neurons in all isthmic cholinergic nuclei both types of responses and with similar dynamics (Figure 5.7A-B; aCh-A 8.7%, N = 173; pCh-A 9.4%, N = 266; Ch-B 10.5%, N = 487). Mapping cell locations belonging to these clusters reveals that cells from both cluster types seem to be well distributed between all domains (Figure 5.7C,D). This suggests that looming responsive neurons might not segregate between isthmic cholinergic sub-nuclei, although this represents a small dataset, and thus more data needs to be acquired to confidently provide a conclusion. Both cluster types seem to be lateralized in the OT, which might reflect either slight asymmetries in the location of the visual stimulus with respect to the position of the fish or, particularly in the Loom late cluster, related to the motor response direction (Figure 5.7E,F). Investigation of the motor kinematics during these presentations will be required to assess these hypotheses.

Nevertheless, these results confirm that NI neurons, albeit on all cholinergic isthmic domains, are responsive to looming stimuli. Further, these responses can be categorized as responses during the initial expansion phase of the looming stimulus and to the later expansion "near collision" stage. This is in agreement with observations in other teleost species, that the NI is particularly responsive to looming stimuli (Gallagher and Northmore, 2006).

5.2 Discussion

The NI has largely been considered as a visually responsive structure, and several studies have investigated the responsiveness of NI neurons to a multitude of visual stimuli, including moving targets (Cui and Malpeli, 2003), luminance changes (Wiggers and Roth, 1991; Northmore and Gallagher, 2003) and looming stimuli (Gallagher and Northmore, 2006; Mysore and Knudsen, 2014; Asadollahi et al., 2010). This study, however, provides the first description of NI activity in animals actively engaged in an ethologically relevant behaviour.

Here, a subset of NI neurons of zebrafish larvae, particularly those lo-

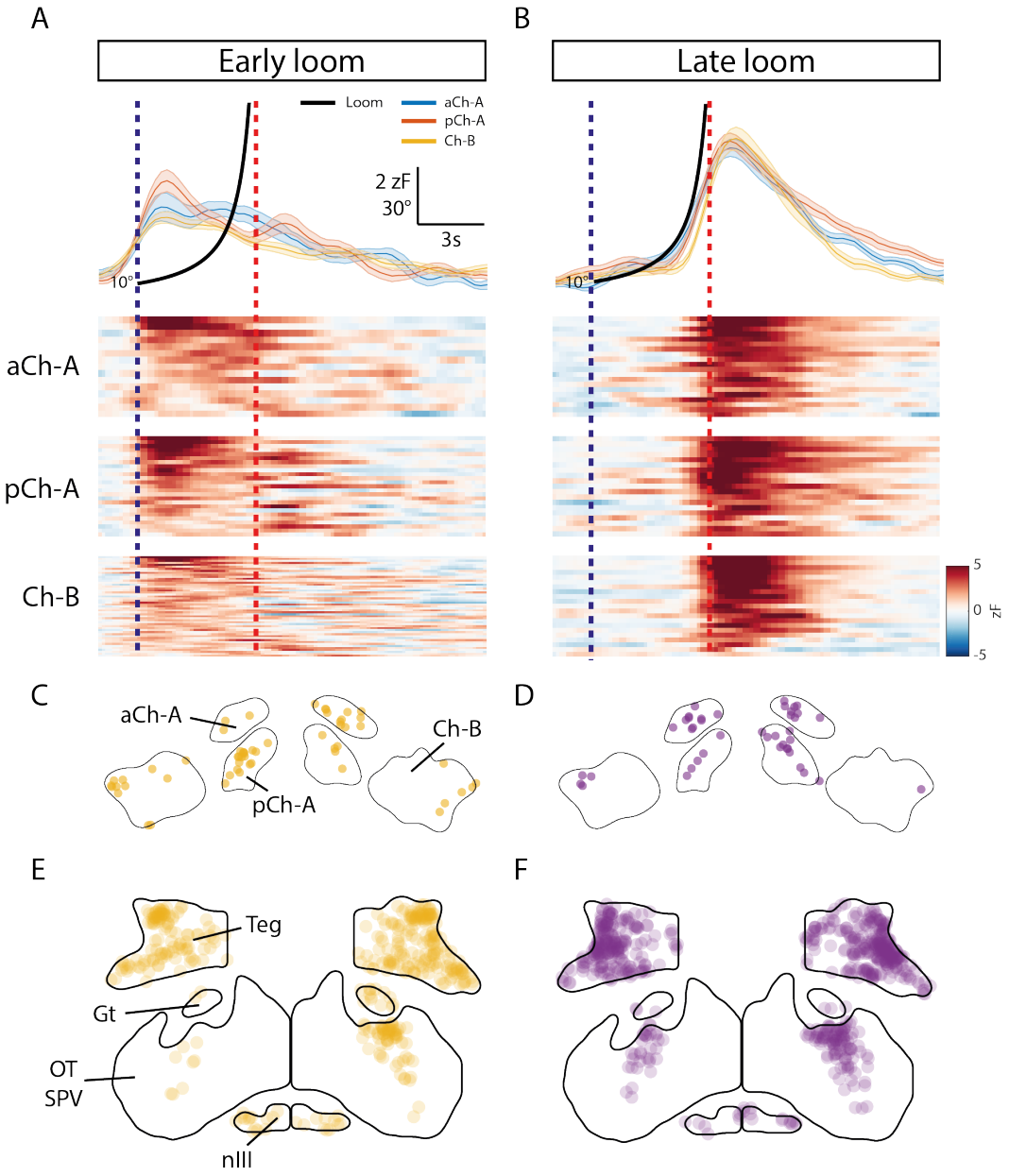

Figure 5.7: Responses to looming stimuli in the NI. (A) Early loom cluster activity of cholinergic isthmic nuclei. (B) Late loom cluster activity of cholinergic isthmic nuclei. Raster represents mean zF responses of clustered ROIs. (C-D) Scatter plot of ROI locations in A and B in the isthmic cholinergic nuclei. (E-F) Scatter plot of ROI locations across the rest of imaged areas of the brain. For illustration purposes, locations of brain regions have been offset, but ROI locations within regions are correct.

cated in the aCh-A domain, were found to respond to prey-like stimuli. The timing of these responses suggests that they receive input from ipsilateral OT neurons and are responsive at most rostral regions of the visual field. These observations make this population particularly well suited to modulate hunting behaviour. Indeed, by decoupling sensory and motor-related activity at the time of convergences (CZ-score), the results presented here strongly indicate that activity of aCh-A neurons is tightly linked to initiation of hunting routines. In contrast, few cells in the pCh-A and Ch-B domains were found to reliably respond to prey-like stimuli, although pCh-A neurons also seem to encode some convergence-related activity. Considering that NI Type I neurons are almost exclusively found in the aCh-A domain and their innervation pattern strongly suggests their role in hunting behaviour, it seems likely that prey-like responses and convergence related activity in the NI is broadcast by this cell type, although direct evidence of this is still needed.

Hunting initiation or maintenance

The results presented thus far indicate that NI, and specifically, aCh-A neurons, play an active role in hunting. Moreover, their activation concordant with convergent saccades might suggest that they mediate hunting initiation rather than maintenance of targeted routines. A careful analysis of the Ca^{2+} in relation to behaviour could provide evidence towards one or both hypothesis. For instance, if NI provided a maintenance signal, we might have observed "spikes" of activity concordant with successive orienting turns during a hunting sequence, if the NI provides phasic input to the OT. Moreover, a sustained increase of activity for the duration of a hunting sequence would suggest a tonic facilitation signal. However, the slow dynamics of GCamP6s ($\tau \approx 3.5$ s, Migault et al. (2018)) compared to the fast behaviour render this analysis challenging. Thus, it is difficult to infer if NI activity commences prior to or just after the initiation of hunting. Moreover, extended hunting routines are rare in tethered preparations, and while they can be observed, as in Figure

5.1B, most terminate after one or two swim bouts (data not shown).

Nevertheless, NI ablation does not impair hunting initiation (Figure 4.4E) or bout kinematics (Figure 4.6D-H) in free swimming conditions, but does severely impair larva's ability to maintain a targeted sequence of orienting turns (Figure 4.4F). Thus, in combination with the loss-of-function results, the results presented here support a model in which NI is recruited during hunting routines and functions to support the maintenance of those routines.

Facilitation of neuronal responses

What might be the effect of NI feedback to the tectum at initiation of hunting? Considering that NI ablation has the specific effect of impairing the ability to sustain hunting routines towards target prey, these results are in favour of the hypothesis that the NI acts to facilitate continued targeting of prey during hunting routines. The simplest mechanistic model for how this might be achieved is that isthmo-tectal/pretectal input selectively excites or modulates activity of neurons in the rostral tectum and AF7 after hunting initiation, facilitating responses to rostrally located prey. This facilitation might be crucial to evoke fast directed behavioural manoeuvres towards a quickly evading prey. A more complex mechanism might involve the parallel activation of globally inhibitory circuitry, likened to the selective attentional winner-take-all mechanism thought to be modulated by the isthmic Ipc/SLu and Imc subpopulations of birds (Knudsen, 2018), although no direct evidence for such a mechanism to exist in other species have been provided yet.

Nevertheless, supporting evidence of the NI's role in response facilitation of OT neurons is provided by experiments where co-stimulation of the optic nerve and the ipsilateral NI are reported to enhance calcium influx of retino-tectal fibers in the frog (Dudkin and Gruberg, 2003), a mechanism thought to be mediated by nicotinic ACh receptors present in these fibres (Butt et al., 2000). Similarly, blocking Ipc excitation in barn owls decreases the gain and spatial discrimination of tectal units associated with the blocked Ipc neurons

(Asadollahi and Knudsen, 2016), although modulation of tectal outupt in birds is likely to be mediated by excitatory glutamate release at dendritic terminals of tectal neurons (González-Cabrera et al., 2015). Whether NI terminals in the larval zebrafish pre-synaptically contact retino-tectal fibres, or tectal dendrites, is still undetermined.

NI encoding of stimulus salience

Neurons of the cat's parabigeminal nucleus (PBG) seem to encode the position of a moving target, as measured by its retinal position error (RPE), even when the target briefly disappears (Ma et al., 2013). Moreover, when two stimuli are presented at the same time, PBG neurons respond to the target that is selected to saccade to, indicating that their activity is primarily determined by the behavioural relevance of a stimulus, rather than their sensory features. Also, Ipc neurons in the avian isthmus respond with increasing firing rates to increased contrast and speed of visual stimuli (Asadollahi et al., 2010; Asadollahi and Knudsen, 2016) and level of sounds (Maczko et al., 2006), and their response is quickly switched off when a competing stimulus outside their receptive field is more salient that the stimulus being presented at their receptive field centre (Asadollahi et al., 2010). In teleost fish, extracellular NI recordings to checker ball stimuli moving in a variety of different paths revealed that NI neurons are particularly responsive to approaching stimuli, and that its activity ramps up as a function of the stimulus' proximity (Gallagher and Northmore, 2006). These responses also tend to habituate to repeated visual stimulation, which conforms with the hypothesis that visual salience or novelty is an important factor determining NI activity. These observations are in line with the hypothesis that NI neurons encoding the salience or relevance of a visual target across different species.

The experiments presented here in the larval zebrafish were not specifically design to unambiguously discriminate the salience of visual stimuli. One can hypothesise, however, that the selective activation of NI neurons at hunting

initiation and ipsilateral to the convergence direction might suggest their role in modulating activity targeting specifically relevant stimuli, such as target prey. It would be interesting in the future to record NI activity in the presence of multiple competing prey-like stimuli and investigate if NI responses follow the target stimulus selected for behaviour. Further, changing feature properties of these stimuli, such as their contrast, might prove useful in determine If NI neurons discriminate between relevant and salient stimuli. Although these two properties might be difficult to disentangle, assessing targeted behaviour during such experiments might provide useful in distinguishing the two.

Future perspectives

Following the apparent segregation of aCh-A and pCh-A neurons in response to hunting, and their different morphologies, it would be interesting to record activity in these populations in response to looming spots in order to investigate if these populations might be specialized to modulate different behavioural responses, such as to escape versus predate. Ideally, one would like to be able to identify responses coming from NI Type I and Type II neurons. Although the lack of live markers of these neurons make this a difficult task, it would be possible to post-mortem independently label these two subpopulations by retrogradely tracing ipsilateral AF7 projections (from NI Type I neurons) and contralateral OT projections (from NI Type II neurons). Registration of retrogradely labelled brains to an image stack of the live brain used for functional imaging might allow a 1:1 match of neuronal responses with their projection identity.

These results also indicate that the larval zebrafish NI, as has been observed in other teleost species, responds to the presentation of looming stimuli (Gallagher and Northmore, 2006). It further adds that at least two types of responses, one in the early expansion phase, and another in the late "near collision" phase of the looming stimuli can be observed. What might be the function of these two populations? It's possible that the early loom population

might signal salient stimuli in the visual field of the larva, perhaps facilitating sensory responses to those locations, while the late loom population might be signal the near collision of a stimulus, and facilitate pre-motor activity in the tectum to induce escape responses. If so, perhaps the first population would also respond to other stimuli such as prey-like spots, while the responses of the second population might relate better with motor variables, such as the convergence related activity reported in neurons of the aCh-A domain. It would be interesting to understand how these functional responses tie with their respective axonal morphologies.

In conclusion, the results presented here provide evidence that the larval zebrafish NI is responsive to prey and looming stimuli, and that neurons predominantly in the aCh-A domain signals the initiation of hunting behaviour and might be required for providing facilitation of continuous behavioural responses towards target prey.

Chapter 6

General Conclusions

6.1 Summary

The work presented was set to provide a better understanding on how the nervous system has the ability to provide animals to sustain behavioural responses towards particular target stimuli which might be relevant to the animal's goals. To that end, the Nucleus Isthmi of the larval zebrafish was thoroughly investigated in the context of hunting behaviour, which in larvae involves a sustained engagement with a moving prey. Several findings provide clues to the involvement of this small midbrain tegmental nucleus in the larva's ability to engage with ethologically relevant visual stimuli:

1. Morphologically, neurons of the larval NI have two types of projection patterns: NI Type I neurons project to the AF7 retinocipient neuropil and the anterior OT and target the most superficial retinocipient laminae of the OT, while NI Type II neurons project bilaterally to the OT and target deeper retinocipient laminae and are more spread-out across the OT space map. The dendrites of these two types of neurons are also different, branching in opposing directions, which might indicate that they're postsynaptic to different neuronal populations.

2. Loss-of-function experiments of the larval NI, where neurons predominantly in the Ch-A domain were bilaterally ablated, impairs the ability of free-swimming larvae to sustain targeted hunting routines towards

live paramecia. This ultimately leads to most routines being aborted midway. Using an extensive characterization of hunting kinematics, including fish-target features during hunting routines, I found that this effect is very specific, as initial prey detection and the larva's sensory and motor capacity to orient towards target prey was not impaired.

3. Although fish were still able to correctly escape from looming visual stimuli simulating approaching threats in after NI ablation, a rightwards shift of the contrast-response function was observed for NI ablated larvae, which suggests that NI neurons modulate behavioural responses to looming stimuli by lowering the contrast sensitivity, likely by modulating responses of tectal neurons. This modulation might act through NI Type II neurons, which seem more likely to provide response facilitation across a large proportion of the tectal space map, a possible requirement as looming threats are likely to show up from any location in the fish's surroundings.

4. Imaging of neuronal responses in the larval NI during a virtual-reality setup where tethered fish were able to engage in sustained hunting of prey-like visual stimuli revealed that NI neurons, and particularly those located in the anterior Ch-A domain, increase their activity at the initiation of hunting. This supports the hypothesis that NI Type I neurons, which are localized to the aCh-A domain, might be specifically recruited to modulate neuronal responses during hunting routines.

6.2 A mechanistic model for NI-mediated response facilitation

Using the evidence provided in this study, and considering the current knowledge of the brain circuitry involved in hunting behaviour of zebrafish larva, I propose the following model (Figure 6.1A) for how the NI modulates the continuous targeting of prey during hunting routines:

1. Visual information of moving prey is received in the retina and transmitted to the contralateral OT and AF7;

2. Non-linear mixed selectivity (NLMS) neurons in the tectum that are tuned to prey-like features recognize the stimulus as prey (Bianco and Engert, 2015);

3. Tectal neurons, perhaps neuronal assemblies that are activated at hunting initiation, activate ipsilateral NI Type I neurons, which topographically feedback onto the anterior OT and AF7;

4. OT and pretectal neurons in the Gt, which might be required to gate the activation of downstream hunting pre-motor circuitry, activate hunt promoting neurons in the reticulospinal system (RS), which elicit orienting bouts through innervation of downstream spinal cord neurons, leading to sustained hunting routines.

5. A feedback loop is established in which sensory responses, but possibly also pre-motor tectal activity, in the anterior visual-field are facilitated. This might be mediated though ACh release from NI Type I terminals in retinotectal superficial terminals.

In the case that NI feedback is disrupted, it is possible that visual information from target prey is unable to reach a response threshold, leading to an aborted routine. It is also possible that other modulatory systems or competing visual stimulation are allowed to overtake target-induced responses, changing the behavioural state of the animal.

On a more speculative note, it is possible that NI Type II neurons might modulate a different behaviour, such as escape responses to looming threats (Figure 6.1B). Given that the axonal processes of these neurons are more widespread across the tectal map and target deeper regions of the OT, it seems plausible to think that they might mediate more generalized arousal states to visual stimulation. However, it cannot be excluded the hypothesis

that these neurons also modulate hunting behaviour, as prospective pCh-A and Ch-B neurons were also found to be active during hunting. Indeed, Type II neurons might facilitate integration of other sensory (eg., olphactory) and/or internal signals (eg., hunger), allowing the maintenance or termination of the hunting state. Specific targeting of these neuronal population with the help of live genetic markers paired with hunting and looming escape behaviours could provide evidence to support these hypotheses.

Finally, although this study does not provide direct evidence that the larval zebrafish's NI functions as mechanism that mediates visual selective attention, as such would require convincing proof that it somehow mediates target selection and suppression of competing distractors (Wiederman and OCarroll, 2013; De Bivort and Van Swinderen, 2016), the results reported in this thesis suggest that this could be the case. Indeed, the topographic and narrow-field mapping of NI Type I projections are in concordance with the site-specific facilitation of target responses in competition assays in birds (Asadollahi et al., 2010). In the future, studies where competing distractor stimuli are presented in a control tethered preparation could provide evidence that NI neurons of zebrafish larvae selectivelly respond to salient/relevant target stimuli.

Taken together, this study's use of state-of-the-art tools to interrogate the role on the NI in the behaviour of zebrafish larva uncovered its role in the larva's ability to sustain hunting responses towards target prey. This is likely to be a part of a conserved vertebrate mechanism to sustain behavioural responses towards ethologically relevant stimuli. More generally, this approach projects onto the general goal of systems neuroscience to understand the computational, algorithmic and implementation levels employed in by nervous system, linking sensory perception to behaviour. In this context, future studies using similar frameworks will be able to provide clear insights on how attention is generated in the brain, and how evolution has shaped these mechanisms, from the tiny zebrafish larva, to those of the adult human.

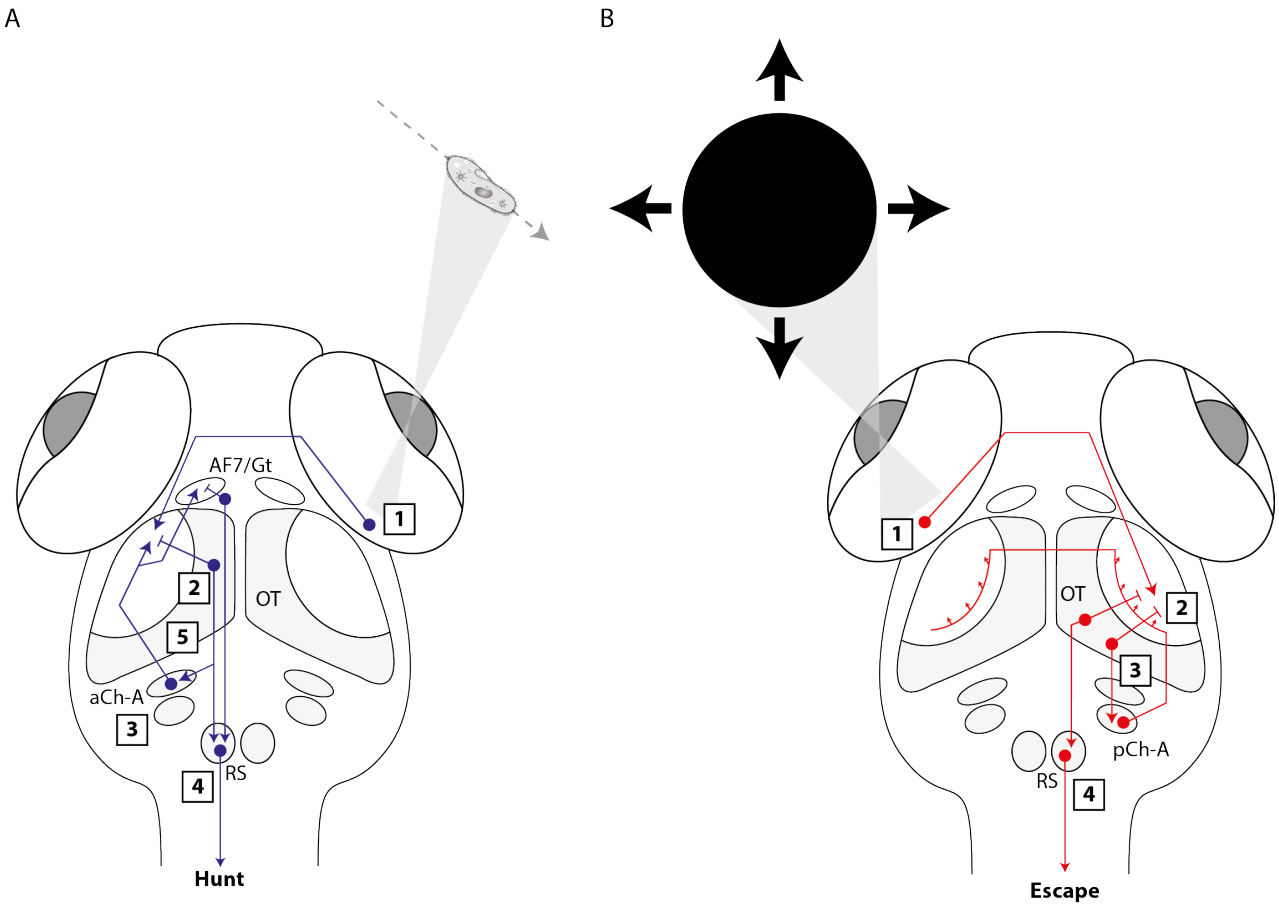

Figure 6.1: Model circuit for NI modulation of visual behaviours. (A) NI Type I mediate facilitation of sustained hunting routines: (1) Visual information of moving prey is received in the retina and is simultaneously transmitted to the contralateral OT and AF7; (2) Non-linear mixed selectivity (NLMS) neurons in the tectum tuned to prey-like features recognize the stimulus as prey; (3) This information is relayed to ipsilateral NI Type I neurons, which topographically feedback onto the anterior OT and AF7; (4) Pre-motor activity, which might be gated by pretectal Gt output, is relayed to the reticulospinal system (RS) to activate hunt promoting neurons, which elicit orienting bouts through innervation of downstream spinal cord neurons. (5) A feedback loop is established in which sensory and/or pre-motor response in the anterior visual-field are facilitated; (B) NI Type II mediated facilitation of escape behaviour: (1) Visual features related to looming spots are transmitted to the contralateral OT; (2) Tectal neurons relay loom-related activity to the NI; (3) NI Type II neurons facilitate responses bilaterally across the tectal map, lowering their response threshold; (4) Pre-motor activity in the OT is relayed to the reticulospinal system to activate escape promoting neurons, which elicit an escape manoeuvre by stimulation of downstream spinal cord neurons.

Chapter 7

Materials and Methods

7.1 Animals

Adult zebrafish (*Danio rerio*) were maintained and bred according to standard procedures. Embryos and larvae were maintained in a 14/10-hour light/dark cycle.

All experiments were conducted on 6 days-post-fertilization zebrafish larvae homozygous for the nacre mutation, except larvae used for single-cell electroporation, where 0.002% phenylthiourea (PTU) was added to fish water from 12 hours-post-fertilization to inhibit pigment formation. Larvae used for free-swimming behaviour, retrograde DiI iontophoresis and Ca^{2+} experiments also expressed nuclear localized GCaMP6s [Tg(elavl3:H2B-GCaMP6s) (Vladimirov et al., 2014). Single-cell electroporation experiments used double transgenic larvae from a cross between Tg(ETvmat2:GFP) (Wen et al., 2008) and Tg(atoh7:GFP) (Masai et al., 2003). Larvae used for behaviour and Ca^{2+} imaging experiments were maintained in the Tuebingen wild-type background strain.

Ethical approval for zebrafish experiments was obtained from the Home Office UK under the Animal Scientific Procedures Act 1986.

7.2 Whole-mount in situ hybridization and immunohistochemistry

Fluorescent in situ hybridization and immunostaining was performed as previously described (Lauter et al., 2011; Macdonald, 1999). Cy3 tyramide (Perkin-Elmer) was used for single *in-situ* hybridizations and combined with Cy5 and Fluorescein (Perkin-Elmer) for triple-fluorescent *in-situ* hybridizations. *mRNA* anti-sense riboprobes for *chata*, *chatb*, *vachta*, *vachtb*, *hacta* and *hactb* were kindly provided by Marnie E. Halpern (Hong et al., 2013). *reelin* (Costagli et al., 2002), *vglut2b* (Chong et al., 2005) and *gad1b* (Mueller and Guo, 2009) riboprobes were synthesised as previously (Thisse and Thisse, 2008).

For antibody detection, rabbit anti-Calretinin antibody (Cwant, Cat 7697, dilution 1:1000), mouse anti-ERK (p44/42 MAPK (Erk1/2) 4696, dilution 1:500) and rabbit anti-GFP (Torrey Pines Biolabs, TP 401, dillution 1:1000) were used as primary antibodies, and Alexa Fluor 488-conjugated (Molecular Probes, dillution 1:200) secondary antibody was used.

7.3 Lipophilic dye tracing by iontophoresis

Larvae of Tg(elavl3:H2B-GCaMP6s) were fixed at 6 dpf by overnight incubation in 4% paraformaldehyde (PFA) in 0.1 M sodium phosphate and 4% Sucrose (Sigma-Aldrich). Larvae were then mounted on a glass slide in drops of 2% low melting point agarose (Sigma) in 0.1 M sodium phosphate buffer, pH 7.4 (PBS). Using a microsurgical blade, a small chamber of agarose was cut from the right or left side of the fish's head, exposing half of the head and eye. Micropipettes with a tip diameter of 1-2 µm were pulled on a P-87 micropipette puller (Sutter Instrument Company, CA) using AlSi glass capillaries containing a filament. Micropipettes were then filled with a solution of the fluorescent carbocyanine dye 1,1'-dioctadecyl-3,3,3',3'-tetramethylindocarbocyanine perchlorate (DiI) (Molecular probes) and guided to either the OT or AF7 neuropil using a MX3000 Huxley-style micromanipulator (Soma Scientific Instruments) under x40 water-immersion DIG optics (Axioskop 2 FS microscope, Carl Zeiss)

and under fluorescent light (FITC filter). DC electrical stimulation was then applied using a 9V Alkaline Battery. The dye flow was directly observed under fluorescence. After dye application, larvae were unmounted and incubated in PBS in the dark at 4° for a period of 7-10 days to allow the dye to travel. Such long incubation period was probably not necessary but was used to make sure the dye was able to travel to the contralateral NI. Larvae were then mounted and imaged under laser scanning confocal microscopy (Leica TCS SPE or SP8) using a water immersion objective (HC FLUOTAR L 25x/0.95 W VISIR, LEICA).

Retrogradely labelled cells were counted manually using the ImageJ Cell Counter plugin using the original image volumes. The elavl3:H2B-GCaMP6s imaging channel was used to assess cell body staining. Images were then registered to the ZBB atlas and cell coordinates were transformed to the atlas' reference frame using the ANTs toolbox with the following parameters for a registered 3D image volume "fish1" and centroid positions file "centroids.csv":

```
antsApplyTransformsToPoints -d 3 -i centroids.csv -o
    ↪ centroids_ZBB.csv -t [fish1_0GenericAffine.mat,1] -t [
    ↪ fish1_1InverseWarp.nii.gz,0]
```

7.4 Focal electroporation

Cell electroporations were done as previously described (Zou et al., 2016). Briefly, double transgenic larvae of Tg(ETvmat2:GFP) and Tg(atoh7:GFP) at 4 dpf were anesthetised with Tricane (0.02%, Sigma) and mounted in a custom made slide (Zou et al., 2016). The microscope and micropipettes used were the same as for lipophilic dye application. Micropipettes were filled with a solution of Dextran, Tetramethylrhodamine and biotin, 3000 MW, Lysine Fixable (0.2 mg/mL in dH2O) and guided to a position anterior to the identifiable Locus coeruleus. Electrical stimulation was then applied with the following parameters: short (< 0.5 s) trains of 2 ms square pulses at 200 Hz and a po-

tential difference of 5-7 V. Trains were delivered 1-5 times with approximately 0.5 s interval between them. Pulses were generated with a Grass SD9 stimulator (Grass-Telefactor, West Warwick, RI). After the procedure, larvae were unmounted and returned to their housing conditions. At 6 dpf, larvae were anesthetised and imaged under laser scanning confocal microscopy.

7.5 3D image registration

Registration of image volumes was performed using the ANTs toolbox version 2.1.0 (Avants et al., 2011). Images were converted to the NIfTi format required by ANTs using the ImageJ plugin nifty_io.jar. As example, to register the 3D image volume in fish1–01.nii.gz, to the reference brain ref.nii, the following parameters were used:

```
antsRegistration -d 3 -float 1 -o [fish1_, fish1_Warped.nii.gz]
   ↪ -n WelchWindowedSinc -r [ref.nii, fish1-01.nii.gz,1] -t
   ↪ Rigid[0.1] -m MI[ref.nii, fish1-01.nii.gz,1,32, Regular
   ↪ ,0.25] -c [200x200x200x0,1e-8,10] -f 12x8x4x2 -s 4x3x2x1 -
   ↪ t Affine[0.1] -m MI[ref.nii, fish1-01.nii.gz,1,32, Regular
   ↪ ,0.25] -c [200x200x200x0,1e-8,10] -f 12x8x4x2 -s 4x3x2x1 -
   ↪ t SyN[0.1,6,0] -m CC[ref.nii, fish1-01.nii.gz,1,2] -c [200
   ↪ x200x200x200x10,1e-7,10] -f 12x8x4x2x1 -s 4x3x2x1x0
```

The deformation matrices computed above were then applied to any other image channel N of fish1 using:

```
antsApplyTransforms -d 3 -v 0 -float -n WelchWindowedSinc -i
   ↪ fish1-0N.nii.gz -r ref.nii -o fish1-0N_Warped.nii -t
   ↪ fish1_1Warp.nii.gz -t fish1_0GenericAffine.mat
```

Registrations were performed using UCLs Legion cluster. Usually, jobs were performed using a Dell C6220 node with 16 cores and 16 GB of RAM.

Registration was usually finished after 2-4h using these specifications for a volume of 1030x616x420 px.

All brains were registered onto the ZBB brain atlas (Marquart et al., 2015), with some differences between experiments:

- For functional Ca^{2+} live image stacks, a three-step registration was used: the imaging volume, which was usually composed of 2-7 image stacks was first registered to a larger volume of the same brain taken after the experiment using only rigid and affine transformations (this aligns the volumes very well as they are taken from the same brain). Then, the larger volume was registered onto a high-resolution 3D whole-brain volume of a 6 dpf brain expressing elavl3:H2B-GCaMP6s, which was imaged using the same 2-photon microscope that was used during functional Ca^{2+} imaging. I found that this works better than registering the large volume directly onto the ZBB atlas. Since the high-resolution volume had already been registered onto the ZBB atlas, the transformations were concatenated to bring the functional imaging volume to the ZBB atlas (Ca^{2+} > post-stack > Hi-Res > ZBB).

- For imaging volumes related to NI cells ablations, the post-ablation stack was registered to the pre-ablation stack of the same brain using only rigid and affine transformations. This was done to ensure that the ablation "scar", which was also apparent in the registration channel, did not interfere with the registration procedure. The pre-ablation volume was registered to the high-resolution elavl3:H2B-GCaMP6s brain. The post-ablation stack was then transported to the ZBB reference by concatenating the transformations (post-ablation > pre-ablation > Hi-res > ZBB)

- For electroporation imaging volumes, since the ZBB atlas did not have a double transgenic brain expressing the same markers, but had the single expressions, an imaging volume computed as the sum of the single trans-

genic expressions of Tg(ETvmat2:GFP) and Tg(atoh7:GFP) already registered onto the ZBB atlas was used as a reference.

All registrations were manually assessed for global and local alignment of brain patterns, particularly around the OT neuropil, midbrain-hindbrain boundary and cerebellar track near the NI. For Tg(ETvmat2:GFP; atoh7:EGFP) expressing brains, volumes were assessed for correct alignment of the OT neuropil layers and AFs, Locus coeruleus neurons and the cerebellar fibre track near the NI. Volumes that were not well registered around these areas were not used for further analysis.

Brain regions correspond to regions in the ZBB atlas and cell ROIs were assigned a region label based on the predefined thresholds on the atlas' browser (Marquart et al., 2015). New region labels including for all mRNA riboprobes and Calretinin antibody expression were done by transforming the median volumes for all registered brains of the same marker into a binary mask. The threshold for these was set manually, as attempts to use automatic thresholding algorithms were not fortuitous.

7.6 Neuronal tracing

All electroporated single cell morphologies were traced using the Simple Neurite Tracer plugin for ImageJ (Longair et al., 2011)

7.7 Laser cell ablations

After behavioural experiment, 5 dpf larvae were anesthetised and mounted on a slide, dorsal side up in 2% low-melting agarose. Control larvae were mounted on the same slide. A pre-ablation image stack was taken for the fish that underwent cell ablation using a large imaging window encompassing the entire width of the brain and covering the whole isthmus in its dorsal-ventral axis. Cell bodies in elavl3:H2B-GCaMP6s were targeted for ablations by their position along the cerebellar track that runs near cells of the NI. Single-cell ablations were performed using a pulsed infrared laser (Coherent

Chameleon II) and the same custom-built microscope as used for imaging. A spiral scan was performed, centred in the target soma for 140 ms at 800 nm, 150–200 mW (measured at sample), using a water immersion objective (Olympus XLUMPLFLN 20X, 1.0 NA). An auto-fluorescent "scar" was apparent on both green and red channels when cells were correctly ablated, which was used to infer correct ablation. Around 100 cells were targeted on each side of the brain where NI cells expressing Ch-A are usually located. After all ablations, a post-imaging stack was taken using the same window specifications as the pre-ablation stack. Fish were then unmounted and placed in single 35 mm petri dishes to recover. All fish survived the ablation procedures.

7.8 Behaviour setup for free-swimming larvae

The behavioural "arena" consisted of a 35 mm petri dish bottom which had been sanded on both internal and external sides with sand paper to remove reflexions and covered on the outside with black tape. This was done to attempt to minimize the fish's thigmotaxic behaviour. The dish was placed on a transparent plastic platform where a diffusive paper (3026, Rosco) was placed on the top. The image from a pico projector (AAXA P2 Jr) was reflected upwards of a cold mirror and ended up back-projected on the diffusive paper (screen). An infrared LED panel (Sourcingmap) was placed bellow the platform to provide illumination throughout the arena. Images from the arena were acquired using an infrared sensitive high-speed camera (Mikrotron EoSens) mounted with a fixed aperture lens (35 mm) with a bandpass filter attached to block visible light. Videos were recorded at 700 Hz. A solenoid "tapper" was placed such that the piston, when extended, would contact the rod that connected the platform with the arena to the central pole of the rig. The solenoid was controlled using an Arduino Uno using custom-built code. All online tracking and stimulus presentation were controlled by custom-built software using LabView (National Instruments) and MATLAB (MathWorks).

7.8.1 Tracking

During experiments, images were background-subtracted and the absolute value of each pixel was used. The fish's centroid position was determined on a thresholded image of the fish. Eye centroids were tracked using a higher threshold (they appear bright due to background subtraction). Eye angles were determined by fitting an ellipse to each eye and recording the angle between the long axis of the ellipse and a line parallel to the midline of the larva. Positive angles were measured clockwise from the midline to the long axis of the ellipse and negative angles counter-clockwise. For both eyes, increases in eye angle indicate rightward rotation and decreases, leftward rotation. The tail was tracked by finding 9 equidistant x-y coordinates along the tail from the swim-bladder position to the tip of the tail and measuring the angles between the 8 resulting segments. The tail angles were computed by the sum of the all inter-segment angles. Rightward bending of the tail is represented by positive angles and leftward bending by negative angles.

For the duration of the experiment, high-speed (700 Hz) videos of a square window (length: 7.25 mm, 24.8 px/mm) centred of the fish's body centroid were saved for offline scoring of hunting routines. Also, 17 Hz videos of the entire arena were recorded for offline tracking of paramecia.

7.8.2 Visual stimuli

Visual stimuli were presented using the Psychophysics Toolbox version 3 (Kleiner et al., 2007) implemented within the LabView software. Looming stimuli are represented by the ration between their length (l) and velocity (v), mimicking a stimulus of fixed size travelling at the same speed (Sun and Frost, 1998). Spots were presented with a fixed l/r ratio of 490 ms and moved from 10° to 100° in size. The contrasts of the spots were defined as linear pixel intensity values between the minimum and maximum values of the projector. Both optomotor gratings and looming spots were presented in egocentric coordinates with respect to the fish, such that directional gratings always moved 90° to left or right sides of the fish and looming spots were centred 5 mm away

from the fish's centroid and at 90° to left or right sides. Looming and directional gratings were presented in pseudo-random order with an inter-stimulus interval of minimum 90 s. Stimuli were only presented if the fish's centroid was $\geq$ 11 mm from the edge of the arena. If this was not the case, stimuli would wait and be presented when the fish retuned to this central area. Also, when fish were outside this area, circular directional gratings that moved towards the centre of the arena was presented to induce optomotor swimming to the centre. Mechano-acoustic stimuli, delivered though the mounted solenoid, were applied after 1h of experimental recording with an inter-stimulus interval of 14 s for a duration of 10 minutes.

At the beginning of each experiment, around 80 paramecia (*Paramecium aurelia* were added to 3.5 mL of fish facility water in the arena. Initial paramecia numbers were counted manually from whole-field video frames from the first 5 minutes of the experiment, selecting only for moving paramecia. Larvae of 5 or 6 dpf were then added to the arena and left to accommodate for 2 minutes. Between each fish, the arena was thoroughly rinsed with fish facility water to remove any unconsumed paramecia.

7.8.3 Data analysis

All data analysis was done using code custom-written in MATLAB. Vergence angle was defined as the sum of the left and right eyes (angles from the right eye were inverted to represent increasing values when the eye converged). To determine when fish converged their eyes to initiate a hunting routine, a vergence threshold was computed for each fish by fitting a two-term Gaussian model to its vergence angle distribution, which is invariably bimodal such that the first peak represents vergence during normal swimming and the second during hunting. The threshold was computed as the centre of the second gaussian term minus one standard deviation. The fish was determined to be hunting if its vergence angle exceeded vergence threshold. Briefly, start and end of swim bouts were found through a tail velocity threshold applied to smoothed cumulative tail angles. Escape responses to loom or tap stimuli were determined by

a fixed tail velocity threshold.

Paramecia from whole-field videos were segmented by finding local intensity maxima in a after images were filtered using a 2D gaussian filter. Then, segmented particles were tracked by a frame-by-frame linking step using the Hungarian algorithm using a version of the simpletracker MATLAB code written by Jean-Yves Tinevez.

7.8.4 Scoring of hunting epochs

Hunting epochs, as defined by the beginning to end of eye convergence, were manually assessed using recorded high-speed videos. To identify target paramecia, if from the beginning of a routine one paramecia was observed being pursued by the larva for more than one successive swim bout, that paramecia was manually labelled as a prospective target. This labelling was done at the experimenter's discretion, however, due in part to the low paramecia density, most hunting routines either had one clearly targeted paramecia, or no paramecia was observed in the fish's vicinity and the epoch terminated. If several paramecia were in the field of view and no clear identifiable target could be discerned, the epoch was labelled as "target unidentified". Then, for each swim bout in the hunting routine the fish-target distance-gain and orientation-gain were computed as the fraction of distance or orientation between fish and prey that was eliminated by the bout (Figure 3A). Prospective targets were only defined as "target" if at the beginning of the epoch they were located within the larva's reaction zone (6 mm from the centre of the eyes and $< 120°$ from each side of the body axis) and the distance-gain and orientation-gain for the first two bouts of a hunting sequence were positive. Fish-target distance was defined as the Euclidean distance between the centre of the fish's eyes and the target centroid. Fish-target orientation was defined as the azimuth between the vector from the centre of the fish's eyes to the target and the fish's heading vector. Capture routines were labelled if the fish attempted to consume the target by either using a fast ram-like swim or a suction (Patterson, 2013). An aborted routine consisted when no capture event occurred. A success was

defined if the fish ingested the target while a miss was labelled in this did not occur. Rare events where the fish regurgitated the paramecia shortly after ingestion were still considered as success. Paramecia consumption plots were draw by analysing success epochs.

7.8.5 Psychometric fitting of looming responses

Logistic functions were fitted to the loom contrast-response escape probabilities for each fish using the Palamedes MATLAB toolbox version 1.8.2 (Prins and Kingdom, 2018). The lower asymptote of the function was set to zero (estimated spontaneous escapes were observed to be near zero). Goodness-of-Fit values were estimated using the same toolbox.

7.9 Closed-loop virtual assay

Larval zebrafish of 5 dpf were anesthetised as previously and mounted in 2.5% low-melting temperature agarose (Invitrogen), dissolved in fish-facility water, in a 35 mm petri-dish lid. Once the agarose had solidified, an opthalmic scalpel was used to carefully remove the agarose anterior to the otic vesicle and caudal to the swim bladder. This allowed the larva to freely move its eyes and tail. They were then left overnight without anaesthetic in the incubator where they were being raised.

2-photon calcium imaging was performed in the same microscope described above with laser tuned to 920 nm and average laser power at sample of 5-10 mW. Images (500 x 500 pixels, 0.61 μm/px) were acquired by frame scanning at 3.6 Hz and for each larva 2-5 image planes were acquired with a z-spacing of 5 um. Image acquisition, eye tracking, and visual stimulus presentation were controlled using software written in LabView and MATLAB. Eye and tail angles were computed in a similar way as in the free-swimming setup.

Stimuli were back-projected (Optoma ML750ST) in a diffusive paper (3026, Rosco) screen placed in half-cylinder in front of the dish where the fish was mounted at a distance of 35 mm from the head of the fish. Another

projector was set to project background luminance bellow the fish. Visual stimuli were designed in MATLAB using the Psychophysics toolbox. A coloured Wratten filter (no. 25, Kodak) was placed in front of both projectors to minimize interference with GCaMP imaging. To monitor eye movements, a 720 nm LED was used to illuminate the larva from below through a diffuser and the eyes were imaged at 60 Hz camera. To monitor tail movements, a cold mirror reflected images from the bottom of the fish to a camera recording at 430 Hz. A 720 nm LED was placed diagonally to the fish's dish to illuminate the tail. In one set of experiments, stimuli were composed of 5° dark spots moving at 30°/s clockwise or counter-clockwise and whole-field bright flashes where both frontal and bottom projectors increased in luminance 2x that of the background. In another set of experiments, looming dark spots were presented with l/r of 490 ms starting at 10° in size and expanding until covering the entire screen at an estimated 70°. It also included a looming control stimulus, where the luminance of the screen followed the same dynamics as the looming stimulus, and small spots as in the previous experiment.

Stimuli were presented in a pseudo-random order and with an interstimulus interval of 30 s (epoch). During small spot presentations, eye vergence was monitored and if the eyes converged with angle above a fixed threshold, the spot was set to travel to the middle to the screen (which would roughly correspond to the middle of the fish's visual field. Tail activity was also monitored such that the spot would move to the middle of the screen if the fish performed successive swim bouts, enabling the fish to perform sustained hunting routines.

7.9.1 Calcium imaging analysis

Data analysis of calcium imaging was performed using custom-written code. Motion correction of imaging frames was performed as in (Bianco and Engert, 2015). ROIs corresponding to imaged cell nuclei were extracted using the neuron detection code from (Kawashima et al., 2016). Extraction of neuronal activity from calcium transients was performed as in (Bianco and Engert, 2015). Fluorescent values for each ROI were z-scored (zF) using the entire

fluorescent traces. Some values are depicted as dF/F, in which case they were computed as in (Bianco and Engert, 2015).

Visual response vectors (VRVs) were computed for each cell by concatenating its mean zF responses for each presented stimulus type. VRV clustering was performed as in (Bianco and Engert, 2015) with the difference that was done with a 2-step methodology. In the first step, The Pearson's correlation between all pairs of VRVs is computed and the two cells with the highest correlation coefficient are joined into a cluster. This process is repeated by progressively joining cells and clusters until no pairwise correlation exceeded threshold. In this first step, a stringent correlation threshold ($\rho \geqslant 0.9$) is used to find the main response archetypes present in the dataset. Then, all cells are re-clustered using these archetypes as templates to cluster previously unassigned cells using a less stringent threshold ($\rho \geqslant 0.7$).

VRVs for looming experiments were clustered using K-means clustering. Briefly, VRV's were Z-scored and PCA was applied to the VRV matrix for all ROIs. The first 25 Principle components were selected to use for clustering, which explained 67.3% of the variance. These PCs were then clustered using K-means with K ranging from 2 to 50. The same elbow method was then applied to the Sum of squared errors (SSE) from all clustering procedures, which resulted in K = 14 being selected. Here, only 2 of those clusters are shown, which represent the clusters with responses to looming stimuli but no responses to the luminance control. The Looming-early cluster represent 6.8% of all ROIs in the dataset (n = 44941), while Looming-late cluster represents 8.8%. Other responses included prey-responsive cells (11.9%), Loom responsive and luminance control responsive (7.5%), and other non-typical responses (65%).

CZ-scores were calculated independently for each ROI. Briefly, for each convergence event that occurred during the presentation of a spot stimulus (GO epochs), the mean zF response of the ROI was calculated during a time window surrounding the convergence event (2 s before and after). Then, mean

zF values are computed for all epochs where the same stimulus was presented but the fish did not respond with a convergence saccade (NO-GO epochs). This mean zF value was taken from a similar window of time as the GO epoch, ensuring that the stimulus was at the same position, and thus, any visual responses are likely to be comparable (not considering differences in eye viewing angles). The following Z-scoring formula is then applied:

$$CZ - Score = \frac{x_{GO} - \mu_{NO-GO}}{\sigma_{NO-GO}} \tag{7.1}$$

This process is then repeated for all other GO epochs, resulting in a list of CZ-scores for each ROI. This list was then divided by GO epochs where the convergence was directed to the left or right sides. SpCZ-scores were computed in a similar fashion as CZ-scores, except that instead of mean zF values around GO convergences, these were taken from zF values around spontaneous convergences that occurred during period where no stimulus was being presented. These values were similarly Z-scored with the distribution of mean zF values taken at a similar timepoint on all other epochs.

7.10 Statistics

Wilcoxon rank sum tests or Two-factor, within-subject repeated measures ANOVA was used for most comparisons. p-values are stated in all cases. Values in figures represent means ± SEM unless stated otherwise.

Bibliography

Misha B Ahrens, Michael B Orger, Drew N Robson, Jennifer M Li, and Philipp J Keller. Whole-brain functional imaging at cellular resolution using light-sheet microscopy. *Nature methods*, 10(5):413, 2013.

Amin Allalou, Yuelong Wu, Mostafa Ghannad-Rezaie, Peter M Eimon, and Mehmet Fatih Yanik. Automated deep-phenotyping of the vertebrate brain. *ELife*, 6:e23379, 2017.

Paride Antinucci, Oniz Suleyman, Clinton Monfries, and Robert Hindges. Neural mechanisms generating orientation selectivity in the retina. *Current Biology*, 26(14):1802–1815, 2016.

Ali Asadollahi and Eric I Knudsen. Spatially precise visual gain control mediated by a cholinergic circuit in the midbrain attention network. *Nature communications*, 7:13472, 2016.

Ali Asadollahi, Shreesh P Mysore, and Eric I Knudsen. Stimulus-driven competition in a cholinergic midbrain nucleus. *Nature neuroscience*, 13(7):889, 2010.

Brian B Avants, Nicholas J Tustison, Gang Song, Philip A Cook, Arno Klein, and James C Gee. A reproducible evaluation of ants similarity metric performance in brain image registration. *Neuroimage*, 54(3):2033–2044, 2011.

Alison J Barker and Herwig Baier. Sins and soms: Neural microcircuits for size tuning in the zebrafish and mouse visual pathway. *Frontiers in neural circuits*, 7:89, 2013.

Alison J Barker and Herwig Baier. Sensorimotor decision making in the zebrafish tectum. *Current Biology*, 25(21):2804–2814, 2015.

Mandy V Bartsch, Kristian Loewe, Christian Merkel, Hans-Jochen Heinze, Mircea A Schoenfeld, John K Tsotsos, and Jens-Max Hopf. Attention to color sharpens neural population tuning via feedback processing in the human visual cortex hierarchy. *Journal of Neuroscience*, pages 0666–17, 2017.

Kevin T Beier, Nathan A Mundell, Y Albert Pan, and Constance L Cepko. Anterograde or retrograde transsynaptic circuit tracing in vertebrates with vesicular stomatitis virus vectors. *Current protocols in neuroscience*, 74(1): 1–26, 2016.

J-P Bellier and H Kimura. Peripheral type of choline acetyltransferase: biological and evolutionary implications for novel mechanisms in cholinergic system. *Journal of chemical neuroanatomy*, 42(4):225–235, 2011.

Mor Ben-Tov, Opher Donchin, Ohad Ben-Shahar, and Ronen Segev. Pop-out in visual search of moving targets in the archer fish. *Nature communications*, 6:6476, 2015.

Isaac H Bianco and Florian Engert. Visuomotor transformations underlying hunting behavior in zebrafish. *Current Biology*, 25(7):831–846, 2015.

Isaac H Bianco, Leung-Hang Ma, David Schoppik, Drew N Robson, Michael B Orger, James C Beck, Jennifer M Li, Alexander F Schier, Florian Engert, and Robert Baker. The tangential nucleus controls a gravito-inertial vestibulo-ocular reflex. *Current biology*, 22(14):1285–1295, 2012.

Isaac Henry Bianco, Adam R Kampff, and Florian Engert. Prey capture behavior evoked by simple visual stimuli in larval zebrafish. *Frontiers in systems neuroscience*, 5:101, 2011.

KE Binns and TE Salt. The functional influence of nicotinic cholinergic recep-

tors on the visual responses of neurones in the superficial superior colliculus. *Visual neuroscience*, 17(2):283–289, 2000.

Susan E Boehnke and Douglas P Munoz. On the importance of the transient visual response in the superior colliculus. *Current opinion in neurobiology*, 18(6):544–551, 2008.

Douglas M Bolzon, Karin Nordström, and David C O'Carroll. Local and large-range inhibition in feature detection. *Journal of Neuroscience*, 29(45): 14143–14150, 2009.

Astra S Bryant, C Alex Goddard, John R Huguenard, and Eric I Knudsen. Cholinergic control of gamma power in the midbrain spatial attention network. *Journal of Neuroscience*, 35(2):761–775, 2015.

Seth A Budick and Donald M O'Malley. Locomotor repertoire of the larval zebrafish: swimming, turning and prey capture. *Journal of Experimental Biology*, 203(17):2565–2579, 2000.

Harold A Burgess and Michael Granato. Sensorimotor gating in larval zebrafish. *Journal of Neuroscience*, 27(18):4984–4994, 2007.

John D Burrill and Stephen S Easter Jr. Development of the retinofugal projections in the embryonic and larval zebrafish (brachydanio rerio). *Journal of Comparative Neurology*, 346(4):583–600, 1994.

Timothy J Buschman and Sabine Kastner. From behavior to neural dynamics: an integrated theory of attention. *Neuron*, 88(1):127–144, 2015.

Christopher M Butt, James R Pauly, and Elizabeth A Debski. Distribution and development of nicotinic acetylcholine receptor subtypes in the optic tectum of rana pipiens. *Journal of Comparative Neurology*, 423(4):603–618, 2000.

Hanan S Caine and EDWARD R Gruberg. Ablation of nucleus isthmi leads to loss of specific visually elicited behaviors in the frog rana pipiens. *Neuroscience Letters*, 54(2-3):307–312, 1985.

Antonio Castro, Manuela Becerra, María Jesús Manso, and Ramón Anadón. Calretinin immunoreactivity in the brain of the zebrafish, danio rerio: distribution and comparison with some neuropeptides and neurotransmitter-synthesizing enzymes. i. olfactory organ and forebrain. *Journal of Comparative Neurology*, 494(3):435–459, 2006.

Shang-Wei Chong, Thi-Thu-Hang Nguyen, Lee-Thean Chu, Yun-Jin Jiang, and Vladimir Korzh. Zebrafish id2 developmental expression pattern contains evolutionary conserved and species-specific characteristics. *Developmental dynamics: an official publication of the American Association of Anatomists*, 234(4):1055–1063, 2005.

TS Collett, SB Udin, and DJ Finch. A possible mechanism for binocular depth judgements in anurans. *Experimental brain research*, 66(1):35–40, 1987.

SA Combes, MK Salcedo, MM Pandit, and JM Iwasaki. Capture success and efficiency of dragonflies pursuing different types of prey. *Integrative and comparative biology*, 53(5):787–798, 2013.

Lin Cong, Zeguan Wang, Yuming Chai, Wei Hang, Chunfeng Shang, Wenbin Yang, Lu Bai, Jiulin Du, Kai Wang, and Quan Wen. Rapid whole brain imaging of neural activity in freely behaving larval zebrafish (danio rerio). *Elife*, 6:e28158, 2017.

Martha Constantine-Paton and Patricia Ferrari-Eastman. Topographic and morphometric effects of bilateral embryonic eye removal on the optic tectum and nucleus isthmus of the leopard frog. *Journal of Comparative Neurology*, 196(4):645–661, 1981.

Arianna Costagli, Marika Kapsimali, Stephen W Wilson, and Marina Mione.

Conserved and divergent patterns of reelin expression in the zebrafish central nervous system. *Journal of Comparative Neurology*, 450(1):73–93, 2002.

Trinity B Crapse, Hakwan Lau, and Michele A Basso. A role for the superior colliculus in decision criteria. *Neuron*, 97(1):181–194, 2018.

He Cui and Joseph G Malpeli. Activity in the parabigeminal nucleus during eye movements directed at moving and stationary targets. *Journal of Neurophysiology*, 89(6):3128–3142, 2003.

Benjamin L De Bivort and Bruno Van Swinderen. Evidence for selective attention in the insect brain. *Current opinion in insect science*, 15:9–15, 2016.

Rodrigo J De Marco, Antonia H Groneberg, Chen-Min Yeh, Mario Treviño, and Soojin Ryu. The behavior of larval zebrafish reveals stressor-mediated anorexia during early vertebrate development. *Frontiers in behavioral neuroscience*, 8:367, 2014.

Filippo Del Bene, Claire Wyart, Estuardo Robles, Amanda Tran, Loren Looger, Ethan K Scott, Ehud Y Isacoff, and Herwig Baier. Filtering of visual information in the tectum by an identified neural circuit. *Science*, 330(6004):669–673, 2010.

Paul H Desan, Edward R Gruberg, Kelly M Grewell, and Felix Eckenstein. Cholinergic innervation of the optic tectum in the frograna pipiens. *Brain research*, 413(2):344–349, 1987.

L Domenici, HJ Waldvogel, C Matute, and P Streit. Distribution of gaba-like immunoreactivity in the pigeon brain. *Neuroscience*, 25(3):931–950, 1988.

Jon Driver. A selective review of selective attention research from the past century. *British Journal of Psychology*, 92(1):53–78, 2001.

Elizabeth A Dudkin and Edward R Gruberg. Nucleus isthmi enhances calcium influx into optic nerve fiber terminals in rana pipiens. *Brain research*, 969 (1-2):44–52, 2003.

Elizabeth A Dudkin, Joel B Sheffield, and Edward R Gruberg. Combining visual information from the two eyes: the relationship between isthmotectal cells that project to ipsilateral and to contralateral optic tectum using fluorescent retrograde labels in the frog, rana pipiens. *Journal of Comparative Neurology*, 502(1):38–54, 2007.

Elizabeth A Dudkin, Teri Peiffer, Benjamin Burkitt, Christopher N Neeb, and Edward R Gruberg. Leopard frog priorities in choosing between prey at different locations. *Behavioural processes*, 86(1):138–142, 2011.

Timothy W Dunn, Christoph Gebhardt, Eva A Naumann, Clemens Riegler, Misha B Ahrens, Florian Engert, and Filippo Del Bene. Neural circuits underlying visually evoked escapes in larval zebrafish. *Neuron*, 89(3):613–628, 2016.

AA Dunn-Meynell and SC Sharma. Changes in the topographically organized connections between the nucleus isthmi and the optic tectum after partial tectal ablation in adult goldfish. *Journal of Comparative Neurology*, 227(4): 497–510, 1984.

Stephen S Easter Jr and Gregory N Nicola. The development of vision in the zebrafish (danio rerio). *Developmental biology*, 180(2):646–663, 1996.

James A Edwards and Hollis T Cline. Light-induced calcium influx into retinal axons is regulated by presynaptic nicotinic acetylcholine receptor activity in vivo. *Journal of neurophysiology*, 81(2):895–907, 1999.

Lee E Eiden. The cholinergic gene locus. *Journal of neurochemistry*, 70(6): 2227–2240, 1998.

Erika M Ellis, Gregory Gauvain, Benjamin Sivyer, and Gabe J Murphy. Shared and distinct retinal input to the mouse superior colliculus and dorsal lateral geniculate nucleus. *American Journal of Physiology-Heart and Circulatory Physiology*, 2016.

Dominic A Evans, A Vanessa Stempel, Ruben Vale, Sabine Ruehle, Yaara Lefler, and Tiago Branco. A synaptic threshold mechanism for computing escape decisions. *Nature*, page 1, 2018.

Howard E Evans. The behavior patterns of solitary wasps. *Annual review of entomology*, 11(1):123–154, 1966.

J-P Ewert, H Buxbaum-Conradi, F Dreisvogt, M Glagow, C Merkel-Harff, A Röttgen, E Schürg-Pfeiffer, and WW Schwippert. Neural modulation of visuomotor functions underlying prey-catching behaviour in anurans: perception, attention, motor performance, learning. *Comparative Biochemistry and Physiology Part A: Molecular & Integrative Physiology*, 128(3):417–460, 2001.

Jörg-Peter Ewert. The neural basis of visually guided behavior. *Scientific American*, 230(3):34–43, 1974.

Jillian H Fecteau and Douglas P Munoz. Salience, relevance, and firing: a priority map for target selection. *Trends in cognitive sciences*, 10(8):382–390, 2006.

Mónica Folgueira, Ramón Anadón, and Julián Yáñez. The organization of the pretectal nuclei in the trout: a revision based on experimental holodogical studies. *Brain research bulletin*, 75(2-4):251–255, 2008.

Dominique Förster, Irene Arnold-Ammer, Eva Laurell, Alison J Barker, António M Fernandes, Karin Finger-Baier, Alessandro Filosa, Thomas O Helmbrecht, Yvonne Kölsch, Enrico Kühn, et al. Genetic targeting and anatomical registration of neuronal populations in the zebrafish brain with a new set of bac transgenic tools. *Scientific Reports*, 7(1):5230, 2017.

Haleh Fotowat and Fabrizio Gabbiani. Collision detection as a model for sensory-motor integration. *Annual review of neuroscience*, 34:1–19, 2011.

Shai Gabay, Tali Leibovich, Avi Ben-Simon, Avishai Henik, and Ronen Segev. Inhibition of return in the archer fish. *Nature communications*, 4:1657, 2013.

Jens P Gabriel, Chintan A Trivedi, Colette M Maurer, Soojin Ryu, and Johann H Bollmann. Layer-specific targeting of direction-selective neurons in the zebrafish optic tectum. *Neuron*, 76(6):1147–1160, 2012.

Ethan Gahtan and Donald M O'Malley. Visually guided injection of identified reticulospinal neurons in zebrafish: a survey of spinal arborization patterns. *Journal of Comparative Neurology*, 459(2):186–200, 2003.

Shawn P Gallagher and David PM Northmore. Responses of the teleostean nucleus isthmi to looming objects and other moving stimuli. *Visual neuroscience*, 23(2):209–219, 2006.

AM Gaybriel and CW Ragsdale. Histochemically distinct compartments in the striatum of human, monkey and cat demonstrated by acetylchlolinesterase staining. *Proc Natl Acad Sci USA*, 75:5723–5726, 1978.

Bart RH Geurten, Karin Nordström, Jordanna DH Sprayberry, Douglas M Bolzon, and David C O'Carroll. Neural mechanisms underlying target detection in a dragonfly centrifugal neuron. *Journal of Experimental Biology*, 210(18):3277–3284, 2007.

Steven Glasser and David Ingle. The nucleus isthmus as a relay station in the ipsilateral visual projection to the frog's optic tectum. *Brain research*, 159 (1):214–218, 1978.

C Alex Goddard, Devarajan Sridharan, John R Huguenard, and Eric I Knudsen. Gamma oscillations are generated locally in an attention-related midbrain network. *Neuron*, 73(3):567–580, 2012.

C Alex Goddard, Shreesh P Mysore, Astra S Bryant, John R Huguenard, and Eric I Knudsen. Spatially reciprocal inhibition of inhibition within a

stimulus selection network in the avian midbrain. *PloS one*, 9(1):e85865, 2014.

Cristian González-Cabrera, Florencia Garrido-Charad, Alejandro Roth, and Gonzalo J Marín. The isthmic nuclei providing parallel feedback connections to the avian tectum have different neurochemical identities: expression of glutamatergic and cholinergic markers in the chick (gallus gallus). *Journal of Comparative Neurology*, 523(9):1341–1358, 2015.

Adam J Granger, Nicole Mulder, Arpiar Saunders, and Bernardo L Sabatini. Cotransmission of acetylcholine and gaba. *Neuropharmacology*, 100:40–46, 2016.

Ann M Graybiel. A satellite system of the superior colliculus: the parabigeminal nucleus and its projections to the superficial collicular layers. *Brain research*, 145(2):365–374, 1978.

Ann M Graybiel. Periodic-compartmental distribution of acetylcholinesterase in the superior colliculus of the human brain. *Neuroscience*, 4(5):643–650, 1979.

Sten Grillner and Brita Robertson. The basal ganglia over 500 million years. *Current Biology*, 26(20):R1088–R1100, 2016.

Paul Grobstein, Christopher Comer, Margaret Hollyday, and Steven M Archer. A crossed isthmo-tectal projection in rana pipiens and its involvement in the ipsilateral visuotectal projection. *Brain Research*, 156(1):117–123, 1978.

Edward Gruberg, Elizabeth Dudkin, Yuan Wang, Gonzalo Marín, Carlos Salas, Elisa Sentis, Juan Letelier, Jorge Mpodozis, Joseph Malpeli, He Cui, et al. Influencing and interpreting visual input: the role of a visual feedback system, 2006.

Edward R Gruberg and Jerome Y Lettvin. Anatomy and physiology of a

binocular system in the frograna pipiens. *Brain Research*, 192(2):313–325, 1980.

Edward R Gruberg and Susan B Udin. Topographic projections between the nucleus isthmi and the tectum of the frog rana pipiens. *Journal of Comparative Neurology*, 179(3):487–500, 1978.

Edward R Gruberg, Mark T Wallace, and Robert F Waldeck. Relationship between isthmotectal fibers and other tectopetal systems in the leopard frog. *Journal of Comparative Neurology*, 288(1):39–50, 1989.

Edward R Gruberg, Mark T Wallace, Hanan S Caine, and Michael I Mote. Behavioral and physiological consequences of unilateral ablation of the nucleus isthmi in the leopard frog. *Brain, behavior and evolution*, 37(2):92–103, 1991.

Martin Haesemeyer, Drew N Robson, Jennifer M Li, Alexander F Schier, and Florian Engert. A brain-wide circuit model of heat-evoked swimming behavior in larval zebrafish. *Neuron*, 98(4):817–831, 2018.

David G Harper and Robert W Blake. On the error involved in high-speed film when used to evaluate maximum accelerations of fish. *Canadian Journal of Zoology*, 67(8):1929–1936, 1989.

Lucy A Heap, Gilles C Vanwalleghem, Andrew W Thompson, Itia Favre-Bulle, Halina Rubinsztein-Dunlop, and Ethan K Scott. Hypothalamic projections to the optic tectum in larval zebrafish. *Frontiers in neuroanatomy*, 11:135, 2018.

Alison Heffer, Gregory D Marquart, Allisan Aquilina-Beck, Nabil Saleem, Harold A Burgess, and Igor B Dawid. Generation and characterization of kctd15 mutations in zebrafish. *PloS one*, 12(12):e0189162, 2017.

Burkhard Hellmann, Martina Manns, and Onur Güntürkün. Nucleus isthmi,

pars semilunaris as a key component of the tectofugal visual system in pigeons. *Journal of Comparative Neurology*, 436(2):153–166, 2001.

Michael J Higley, Aryn H Gittis, Ian A Oldenburg, Nina Balthasar, Rebecca P Seal, Robert H Edwards, Bradford B Lowell, Anatol C Kreitzer, and Bernardo L Sabatini. Cholinergic interneurons mediate fast vglut3-dependent glutamatergic transmission in the striatum. *PloS one*, 6(4): e19155, 2011.

William Hodos and James C Bonbright. Intensity difference thresholds in pigeons after lesions of the tectofugal and thalamofugal visual pathways. *Journal of Comparative and Physiological Psychology*, 87(6):1013, 1974.

Elim Hong, Kirankumar Santhakumar, Courtney A Akitake, Sang Jung Ahn, Christine Thisse, Bernard Thisse, Claire Wyart, Jean-Marie Mangin, and Marnie E Halpern. Cholinergic left-right asymmetry in the habenulo-interpeduncular pathway. *Proceedings of the National Academy of Sciences*, 110(52):21171–21176, 2013.

MF Huerta. The mammalian superior colliculus: studies of its morphology and connections. *The comparative neurology of the optic tectum*, pages 687–772, 1984.

David Ingle. Disinhibition of tectal neurons by pretectal lesions in the frog. *Science*, 180(4084):422–424, 1973.

David Ingle. Focal attention in the frog: behavioral and physiological correlates. *Science*, 188(4192):1033–1035, 1975.

David Ingle and Jeffrey Cook. The effect of viewing distance upon size preference of frogs for prey. *Vision research*, 17(9):1009–1013, 1977.

Mohammad Rafiqul Islam and Yasuro Atoji. Distribution of vesicular glutamate transporter 2 and glutamate receptor 1 mrna in the central nervous

system of the pigeon (columba livia). *Journal of Comparative Neurology*, 511(5):658–677, 2008.

Hironobu Ito, Noboru Sakamoto, and Koichi Takatsuji. Cytoarchitecture, fiber connections, and ultrastructure of nucleus isthmi in a teleost (navodon modestus) with a special reference to degenerating isthmic afferents from optic tectum and nucleus pretectalis. *Journal of Comparative Neurology*, 205(3): 299–311, 1982.

Laurent Itti and Christof Koch. Computational modelling of visual attention. *Nature reviews neuroscience*, 2(3):194, 2001.

William James. The principles of. *Psychology*, 2:94, 1890.

Charlene D Jarvis. Visual discrimination and spatial localization deficits after lesions of the tectofugal pathway in pigeons; pp. 213–228. *Brain, behavior and evolution*, 9(3):213–228, 1974.

Miao Jing, Peng Zhang, Guangfu Wang, Jiesi Feng, Lukas Mesik, Jianzhi Zeng, Huoqing Jiang, Shaohua Wang, Jess C Looby, Nick A Guagliardo, et al. A genetically encoded fluorescent acetylcholine indicator for in vitro and in vivo studies. *Nature biotechnology*, 36(8):726, 2018.

Nicholas P Johnson, Thomas F Schwab, and William M Saidel. Bilateral efferents from nucleus isthmi to the optic tectum in goldfish (carassius auratus) are spatially restricted. *Neuroscience letters*, 534:311–315, 2013.

Naomi Karoubi, Ronen Segev, and Mario F Wullimann. The brain of the archerfish toxotes chatareus: a nissl-based neuroanatomical atlas and catecholaminergic/cholinergic systems. *Frontiers in neuroanatomy*, 10:106, 2016.

Jan Kaslin, Johanna M Nystedt, Maria Östergård, Nina Peitsaro, and Pertti Panula. The orexin/hypocretin system in zebrafish is connected to the aminergic and cholinergic systems. *Journal of Neuroscience*, 24(11):2678–2689, 2004.

Takashi Kawashima, Maarten F Zwart, Chao-Tsung Yang, Brett D Mensh, and Misha B Ahrens. The serotonergic system tracks the outcomes of actions to mediate short-term motor learning. *Cell*, 167(4):933–946, 2016.

Dal Hyung Kim, Jungsoo Kim, João C Marques, Abhinav Grama, David GC Hildebrand, Wenchao Gu, Jennifer M Li, and Drew N Robson. Pan-neuronal calcium imaging with cellular resolution in freely swimming zebrafish. *nAture methods*, 14(11):1107, 2017.

Charles B Kimmel, Jill Patterson, and Richard O Kimmel. The development and behavioral characteristics of the startle response in the zebra fish. *Developmental psychobiology*, 7(1):47–60, 1974.

WM King and JT Schmidt. The long latency component of retinotectal transmission: enhancement by stimulation of nucleus isthmi or tectobulbar tract and block by nicotinic cholinergic antagonists. *Neuroscience*, 40(3):701–712, 1991.

Raymond M Klein. Inhibition of return. *Trends in cognitive sciences*, 4(4): 138–147, 2000.

Mario Kleiner, David Brainard, Denis Pelli, Allen Ingling, Richard Murray, Christopher Broussard, et al. Whats new in psychtoolbox-3. *Perception*, 36 (14):1, 2007.

Eric I Knudsen. Control from below: the role of a midbrain network in spatial attention. *European Journal of Neuroscience*, 33(11):1961–1972, 2011.

Eric I Knudsen. Neural circuits that mediate selective attention: a comparative perspective. *Trends in neurosciences*, 2018.

Eric I Knudsen, Jason S Schwarz, Phyllis F Knudsen, and Devarajan Sridharan. Space-specific deficits in visual orientation discrimination caused by lesions in the midbrain stimulus selection network. *Current Biology*, 27(14): 2053–2064, 2017.

Sandra K Kostyk and Paul Grobstein. Visual orienting deficits in frogs with various unilateral lesions. *Behavioural brain research*, 6(4):379–388, 1982.

Sandra K Kostyk and Paul Grobstein. Neuronal organization underlying visually elicited prey orienting in the frogi. effects of various unilateral lesions. *Neuroscience*, 21(1):41–55, 1987.

Minoru Koyama, Francesca Minale, Jennifer Shum, Nozomi Nishimura, Chris B Schaffer, and Joseph R Fetcho. A circuit motif in the zebrafish hindbrain for a two alternative behavioral choice to turn left or right. *eLife*, 5:e16808, 2016.

John W Krakauer, Asif A Ghazanfar, Alex Gomez-Marin, Malcolm A MacIver, and David Poeppel. Neuroscience needs behavior: correcting a reductionist bias. *Neuron*, 93(3):480–490, 2017.

Richard J Krauzlis, Lee P Lovejoy, and Alexandre Zénon. Superior colliculus and visual spatial attention. *Annual review of neuroscience*, 36:165–182, 2013.

Richard J Krauzlis, Amarender R Bogadhi, James P Herman, and Anil Bollimunta. Selective attention without a neocortex. *Cortex*, 102:161–175, 2018.

Dihui Lai, Sebastian Brandt, Harald Luksch, and Ralf Wessel. Recurrent antitopographic inhibition mediates competitive stimulus selection in an attention network. *Journal of neurophysiology*, 105(2):793–805, 2010.

Gilbert Lauter, Iris Söll, and Giselbert Hauptmann. Two-color fluorescent in situ hybridization in the embryonic zebrafish brain using differential detection systems. *BMC developmental biology*, 11(1):43, 2011.

Jerome Y Lettvin, Humberto R Maturana, Warren S McCulloch, and Walter H Pitts. What the frog's eye tells the frog's brain. *Proceedings of the IRE*, 47 (11):1940–1951, 1959.

Zheng Li and Katherine V Fite. Gabaergic visual pathways in the frog rana pipiens. *Visual neuroscience*, 18(3):457–464, 2001.

Huai-Ti Lin and Anthony Leonardo. Heuristic rules underlying dragonfly prey selection and interception. *Current Biology*, 27(8):1124–1137, 2017.

Yongjian Liu, David E Krantz, Clarissa Waites, and Robert H Edwards. Membrane trafficking of neurotransmitter transporters in the regulation of synaptic transmission. *Trends in cell biology*, 9(9):356–363, 1999.

Michael A Long, Dezhe Z Jin, and Michale S Fee. Support for a synaptic chain model of neuronal sequence generation. *Nature*, 468(7322):394, 2010.

Mark H Longair, Dean A Baker, and J Douglas Armstrong. Simple neurite tracer: open source software for reconstruction, visualization and analysis of neuronal processes. *Bioinformatics*, 27(17):2453–2454, 2011.

Lee P Lovejoy and Richard J Krauzlis. Inactivation of primate superior colliculus impairs covert selection of signals for perceptual judgments. *Nature neuroscience*, 13(2):261, 2010.

Lee P Lovejoy and Richard J Krauzlis. Changes in perceptual sensitivity related to spatial cues depends on subcortical activity. *Proceedings of the National Academy of Sciences*, page 201609711, 2017.

Thomas Zhihao Luo and John HR Maunsell. Neuronal modulations in visual cortex are associated with only one of multiple components of attention. *Neuron*, 86(5):1182–1188, 2015.

Rui Ma, He Cui, Sang-Hun Lee, Thomas J Anastasio, and Joseph G Malpeli. Predictive encoding of moving target trajectory by neurons in the parabigeminal nucleus. *Journal of neurophysiology*, 109(8):2029–2043, 2013.

Rachel Macdonald. Zebrafish immunohistochemistry. In *Molecular Methods in Developmental Biology*, pages 77–88. Springer, 1999.

NA Macmillan and CD Creelman. Detection theory: A users guide lawrence erlbaum associates. *New York*, page 73, 2005.

Kristin A Maczko, Phyllis F Knudsen, and Eric I Knudsen. Auditory and visual space maps in the cholinergic nucleus isthmi pars parvocellularis of the barn owl. *Journal of Neuroscience*, 26(49):12799–12806, 2006.

Gonzalo Marín, Jorge Mpdozis, Elisa Sentis, Tomás Ossandón, and Juan Carlos Letelier. Oscillatory bursts in the optic tectum of birds represent reentrant signals from the nucleus isthmi pars parvocellularis. *Journal of Neuroscience*, 25(30):7081–7089, 2005.

Gregory D Marquart, Kathryn M Tabor, Mary Brown, Jennifer L Strykowski, Gaurav K Varshney, Matthew C LaFave, Thomas Mueller, Shawn M Burgess, Shin-ichi Higashijima, and Harold A Burgess. A 3d searchable database of transgenic zebrafish gal4 and cre lines for functional neuroanatomy studies. *Frontiers in neural circuits*, 9:78, 2015.

Gregory D Marquart, Kathryn M Tabor, Eric J Horstick, Mary Brown, Alexandra K Geoca, Nicholas F Polys, Damian Dalle Nogare, and Harold A Burgess. High-precision registration between zebrafish brain atlases using symmetric diffeomorphic normalization. *GigaScience*, 6(8):gix056, 2017.

João C Marques, Simone Lackner, Rita Félix, and Michael B Orger. Structure of the zebrafish locomotor repertoire revealed with unsupervised behavioral clustering. *Current Biology*, 28(2):181–195, 2018.

Ichiro Masai, Zsolt Lele, Masahiro Yamaguchi, Atsuko Komori, Asuka Nakata, Yuko Nishiwaki, Hironori Wada, Hideomi Tanaka, Yasuhiro Nojima, Matthias Hammerschmidt, et al. N-cadherin mediates retinal lamination, maintenance of forebrain compartments and patterning of retinal neurites. *Development*, 130(11):2479–2494, 2003.

Melissa B McElligott and Donald M OMalley. Prey tracking by larval zebrafish:

axial kinematics and visual control. *Brain, behavior and evolution*, 66(3): 177–196, 2005.

Robert M McPeek and Edward L Keller. Deficits in saccade target selection after inactivation of superior colliculus. *Nature neuroscience*, 7(7):757, 2004.

Rosalia Méndez-Otero, Carlos Eduardo Rocha-Miranda, and Victor Hugh Perry. The organization of the parabigemino-tectal projections in the opossum. *Brain research*, 198(1):183–189, 1980.

Geoffrey Migault, Thijs L van der Plas, Hugo Trentesaux, Thomas Panier, Raphaël Candelier, Rémi Proville, Bernhard Englitz, Georges Debrégeas, and Volker Bormuth. Whole-brain calcium imaging during physiological vestibular stimulation in larval zebrafish. *Current Biology*, 28(23):3723–3735, 2018.

Matteo Mischiati, Huai-Ti Lin, Paul Herold, Elliot Imler, Robert Olberg, and Anthony Leonardo. Internal models direct dragonfly interception steering. *Nature*, 517(7534):333, 2015.

Gadisti Aisha Mohamed, Ruey-Kuang Cheng, Joses Ho, Seetha Krishnan, Farhan Mohammad, Adam Claridge-Chang, and Suresh Jesuthasan. Optical inhibition of larval zebrafish behaviour with anion channelrhodopsins. *BMC biology*, 15(1):103, 2017.

Yu Mu, Xiao-quan Li, Bo Zhang, and Jiu-lin Du. Visual input modulates audiomotor function via hypothalamic dopaminergic neurons through a cooperative mechanism. *Neuron*, 75(4):688–699, 2012.

Thomas Mueller and Su Guo. The distribution of gad67-mrna in the adult zebrafish (teleost) forebrain reveals a prosomeric pattern and suggests previously unidentified homologies to tetrapods. *Journal of Comparative Neurology*, 516(6):553–568, 2009.

Thomas Mueller, Philippe Vernier, and Mario F Wullimann. The adult central nervous cholinergic system of a neurogenetic model animal, the zebrafish danio rerio. *Brain research*, 1011(2):156–169, 2004.

Florian T Muijres, Michael J Elzinga, Johan M Melis, and Michael H Dickinson. Flies evade looming targets by executing rapid visually directed banked turns. *Science*, 344(6180):172–177, 2014.

Shreesh P Mysore and Eric I Knudsen. Reciprocal inhibition of inhibition: a circuit motif for flexible categorization in stimulus selection. *Neuron*, 73(1): 193–205, 2012.

Shreesh P Mysore and Eric I Knudsen. A shared inhibitory circuit for both exogenous and endogenous control of stimulus selection. *Nature neuroscience*, 16(4):473, 2013.

Shreesh P Mysore and Eric I Knudsen. Descending control of neural bias and selectivity in a spatial attention network: rules and mechanisms. *Neuron*, 84(1):214–226, 2014.

Shreesh P Mysore, Ali Asadollahi, and Eric I Knudsen. Global inhibition and stimulus competition in the owl optic tectum. *Journal of Neuroscience*, 30 (5):1727–1738, 2010.

Shreesh P Mysore, Ali Asadollahi, and Eric I Knudsen. Signaling of the strongest stimulus in the owl optic tectum. *Journal of Neuroscience*, 31 (14):5186–5196, 2011.

DAVID Nachmansohn and AL Machado. The formation of acetylcholine. a new enzyme:" choline acetylase". *Journal of neurophysiology*, 6(5):397–403, 1943.

Anirvan S Nandy, Jonathan J Nassi, and John H Reynolds. Laminar organization of attentional modulation in macaque visual area v4. *Neuron*, 93(1): 235–246, 2017.

Eva A Naumann, Adam R Kampff, David A Prober, Alexander F Schier, and Florian Engert. Monitoring neural activity with bioluminescence during natural behavior. *Nature neuroscience*, 13(4):513, 2010.

Eva A Naumann, James E Fitzgerald, Timothy W Dunn, Jason Rihel, Haim Sompolinsky, and Florian Engert. From whole-brain data to functional circuit models: the zebrafish optomotor response. *Cell*, 167(4):947–960, 2016.

Stephan CF Neuhauss, Oliver Biehlmaier, Mathias W Seeliger, Tilak Das, Konrad Kohler, William A Harris, and Herwig Baier. Genetic disorders of vision revealed by a behavioral screen of 400 essential loci in zebrafish. *Journal of Neuroscience*, 19(19):8603–8615, 1999.

Cristopher M Niell and Stephen J Smith. Functional imaging reveals rapid development of visual response properties in the zebrafish tectum. *Neuron*, 45(6):941–951, 2005.

Nikolas Nikolaou and Martin P Meyer. Imaging circuit formation in zebrafish. *Developmental neurobiology*, 72(3):346–357, 2012.

Anna C Nobre and Freek van Ede. Anticipated moments: temporal structure in attention. *Nature Reviews Neuroscience*, 19(1):34, 2018.

David Northmore. Optic tectum. *Encyclopedia of Fish Physiology: From Genome to Environment. Elsevier*, pages 131–142, 2011.

David PM Northmore and Shawn P Gallagher. Functional relationship between nucleus isthmi and tectum in teleosts: synchrony but no topography. *Visual neuroscience*, 20(3):335–348, 2003.

DPM Northmore. Visual responses of nucleus isthmi in a teleost fish (lepomis macrochirus). *Vision research*, 31(3):525–535, 1991.

Takashi Okuda, Tatsuya Haga, Yoshikatsu Kanai, Hitoshi Endou, Takeshi Ishihara, and Isao Katsura. Identification and characterization of the high-affinity choline transporter. *Nature neuroscience*, 3(2):120, 2000.

RM Olberg, AH Worthington, and KR Venator. Prey pursuit and interception in dragonflies. *Journal of Comparative Physiology A*, 186(2):155–162, 2000.

RM Olberg, RC Seaman, MI Coats, and AF Henry. Eye movements and target fixation during dragonfly prey-interception flights. *Journal of Comparative Physiology A*, 193(7):685–693, 2007.

Robert M Olberg. Visual control of prey-capture flight in dragonflies. *Current opinion in neurobiology*, 22(2):267–271, 2012.

Michael B Orger. The cellular organization of zebrafish visuomotor circuits. *Current Biology*, 26(9):R377–R385, 2016.

Michael B Orger, Adam R Kampff, Kristen E Severi, Johann H Bollmann, and Florian Engert. Control of visually guided behavior by distinct populations of spinal projection neurons. *Nature neuroscience*, 11(3):327, 2008.

Pablo Oteiza, Iris Odstrcil, George Lauder, Ruben Portugues, and Florian Engert. A novel mechanism for mechanosensory-based rheotaxis in larval zebrafish. *Nature*, 547(7664):445, 2017.

Bradley W Patterson, Aliza O Abraham, Malcolm A MacIver, and David L McLean. Visually guided gradation of prey capture movements in larval zebrafish. *Journal of Experimental Biology*, pages jeb–087742, 2013.

Silvia Eva Pérez, Julián Yáñez, Oscar Marín, Ramón Anadón, Agustín González, and Isabel Rodríguez-Moldes. Distribution of choline acetyltransferase (chat) immunoreactivity in the brain of the adult trout and tract-tracing observations on the connections of the nuclei of the isthmus. *Journal of Comparative Neurology*, 428(3):450–474, 2000.

VH Perry and A Cowey. Retinal ganglion cells that project to the superior colliculus and pretectum in the macaque monkey. *Neuroscience*, 12(4):1125–1137, 1984.

Ruben Portugues and Florian Engert. The neural basis of visual behaviors in the larval zebrafish. *Current opinion in neurobiology*, 19(6):644–647, 2009.

Michael I Posner. Orienting of attention. *Quarterly journal of experimental psychology*, 32(1):3–25, 1980.

Michael I Posner and Yoav Cohen. Components of visual orienting. *Attention and performance X: Control of language processes*, 32:531–556, 1984.

Michael I Posner and Steven W Keele. On the genesis of abstract ideas. *Journal of experimental psychology*, 77(3p1):353, 1968.

John H Postlethwait, Ian G Woods, Phuong Ngo-Hazelett, Yi-Lin Yan, Peter D Kelly, Felicia Chu, Hui Huang, Alicia Hill-Force, and William S Talbot. Zebrafish comparative genomics and the origins of vertebrate chromosomes. *Genome research*, 10(12):1890–1902, 2000.

Stephanie J Preuss, Chintan A Trivedi, Colette M vom Berg-Maurer, Soojin Ryu, and Johann H Bollmann. Classification of object size in retinotectal microcircuits. *Current Biology*, 24(20):2376–2385, 2014.

Nicolaas Prins and Frederick AA Kingdom. Applying the model-comparison approach to test specific research hypotheses in psychophysical research using the palamedes toolbox. *Frontiers in psychology*, 9, 2018.

Owen Randlett, Caroline L Wee, Eva A Naumann, Onyeka Nnaemeka, David Schoppik, James E Fitzgerald, Ruben Portugues, Alix MB Lacoste, Clemens Riegler, Florian Engert, et al. Whole-brain activity mapping onto a zebrafish brain atlas. *Nature methods*, 12(11):1039, 2015.

Estuardo Robles, Alessandro Filosa, and Herwig Baier. Precise lamination of retinal axons generates multiple parallel input pathways in the tectum. *Journal of Neuroscience*, 33(11):5027–5039, 2013.

Estuardo Robles, Eva Laurell, and Herwig Baier. The retinal projectome reveals brain-area-specific visual representations generated by ganglion cell diversity. *Current Biology*, 24(18):2085–2096, 2014.

Tobias Roeser and Herwig Baier. Visuomotor behaviors in larval zebrafish after gfp-guided laser ablation of the optic tectum. *Journal of Neuroscience*, 23(9):3726–3734, 2003.

Sebastián A Romano, Thomas Pietri, Verónica Pérez-Schuster, Adrien Jouary, Mathieu Haudrechy, and Germán Sumbre. Spontaneous neuronal network dynamics reveal circuits functional adaptations for behavior. *Neuron*, 85(5): 1070–1085, 2015.

Olaf Ronneberger, Kun Liu, Meta Rath, Dominik Rueβ, Thomas Mueller, Henrik Skibbe, Benjamin Drayer, Thorsten Schmidt, Alida Filippi, Roland Nitschke, et al. Vibe-z: a framework for 3d virtual colocalization analysis in zebrafish larval brains. *Nature Methods*, 9(7):735, 2012.

Samuel Rossel, Julia Corlija, and Stefan Schuster. Predicting three-dimensional target motion: how archer fish determine where to catch their dislodged prey. *Journal of experimental biology*, 205(21):3321–3326, 2002.

Yuri B Saalmann and Sabine Kastner. Cognitive and perceptual functions of the visual thalamus. *Neuron*, 71(2):209–223, 2011.

Noboru Sakamoto, Hironobo Ito, and Shinsuke Ueda. Topographic projections between the nucleus isthmi and the optic tectum in a teleost, navodon modestus. *Brain research*, 224(2):225–234, 1981.

Peter B Sargent, Susan H Pike, Deborah B Nadel, and Jon M Lindstrom. Nicotinic acetylcholine receptor-like molecules in the retina, retinotectal pathway, and optic tectum of the frog. *Journal of Neuroscience*, 9(2):565–573, 1989.

Martin Sarter, Cindy Lustig, William M Howe, Howard Gritton, and Anne S

Berry. Deterministic functions of cortical acetylcholine. *European Journal of Neuroscience*, 39(11):1912–1920, 2014.

Thomas Schlegel, Christine J Schmid, and Stefan Schuster. Archerfish shots are evolutionarily matched to prey adhesion. *Current Biology*, 16(19):R836–R837, 2006.

Andrew M Seeds, Primoz Ravbar, Phuong Chung, Stefanie Hampel, Frank M Midgley Jr, Brett D Mensh, and Julie H Simpson. A suppression hierarchy among competing motor programs drives sequential grooming in drosophila. *Elife*, 3:e02951, 2014.

Julia L Semmelhack, Joseph C Donovan, Tod R Thiele, Enrico Kuehn, Eva Laurell, and Herwig Baier. A dedicated visual pathway for prey detection in larval zebrafish. *Elife*, 3:e04878, 2014.

Martin I Sereno and Philip S Ulinski. Caudal topographic nucleus isthmi and the rostral nontopographic nucleus isthmi in the turtle, pseudemys scripta. *Journal of Comparative Neurology*, 261(3):319–346, 1987.

Rowena Spence, Gabriele Gerlach, Christian Lawrence, and Carl Smith. The behaviour and ecology of the zebrafish, danio rerio. *Biological reviews*, 83 (1):13–34, 2008.

Devarajan Sridharan and Eric I Knudsen. Gamma oscillations in the midbrain spatial attention network: linking circuits to function. *Current opinion in neurobiology*, 31:189–198, 2015.

Devarajan Sridharan, Nicholas A Steinmetz, Tirin Moore, and Eric I Knudsen. Distinguishing bias from sensitivity effects in multialternative detection tasks. *Journal of vision*, 14(9):16–16, 2014.

Devarajan Sridharan, Nicholas A Steinmetz, Tirin Moore, and Eric I Knudsen. Does the superior colliculus control perceptual sensitivity or choice bias dur-

ing attention? evidence from a multialternative decision framework. *Journal of Neuroscience*, 37(3):480–511, 2017.

Georg F Striedter and R Glenn Northcutt. Two distinct visual pathways through the superficial pretectum in a percomorph teleost. *Journal of Comparative Neurology*, 283(3):342–354, 1989.

CA Stuermer. Retinotopic organization of the developing retinotectal projection in the zebrafish embryo. *Journal of Neuroscience*, 8(12):4513–4530, 1988.

Adrian K Stull and Edward R Gruberg. Prey selection in the leopard frog: choosing in biased and unbiased situations. *Brain, behavior and evolution*, 52(1):37–45, 1998.

Hongjin Sun and Barrie J Frost. Computation of different optical variables of looming objects in pigeon nucleus rotundus neurons. *Nature neuroscience*, 1(4):296, 1998.

D Tay and C Straznicky. The development of the nucleus isthmi in xenopus: An autoradiographic study. *Neuroscience letters*, 16(3):313–318, 1980.

Incinur Temizer, Joseph C Donovan, Herwig Baier, and Julia L Semmelhack. A visual pathway for looming-evoked escape in larval zebrafish. *Current Biology*, 25(14):1823–1834, 2015.

Alexander Thiele and Mark A Bellgrove. Neuromodulation of attention. *Neuron*, 97(4):769–785, 2018.

Tod R Thiele, Joseph C Donovan, and Herwig Baier. Descending control of swim posture by a midbrain nucleus in zebrafish. *Neuron*, 83(3):679–691, 2014.

Christine Thisse and Bernard Thisse. High-resolution in situ hybridization to whole-mount zebrafish embryos. *Nature protocols*, 3(1):59, 2008.

PJA Timmermans. Prey catching in the archer fish: angles and probability of hitting an aerial target. *Behavioural Processes*, 55(2):93–105, 2001.

Anne M Treisman. Strategies and models of selective attention. *Psychological review*, 76(3):282, 1969.

Anne M Treisman and Garry Gelade. A feature-integration theory of attention. *Cognitive psychology*, 12(1):97–136, 1980.

Chintan A Trivedi and Johann H Bollmann. Visually driven chaining of elementary swim patterns into a goal-directed motor sequence: a virtual reality study of zebrafish prey capture. *Frontiers in neural circuits*, 7:86, 2013.

Susan Boymel Udin and Mark D Fisher. The development of the nucleus isthmi in xenopus laevis. i. cell genesis and the formation of connections with the tectum. *Journal of Comparative Neurology*, 232(1):25–35, 1985.

Nikita Vladimirov, Yu Mu, Takashi Kawashima, Davis V Bennett, Chao-Tsung Yang, Loren L Looger, Philipp J Keller, Jeremy Freeman, and Misha B Ahrens. Light-sheet functional imaging in fictively behaving zebrafish. *Nature methods*, 11(9):883, 2014.

Katrin Volkmann, Yi-Yen Chen, Matthew P Harris, Mario F Wullimann, and Reinhard W Köster. The zebrafish cerebellar upper rhombic lip generates tegmental hindbrain nuclei by long-distance migration in an evolutionary conserved manner. *Journal of Comparative Neurology*, 518(14):2794–2817, 2010.

Catherine R von Reyn, Aljoscha Nern, W Ryan Williamson, Patrick Breads, Ming Wu, Shigehiro Namiki, and Gwyneth M Card. Feature integration drives probabilistic behavior in the drosophila escape response. *Neuron*, 94 (6):1190–1204, 2017.

MT Wallace, AJ Ricciuti, and ER Gruberg. Nucleus isthmi: its contribution

to tectal acetylcholinesterase and choline acetyltransferase in the frog rana pipiens. *Neuroscience*, 35(3):627–636, 1990.

Shu-Rong Wang. The nucleus isthmi and dual modulation of the receptive field of tectal neurons in non-mammals. *Brain Research Reviews*, 41(1): 13–25, 2003.

Shu-Rong Wang, Kun Yan, Yin-Ting Wang, Shi-Ying Jiang, and Xuan-Shen Wang. Neuroanatomy and electrophysiology of the lacertilian nucleus isthmi. *Brain research*, 275(2):355–360, 1983.

Yuan Wang, Daniel E Major, and Harvey J Karten. Morphology and connections of nucleus isthmi pars magnocellularis in chicks (gallus gallus). *Journal of Comparative Neurology*, 469(2):275–297, 2004.

Yuan Wang, Harald Luksch, Nicholas C Brecha, and Harvey J Karten. Columnar projections from the cholinergic nucleus isthmi to the optic tectum in chicks (gallus gallus): a possible substrate for synchronizing tectal channels. *Journal of Comparative Neurology*, 494(1):7–35, 2006.

Brett C Weber, Robert F Waldeck, and Edward R Gruberg. Seeing beyond the midline: the role of the contralateral isthmotectal projection in the leopard frog. *Visual neuroscience*, 13(3):467–476, 1996.

Lu Wen, Wei Wei, Wenchao Gu, Peng Huang, Xi Ren, Zheng Zhang, Zuoyan Zhu, Shuo Lin, and Bo Zhang. Visualization of monoaminergic neurons and neurotoxicity of mptp in live transgenic zebrafish. *Developmental biology*, 314(1):84–92, 2008.

Rebecca E Westphal and Donald M OMalley. Fusion of locomotor maneuvers, and improving sensory capabilities, give rise to the flexible homing strikes of juvenile zebrafish. *Frontiers in neural circuits*, 7:108, 2013.

Steven D Wiederman and David C OCarroll. Selective attention in an insect visual neuron. *Current Biology*, 23(2):156–161, 2013.

Steven D Wiederman, Joseph M Fabian, James R Dunbier, and David C OCarroll. A predictive focus of gain modulation encodes target trajectories in insect vision. *Elife*, 6:e26478, 2017.

Wolfgang Wiggers. Isthmotectal connections in plethodontid salamanders. *Journal of Comparative Neurology*, 395(2):261–272, 1998.

Wolfgang Wiggers and Gerhard Roth. Anatomy, neurophysiology and functional aspects of the nucleus isthmi in salamanders of the family plethodontidae. *Journal of Comparative Physiology A*, 169(2):165–176, 1991.

Beatriz Williams, Norma Hernández, and Horacio Vanegas. Electrophysiological analysis of the teleostean nucleus isthmi and its relationships with the optic tectum. *Journal of comparative physiology*, 152(4):545–554, 1983.

Donghai Wu and Louis B Hersh. Choline acetyltransferase: celebrating its fiftieth year. *Journal of neurochemistry*, 62(5):1653–1663, 1994.

Claire Wyart, Filippo Del Bene, Erica Warp, Ethan K Scott, Dirk Trauner, Herwig Baier, and Ehud Y Isacoff. Optogenetic dissection of a behavioural module in the vertebrate spinal cord. *Nature*, 461(7262):407, 2009.

Cameron Wyatt, Ewelina M Bartoszek, and Emre Yaksi. Methods for studying the zebrafish brain: past, present and future. *European Journal of Neuroscience*, 42(2):1746–1763, 2015.

Julián Yáñez, Yara Souto, Laura Piñeiro, Mónica Folgueira, and Ramón Anadón. Gustatory and general visceral centers and their connections in the brain of adult zebrafish: a carbocyanine dye tract-tracing study. *Journal of Comparative Neurology*, 525(2):333–362, 2017.

Julián Yáñez, Tania Suárez, Ana Quelle, Mónica Folgueira, and Ramón Anadón. Neural connections of the pretectum in zebrafish (danio rerio). *Journal of Comparative Neurology*, 526(6):1017–1040, 2018.

Tohei Yokogawa, Markus C Hannan, and Harold A Burgess. The dorsal raphe modulates sensory responsiveness during arousal in zebrafish. *Journal of Neuroscience*, 32(43):15205–15215, 2012.

Alexandre Zénon and Richard J Krauzlis. Attention deficits without cortical neuronal deficits. *Nature*, 489(7416):434, 2012.

Maxime JY Zimmermann, Noora E Nevala, Takeshi Yoshimatsu, Daniel Osorio, Dan-Eric Nilsson, Philipp Berens, and Tom Baden. Zebrafish differentially process color across visual space to match natural scenes. *Current Biology*, 2018.

Marc Zirnsak, Nicholas A Steinmetz, Behrad Noudoost, Kitty Z Xu, and Tirin Moore. Visual space is compressed in prefrontal cortex before eye movements. *Nature*, 507(7493):504, 2014.

Steven J Zottoli, Adrienne P Bentley, Brian J Prendergast, and Heather I Rieff. Comparative studies on the mauthner cell of teleost fish in relation to sensory input. *Brain, behavior and evolution*, 46(3):151–164, 1995.

Ming Zou, Rainer W Friedrich, and Isaac H Bianco. Targeted electroporation in embryonic, larval, and adult zebrafish. In *Zebrafish*, pages 259–269. Springer, 2016.